PENNSTATE

1855

VOID DETECTION IN BITUMINOUS MINES WITH AN IN-SEAM SEISMIC TECHNIQUE

FINAL REPORT FOR PHASE II
OF
AN IN-SEAM SEISMIC (ISS) METHOD BASED MINE VOID DETECTION TECHNIQUE

Prepared for

U. S. Department of Labor
Mine Safety and Health Administration
1100 Wilson Boulevard
Suite 2132
Arlington, Virginia 22209 – 3939

RFP# MSHA J53R1011
(Geo-physical Void Detection Demonstrations)

September 4, 2008

By
Maochen Ge

The Pennsylvania State University
Department of Energy and Mineral Engineering
201 Hosler Building, University Park, PA 16802

Acknowledgements

The Penn State ISS void detection project team gratefully thanks all of the individuals and the organizations that supported this project:

To the mining companies which graciously offered their mines to Penn State as testing sites: Amfire Mining Co. and Nolo Mine; Massey Energy Co., Elk Run Coal Co. and Black King Mine; Foundation Coal and Cumberland Mine; RoxCoal Inc. and Roytown Mine; Peabody Energy Co. and Twentymile Mine; and Sterling Mining Co..

To numerous individuals from the mining industry, who helped Penn State with site identification and field tests. Without their help, the project would be impossible. In particular, we would like to thank: *Amfire Mining Co. and Nolo Mine*: R. Bottegal, Manager of Engineering, L. Pianetti, Jr., Mine Manager, Jim Pablic, Director of Safety, Gary Deemer, Mine Manager, Rick Smith, Mine Superintendent, Paul Zamba and Kevin Pollock; *Massey Energy Co., Elk Run Coal Co. and Black King Mine*: Chris Adkins, COO, Massey, Stanley Suboleski, Consultant and Former COO, Massey, Wayne Persinger, Vice President, Elk Run Coal, Chris Blanchard, President, Marfork Coal Company, Peanep Robinson, Mine Superintendent, Black King, Graig Boggs, and Sam Morton; *Foundation Coal and Cumberland Mine*: John Gallick, William Hudak, and Arunkumar Rai; *RoxCoal Inc. and Roytown Mine:* David Rebuck, President, Quecreek Mine, John Hickman, Mine Chief Engineer, and Rod Shabbick; *Peabody Energy Co. and Twentymile Mine*: Mike Berdine, Manager of Technical Resources; *Sterling Mining Co.*: Timothy Miller and Mike Bohan; *Rosebud Mining*: Jerry Hefferan, Vice President, and *Wampum Hardware*: Jay Elkins.

To Dr. W. Khair and West Virginia University for lending the velocity measurement equipment to the Penn State team. This measurement instrumentation was one of the key pieces of equipments used for the project.

To Webb Manufacturing of Midkiff, WV and Minova USA of Georgetown KY for their donation of stem clay and resin, respectively, the materials used for the field tests.

To the Pennsylvania Bureau of Deep Mine Safety for its ongoing support of the ISS project: Mr. J. A. Sbaffoni, Director, Mr. M. McCaffrey; D. Williams, T. A. Wolfgang, and J. L. Kerch.

We would like to thank the Mine Safety and Health Administration for providing funding for the ISS Demonstration Project. We thank Mr. D. Cooper, Director, Acquisition Management Division, Dr. K. Wu, Chief, Mine Waste and Geotechnical Engineering Division (Retired), Mr. Stanley J. Michalek, Chief, Mine Waste and Geotechnical Engineering Division, Mr. G. Gardner, Manager, MSHA's void detection program, Mr. Irving McCrae, and Dr. D. Choi, the Contracting Officer's Technical Representative.

I would like to thank the researchers from Penn State: Dr. Raja Ramani, Dr. Larry Grayson, Dr. Mark Radomsky, and Mr. Shugang Wang for their contributions. I would also like to thank Dr. Tao Feng, a visiting professor from Hunan University of Science and Technology, and Mr. Zhen Yang and Mr. Baisheng Zhen, visiting scholars from China University of Mining and Technology for their contributions to the successful field tests at Black King and Cumberland.

Finally, we would like to thank Dr. R. L. Nigbor from University of California at Los Angeles, Dr. Dai S. Choi, and Dr. Steve Cotton from Raytheon UTD for their constructive comments and suggestions in revising the report.

In 2008, Dr. H. Reginald Hardy Jr., Professor Emeritus at Penn State and Mr. E. Smock, President of Westpoint, two of the most valuable members of our project, passed away. Dr. Hardy was responsible for the laboratory testing and instrumental in the development of the retrievable sensor installation technique. Mr. Smock was the initial partner of the void detection project and hosted three field tests at the Harmony Mine. Their contributions to this project and to the mining industry will be always remembered.

Table of Content

1. Introduction

1.1 Project background

On October 8, 2004, the Mine Safety and Health Administration (MSHA) awarded to The Pennsylvania State University ("Penn State") a contract for the demonstration of the In-seam seismic (ISS) based void detection technique. The award was based on the Penn State proposal entitled *An In-seam seismic (ISS) method based mine void detection technique* submitted to MSHA on November 17, 2003 and the *Revised working plan* for this proposal submitted to MSHA by Penn State on August 25, 2004. The revisions were made in accordance with guidelines given by MSHA during contract negotiations held on July 28 and August 24, 2004.

Phase I of the project commenced on October 8, 2004 and finished on October 31, 2006. During this period, Penn State carried out a total of seven field tests at several locations: two trona mines, one anthracite mine and one bituminous mine. Among these seven tests, two were the contracted demonstrations. The first demonstration was held at FMC, a trona mine in Wyoming, on August 15, 2005, and the second demonstration was performed at the Harmony Mine, an anthracite mine in Pennsylvania, on November 15, 2005. A contracted demonstration was an official demonstration of the technique for the given field condition. Both the MSHA officials and industry representatives were present during the demonstrations.

Penn State completed the field tests and data analysis work for Phase I in March 2006 and submitted the draft version of the final report for Phase I (Ge, 2006a) and the draft version of the users' manual for the ISS technique (Ge, 2006b) to MSHA on March 30, 2006. On June 9, 2006, MSHA informed Penn State the result of the external review of Phase I work by two experts retained by MSHA. Both of the reviews confirmed the value of the reported work as well as the potential of the ISS based void detection technique. Based on the positive outcome of Phase I, MSHA approved Penn State to proceed with Phase II, starting on November 1, 2006.

1.2 Phase II objective

Phase II of the void detection project carried out by Penn State began on November 1, 2006 and ended on June 30, 2008.

The objective of Phase II was to investigate the effectiveness of the In-seam seismic (ISS) based void detection technique for bituminous coal mines.

The importance of Phase II may be viewed from three perspectives. First, a great majority of coal mines in the United States are bituminous mines, and many of them are adjacent to or even surrounded by abandoned mines. As such, bituminous mines are particularly vulnerable to the inundation problem and, therefore, void detection is most critical for these mines.

Secondly, the ISS technique to date has been generally applied to mines with coal seams typically greater than 7 - 8 feet in thickness. Little is known about thin and "soft" seams, a typical condition for small to medium size bituminous mines in the United States. A thin and soft coal seam is considered a much more difficult condition for the ISS based technique. This

concern is further aggravated by the fact that void detection is a new application of the ISS technique.

1.3 Approaches

In order to fulfill the objective of Phase II, our attention was focused on two specific issues: site selection and signal detection. The significance of these two issues and the approach we used to address them are discussed as follows.

1.3.1 Site selection

The Love waves used for the ISS technique are a phenomenon closely associated with seam conditions and the seam conditions for the bituminous mines in the United States vary significantly. In order to evaluate the feasibility of the ISS based void detection technique for bituminous mines, test site selection must represent these diversified conditions. Furthermore, since most bituminous mines operated in the United States today have the characteristic of a thin and "soft" seam, the focus of testing and demonstration should be on these less than ideal conditions.

Four sites from three mines were selected to investigate the effectiveness of the ISS based void detection technique for bituminous mines in Phase II. These three mines are the Nolo Mine of the Amfire Mining Co., the Black King Mine of Massey Energy, and the Cumberland Mine of Foundation Coal. The Nolo Mine hosted two test sites. The basic conditions for these test sites are briefly summarized in Table 1.1.

Table 1.1 Site conditions for testing the ISS based void detection technique

Mine Site	Coal seam	Seam height (inch)	Pillar width (feet)	Roof, floor formation	Depth (feet)	Remarks
Nolo (Site I)	Lower Kittanning	48	120	clay shale	300	Coal is highly fractured, clay shale is weak, roof condition is poor.
Nolo (Site II)	Lower Kittanning	48	180	clay shale	300	Same as above.
Black King	Lower Cedar Grove	36	100	sandstone	700	Coal is stronger than the coal from Nolo mine. Good roof condition.
Cumberland	Pittsburgh	84	200	shale	600	Coal is stronger than the coal from Nolo mine. Reasonable roof condition.

Among these mine sites, the test conditions at the Nolo Mine are most challenging. In addition to a very thin seam, the coal is highly fractured. Furthermore, the shales which formed the roof and the floor are very weak, indicated by severe roof control problems at the mine. From the ISS test point of view, the Nolo Mine almost certainly represents one of the most difficult conditions. The condition encountered at the Nolo Mine is typical for low seam mines in Pennsylvania, West Virginia and Kentucky. Because of the extreme nature of these conditions, the test at the Nolo Mine was considered very important.

The Cumberland Mine, on the other hand, is considered much more ideal for the ISS technique. The Pittsburgh seam recovered at the Cumberland Mine is the best known coal seam in the United States. This coal seam is relatively thick, 7 feet at the site. In addition, the Pittsburgh seam has good strength and is much stronger when compared to the coal seam of Lower Kittanning mined at the Nolo Mine. The shale which forms the immediate roof and floor appears reasonably strong as there are no excessive ground control problems at the Cumberland Mine.

The test site at the Black King Mine combines several extreme conditions. First, the coal seam at the site is extremely thin, measuring only 36-inch thick. The pillar rib is very uneven and undulates in a wave like manner. On the other hand, the coal is much stronger than the coal from Lower Kittanning. The best conditions at the site are the strong roof and floor formed by sandstone.

One of the important issues in testing the ISS based void detection technique is the detection range for the technique. In order to address the problem, two sites were selected from the Nolo Mine. The two sites share identical physical condition and are different only in the two widths, 120-feet wide and 180-feet wide. As such, the detection distance can be determined in an objective manner. The other important consideration in selection of the Nolo Mine is that the test condition at the Nolo Mine represents one of the most difficult situations for the void detection technique. If a detection distance is confirmed at this mine using the ISS based system, then it may be considered as a benchmark of the detection distance for the technique.

1.3.2 Signal detection

The concern with using the ISS based void detection technique for bituminous mines is that the typical condition for the bituminous mines in the United States, a thin and “soft” coal seam with weak country rock, is not ideal for the ISS based technique. The essence of this concern is that it may be difficult to detect the in-seam Love waves.

Geophones are conventionally used for ISS studies. This practice is reasonable when coal seams are thick. For instance, the expected Love wave frequencies will be typically less 200 Hz if the seam thickness is more than 10 feet. However, the typical seam height for the bituminous mines in the United States is much lower as many of the seams are less than 5 feet. As such, the expected frequencies for in-seam Love waves are much higher. Because of this range in frequencies, the utilization of sensors with broader frequency response is essential.

In Phase II, high sensitivity accelerometers with a frequency response of 50 – 5000 Hz were used as the primary sensors. Among a total of 14 sensors used for data acquisition, 10 were accelerometers. The remaining 4 sensors were geophones for detecting low frequency signals. The frequency response of these geophones is 4.5 – 200 Hz.

In addition to the sensor selection, the other important measure to improve the capability of signal detection was to use the sensor installation technique developed during Phase I. Typically, geophones used for the ISS study are simply spiked into the coal. This installation method is acceptable if signal frequencies are low and the rib is competent. For the ISS based void detection technique, this installation method would present two fatal problems. First, the coupling effect of this method with high frequency signals is very poor. Secondly, coal ribs are often highly fractured which causes rapid attenuation of the signals before they reach the sensor.

In order to overcome these problems a retrievable sensor installation technique was developed during Phase I. With this technique, sensors are tightly screwed on the sensor anchors that are grouted at the bottom of the boreholes. This location ensures that the sensors are located beyond the fracture zone. This technique not only greatly improves the coupling effect, but also eliminates the problem caused by the fractured surface.

The last important measure for improving signal detection in Phase II was to use a simple and effective air-tight sealing technique for sensor holes. A unique problem presented to the ISS based void detection technique during the reflection survey is the disturbance caused by strong (air) shock waves. This problem occurs due to a very close range between the blasting locations and the sensors locations and also because of the very confined environment, which could completely overshadow later arriving Love waves, a problem encountered in Phase I during the field test at the Agustus Mine (Ge, 2006a). To eliminate this problem, a number of materials were tested at the beginning of Phase II. As the result, Play-Doh, a playing material for young children, was selected for its effectiveness in providing the air-tight seal for the sensor holes and also for its convenience.

1.4 Report structure

Phase II was a continuation of the work carried out in Phase I and the ISS research by many others in the past.

During the past fifty years, the in-seam seismics has grown into a recognized science and engineering discipline. The basic theory and method of the ISS technique were well summarized and elucidated by Dresen and Ruter in their book: *Seismic Coal Exploration, Part B: In-seam Seismics* (Dresen and Ruter, 1994). Among researchers who contributed the development of the ISS technique, Evison (1955), Krey (1962, 1963, 1976a, 1976b), and Brentrup (1970, 1971, 1979a, 1979b) are considered the representatives of the early developers. The ISS research in US stared in 1960s. The early work included Leitinger (1969), Darken (1975), Guu (1975), Su (1976), Young (1976), etc. Among the recent studies, the work by Rodriguez is most notable (Rodriguez, *et al*., 1994; Rodriguez and Naumann, 1995; Rodriguez, 1996).

In Phase I, seven field tests, including two demonstration tests, were carried out for evaluating the feasibility of the ISS technique for the purpose of void detection. The results of these field tests were presented in the final report for Phase I (Ge, 2006a). The special technical issues, including sensor installation, experimental design, data analysis, and void mapping, were also discussed in a separate report (Ge, 2006b).

This report covers Phase II work only, which consists of six chapters. Chapters 2 – 5 discuss the four field tests and the associated data analysis. Chapter 6 is a summary of the Phase II work and presents our view on the effectiveness of the ISS based void detection technique for bituminous mines.

1.5 Penn State project team

Members of Penn State project team for Phase II:

Dr. Maochen Ge,	PI, Associate Professor of Mining Engineering,
Dr. Mark Radomsky	Director of Field Services, Miner Training Program
Dr. H. Reginald Hardy	Professor Emeritus,
Dr. Raja Ramani	Professor Emeritus
Dr. Larry Grayson	Professor of Mining Engineering
Mr. Hongliang Wang	Graduate Research Assistant
Mr. Jin Wang	Graduate Research Assistant
Mr. Shugang Wang	Graduate Research Assistant

2. First Field Test at Nolo Mine

2.1 Introduction

On June 23, 2007, the Penn State project team carried out a field test on the ISS based void detection technique at the Nolo Mine. It was the first test for Phase II of the void detection project awarded by MSHA. The objective of Phase II was to investigate the feasibility of utilizing in-seam Love waves for void detection in bituminous mines.

Nolo mine

The Nolo Mine is an underground bituminous coal mine, located approximately 3 miles southwest of the community of Nolo in Buffington Township, Indiana County, Pennsylvania (Figure 2.1). The coal seam is known as the Lower Kittanning, which has an average height of 50 inches. The roof and floor are formed from sandy shale and clay shale, respectively. The overburden in the mine varies from 200 to 300 feet.

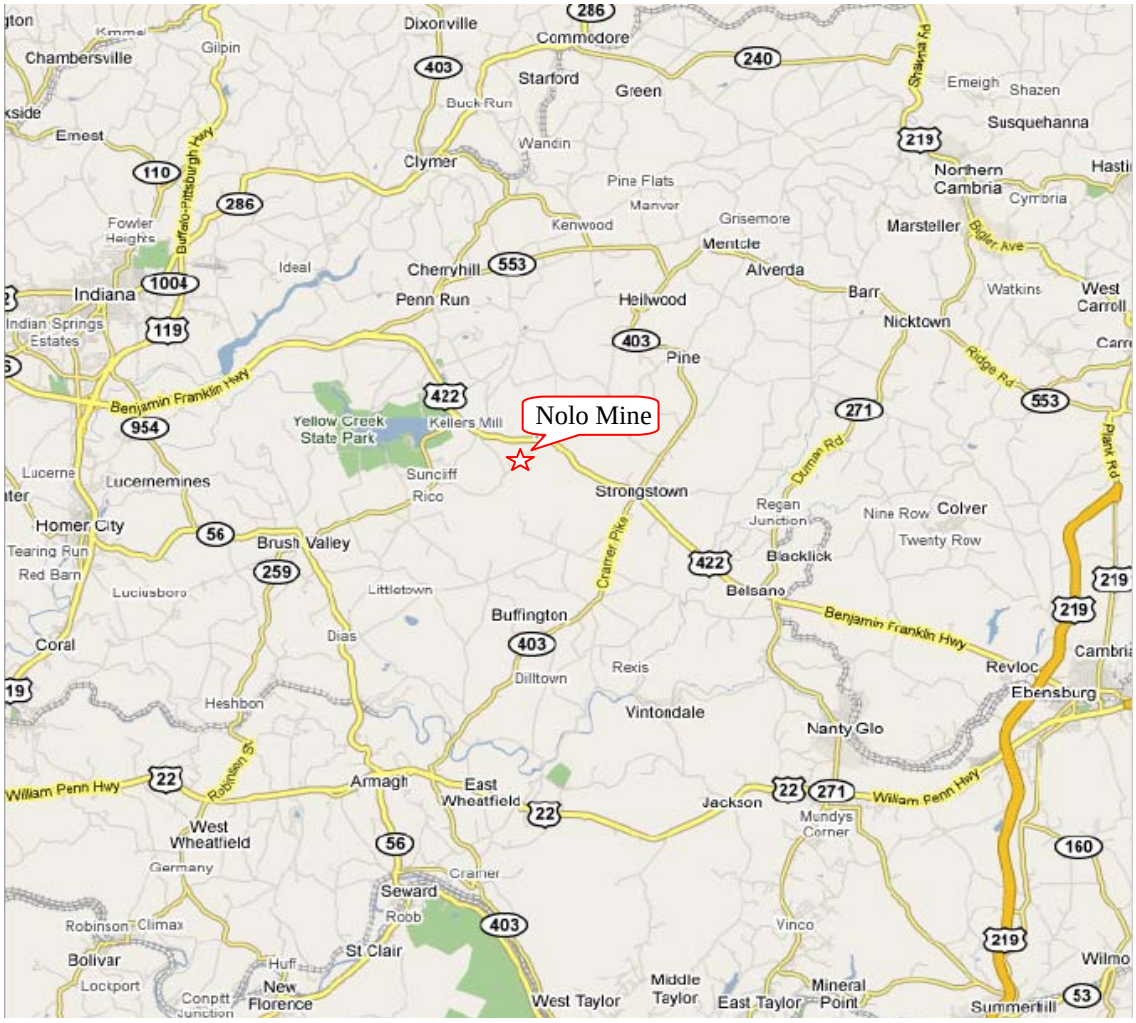

Figure 2.1 Geographic location of the Nolo Mine

2.2. Testing site and experimental design

Penn State executed two tests on the ISS based void detection technique at two different sites down the length of a long pillar (Figure 2.2). The first test site was positioned at the narrow section of the pillar, which was about 120-feet wide. This site was termed Site I. The second test site, Site II, was located at the mid-point of the wide section which was approximately 180-ft wide.

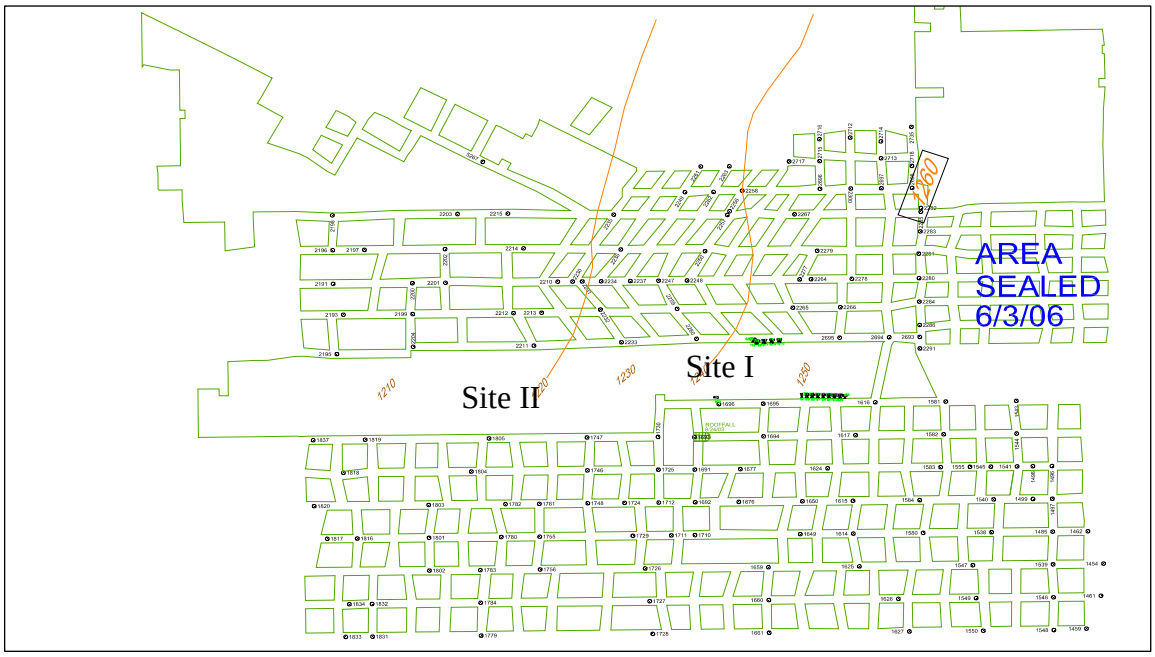

Figure 2.2 The locations of two test sites at the Nolo Mine.

2.2.1 Testing site condition

The coal seam, Lower Kittanning, is highly fractured at the mine site. As a result, the pillar ribs are also highly fractured. This can be seen in the picture shown in Figure 2.3, where coal fragments broken off from the rib consist of very small pieces and are piled along the rib on the floor.

The roof strata which are formed by clay and sandy shale are weak. As a result, the roof condition at the mine is very poor. This is also evident from the picture in Figure 2.3. Roof control is a severe problem at the Nolo Mine.

The site condition at the Nolo Mine, a thin and "soft" seam with weak roof and floor, is typical for many small bituminous mines in the Appalachian region. The selection of the Nolo Mine as the test site was largely due to its representative condition for small bituminous mines in the eastern region of the United States. This typical condition, however, is not favorable for the development and propagation of in-seam Love waves. It is therefore considered a challenge to apply the ISS based void detection technique to the bituminous mines.

Figure 2.3 A view of the rib and roof condition at the test site of the Nolo Mine.

2.2.2 Test layout for Site I

The test layout for Site I is shown in Figure 2.4. The site was utilized for both transmission and reflection surveys. The testing setup included three sections: a sensor section, a blasting section for transmission surveys, and a blasting section for reflection surveys.

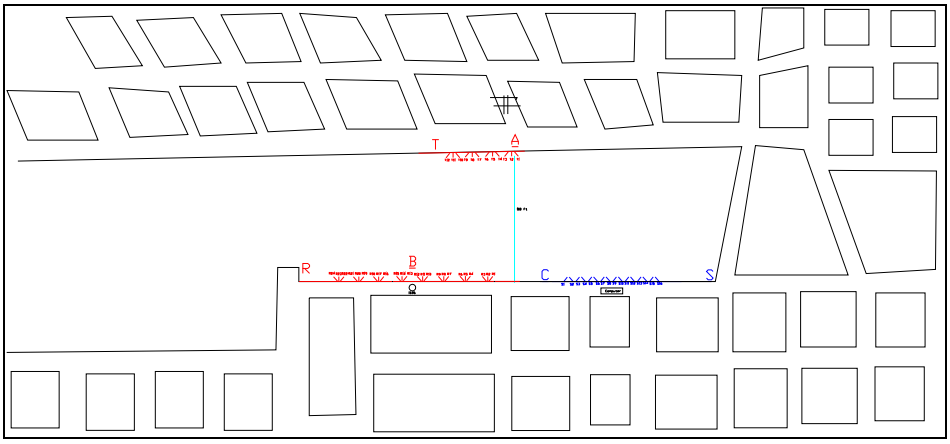

Figure 2.4 An overview of the test site. The blue and red segments on the lower side of the pillar denote the locations of sensor holes and blasting holes for reflection surveys, respectively. The red segment on the top side of the pillar represents the locations of blasting holes for transmission surveys.

2.2.3 Sensor section

The sensor section was located on the lower side of the pillar, 50 feet from the east end of the pillar marked by S. A total of 16 sensor holes were prepared for transmission and reflection surveys, which were numbered from S1 to S16. The locations and orientation of these sensor holes are shown in Figure 2.5. These sensor holes are 5-feet deep, drilled in pairs and oriented with a 45° angle in the middle of the coal seam. The diameter of the sensor holes is 1.75 inches. Among these 16 sensor holes, 14 were used for the test. Table 2.1 lists the related information for these sensor holes.

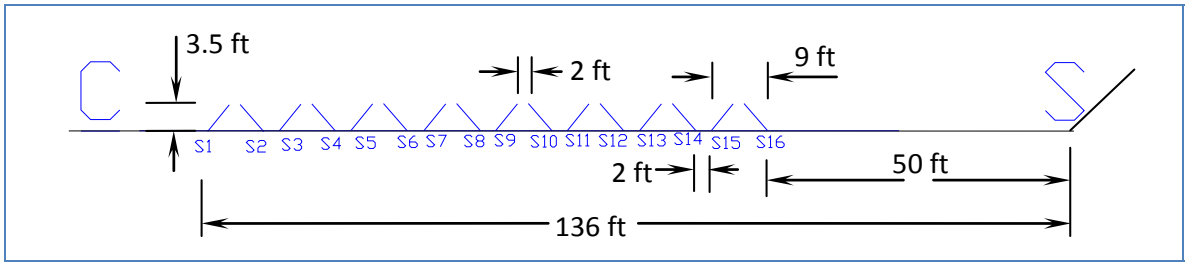

Figure 2.5 Layout of sensor section at Site I, Nolo Mine.

Table 2.1 Sensor hole information for Site I, Nolo Mine.

Hole #	Channel #	Length (ft)	Sensor coordinate (ft)	
			East (x)	North (y)
S1	2	5	1625767.0	450041.9
S2	3	5	1625768.8	450041.9
S3	4	5	1625777.9	450041.6
S4	5	5	1625779.3	450041.6
S5	7	5	1625788.6	450041.3
S6	8	5	1625790.2	450041.3
S7	9	5	1625799.4	450041.0
S8	10	5	1625801.1	450041.0
S9	11	5	1625810.1	450040.8
S10	12	5	1625812.1	450040.8
S11	13	5	1625821.0	450040.5
S12	14	5	1625823.1	450040.5
S13	15	5	1625832.2	450040.2
S14	16	5	1625834.1	450040.2

Two types of sensors, the accelerometers and the geophones, were used. Accelerometers were placed in the first ten holes, S1 - S10, and geophones were placed in the remaining four holes, S11 - S14.

2.2.4 Blasting section for the transmission surveys

The blasting section for the transmission surveys was located on the upper side of the pillar. Twelve blasting holes were prepared for transmission surveys, which were numbered from T1 to T12 (Figure 2.6). The length of these holes varied, with perpendicular holes designed to be 3.5-feet deep and angled holes designed to be 5-feet deep. All holes were 1.5 inches in diameter. The coordinates for sources in these holes are presented in Table 2.2. Among these 12 prepared blasting holes, 8 were actually used during the field test.

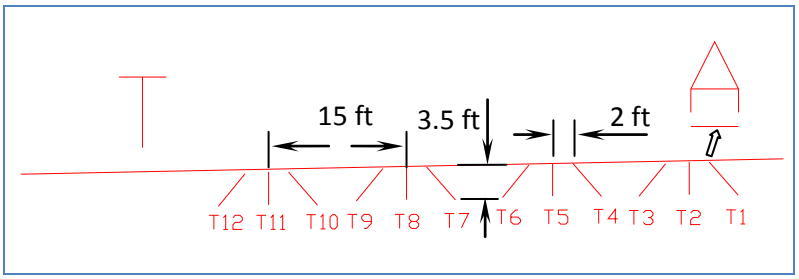

Figure 2.6 Blasting boreholes prepared for transmission survey**.**

Table 2.2 Coordinates of blasting hole sources for transmission survey at Site I, Nolo Mine.

Hole #	Source coordinate (ft)	
	East (x)	North (y)
T1	1625725.3	450152.3
T2	1625718.8	450151.9
T3	1625713.8	450151.6
T4	1625710.3	450151.4
T5	1625704.5	450151.0
T6	1625699.2	450150.6
T7	1625695.3	450150.4
T8	1625689.9	450150.1
T9	1625684.2	450149.7
T10	1625680.5	450149.4
T11	1625675.2	450149.1
T12	1625669.7	450148.7

2.2.5 Blasting section for the reflection survey

The blasting section for the reflection surveys was located on the lower side of the pillar. The section location was determined during the site inspection and consequently centered at Mark B. A total of 24 blasting holes were prepared for the reflection survey and were numbered from R1 to R24, as shown in Figure 2.7. The length of these holes varied, with vertical holes designed to be 3.5-feet deep and angled holes designed to be 5-feet deep All holes were 1.5 inches in diameter. The coordinates of the sources in these holes are listed in Table 2.3.

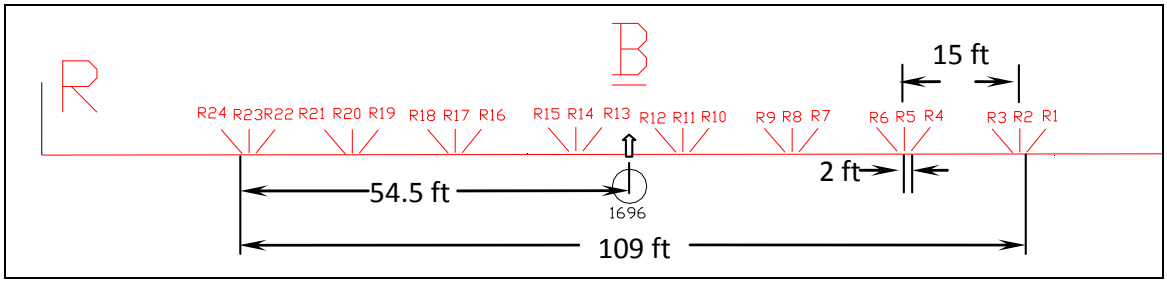

Figure 2.7 Blasting section for reflection surveys at Site I, Nolo Mine.

Table 2.3 Coordinates of blasting hole sources for reflection survey at Site I, Nolo Mine

Hole#	Source coordinate (ft)	
	East (x)	North (y)
R1	1625657.7	450038.2
R2	1625652.2	450037.9
R3	1625646.7	450037.7
R4	1625643.0	450037.5
R5	1625637.4	450037.2
R6	1625631.8	450037.0
R7	1625628.1	450036.8
R8	1625622.6	450036.6
R9	1625617.0	450036.3
R10	1625613.7	450036.2
R11	1625609.0	450035.9
R12	1625602.3	450035.7
R13	1625598.8	450035.5
R14	1625593.2	450035.2
R15	1625587.5	450035.0
R16	1625583.7	450034.8
R17	1625578.3	450034.5
R18	1625572.5	450034.3
R19	1625568.8	450034.2
R20	1625563.2	450033.9
R21	1625557.8	450033.7
R22	1625553.6	450033.5
R23	1625547.9	450033.1
R24	1625542.5	450033.0

2.3 Transmission surveys

A total of 8 transmission surveys were performed at Site I. The ray paths associated with these surveys are illustrated in Figure 2.8. The seismic source for most of the surveys was 120 grams dynamite. The strength of the dynamite delivered by the blasting company for the test was much lower than the ones we normally used (about one third of the strength we normally used) for the tests in Phase I as well as the other tests in Phase II. The event information for these surveys is summarized in Table 2.4.

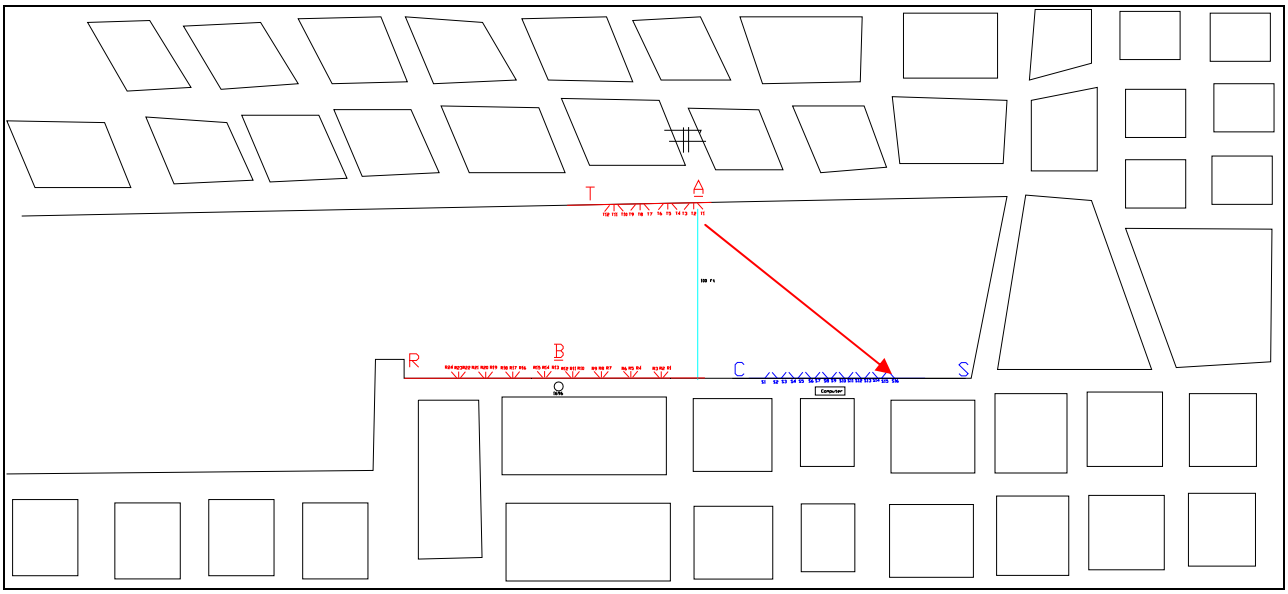

Figure 2.8 Illustration of ray paths associated with the transmission survey.

Table 2.4 A summary of the transmission survey at Site I

Hole #	Explosive (gram.)	Event #
T1	120	71
T2	120	67
T3*	120	63
T7	120	57
T9	120	52
T10	120	44
T11	120	28
T12	40	17

*Two caps were used.

Among these eight surveys, seven were successfully recorded and the results for these seven recorded events were similar. Event 57 is selected to show the general characteristics of the transmission data. The survey layout for the event is shown in Figure 2.9, where T7 is the

location of the seismic source. The average signals travel distance for this survey is approximately 150 feet.

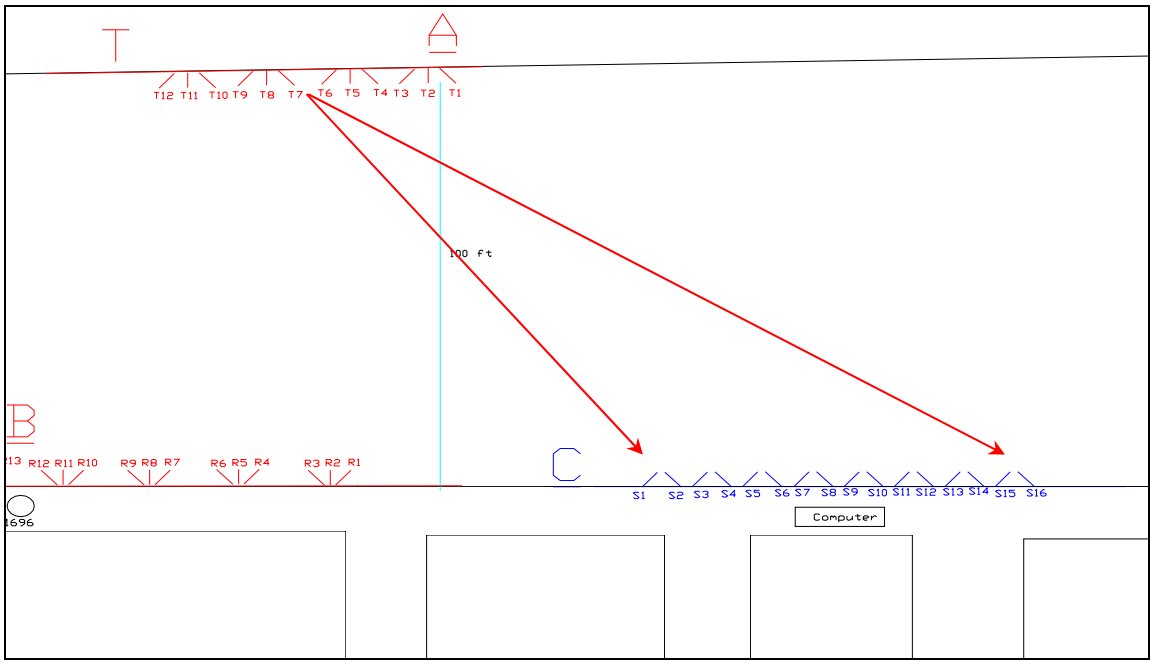

Figure 2.9 Testing setup for Event 57.

The original waveform record for Event 57 is presented in Figure 2.10. The first arrival signals are P- and S-waves transmitted through the roof and the floor. The frequencies for these signals are very high, varying from 1,000 to 2000 Hz with a typical value of 1,500 Hz. The in-seam Love waves arrived at a much later time.

To highlight the in-seam Love waves, a 50-400 Hz bandpass filter was applied to the original signals. The result of this filtering process is shown in Figure 2.11. The in-seam Love waves, which were originally overshadowed by strong P- and S-waves from the roof and floor, become apparent for most channels after this filtering process. The frequencies for the in-seam Love waves are about 200 -300 Hz. The frequency spectra for the signals originally plotted in Figure 2.10 are shown in Figure 2.12.

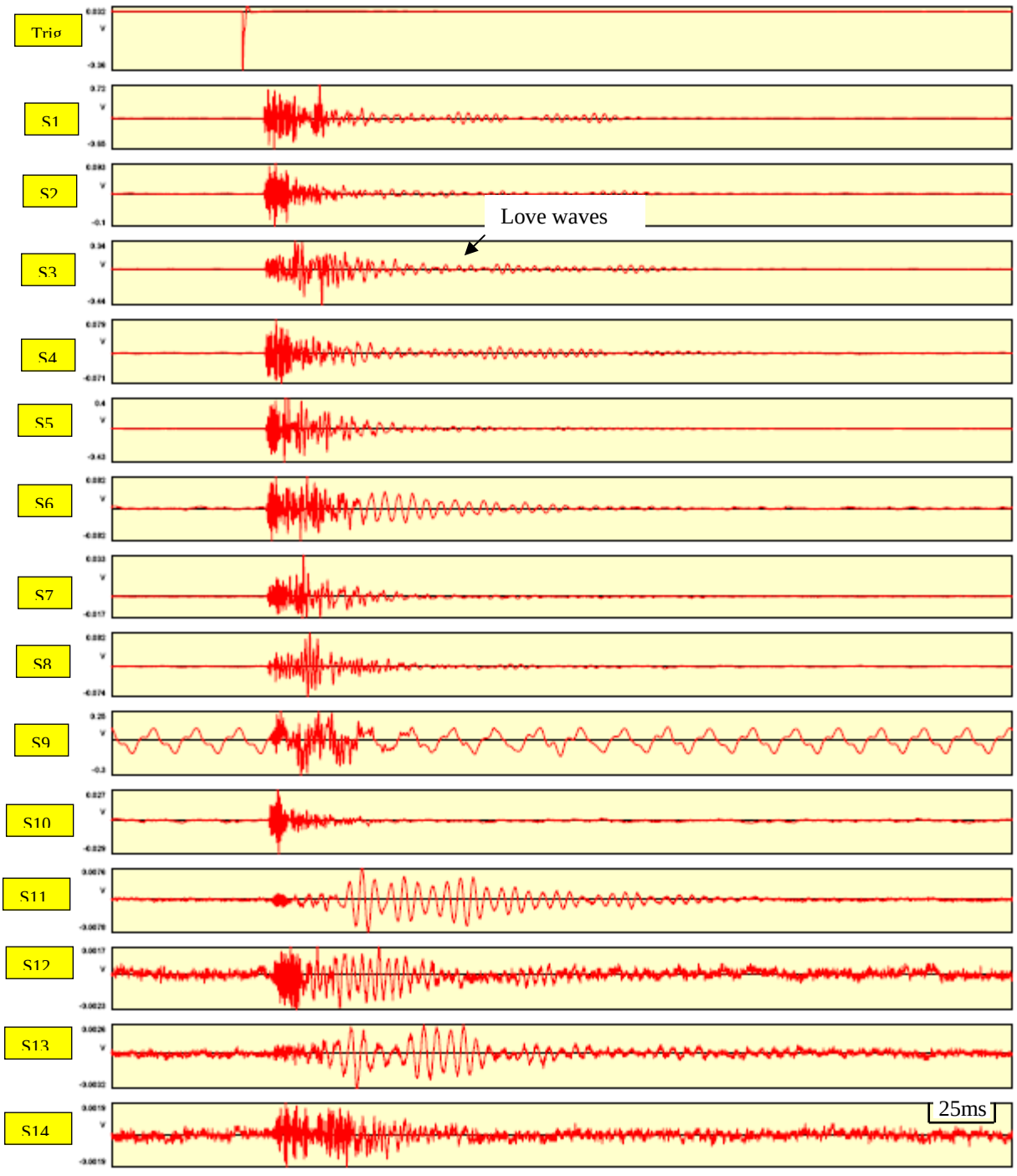

Figure 2.10 Original waveform record for a transmission survey (Event 57) carried out at Site I, Nolo Mine (display window: 50-400 ms).

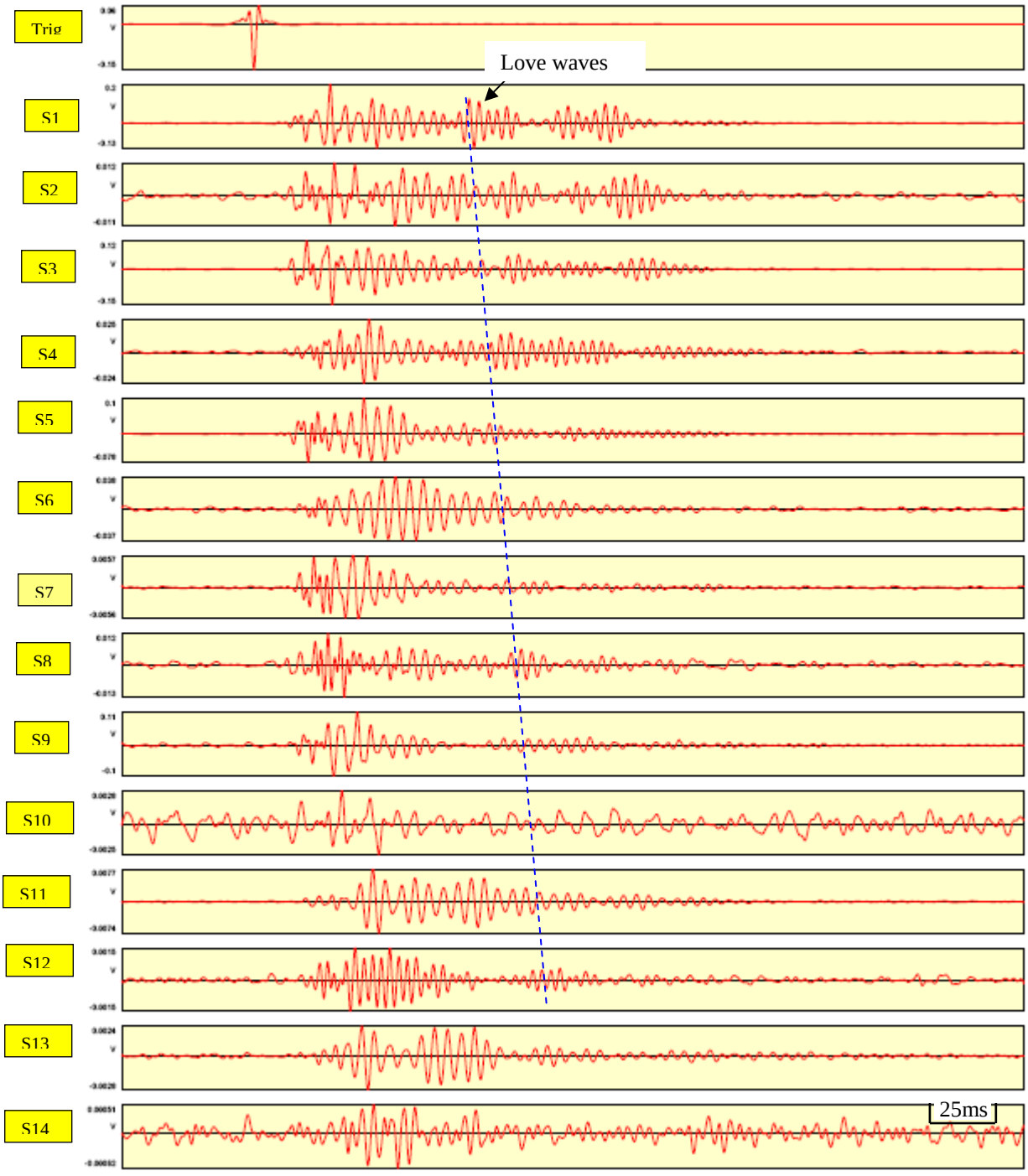

Figure 2.11 Resulting signal waveform for Event 57 after applying a 50-400 Hz bandpass filter (display window: 50-400 ms).

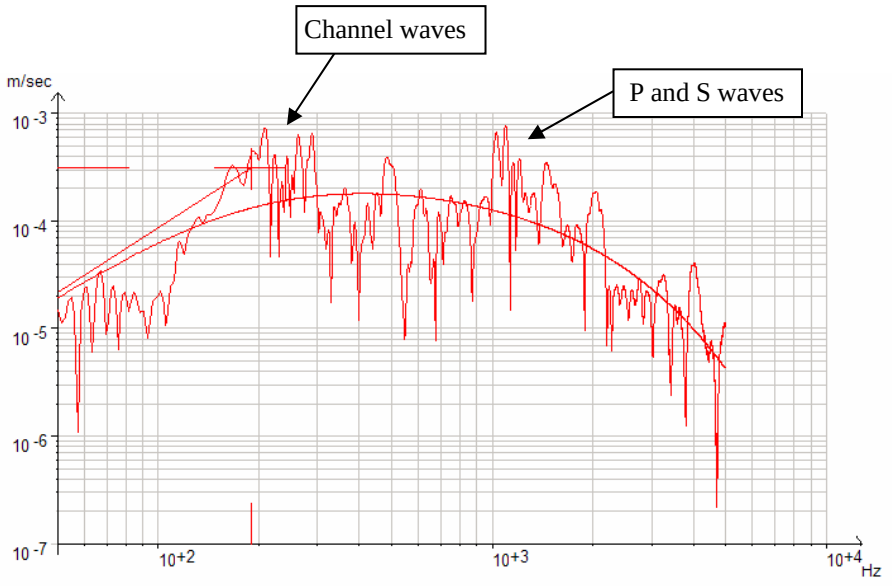

Figure 2.12 Frequency spectrums for signals recorded by sensor S1 shown in Figure 2.10.

Wavelet Analysis

It is known that ISS signals are non-stationary in both their frequency and amplitude statistics. These signals usually vary in amplitude and frequency over long periods of time. Ideally, for the ISS signal analysis, one would like to separate short period oscillations from long period oscillations. Wavelet analysis is used to simultaneously decompose a signal into time and frequency space. With wavelet analysis, one can determine the characteristics of the frequency of a signal, and the variation of the frequency with time.

One of the major difficulties in ISS data analysis is to identify newly arrivals because signals from the roof and floor and signals from the coal seam are often superimposed. Differentiating channel waves from refracted S- waves is challenging. Furthermore, reflection signals are often hampered by background noises and long-lasting transmission waves. One of the approaches to resolve these complicated problems, as demonstrated in Phase I (Ge, 2006), is wavelet analysis. The wavelet transform provides a convenient means to identify newly arrivals by examining their time related frequency characteristics. Such an example is given in Figure 2.13.

Part *a* in Figure 2.13 is the original waveform of the transmission signal received by sensor S1 presented earlier in Figure 2.10. Part *b* in Figure 2.13 is the plot of the wavelet transform coefficient with Gabor wavelets, and part *c* in Figure 2.13 is the 3-dimensional display of part *b*.

In this example, signals are distinguished by their local (time) characteristics: frequency and wavelet coefficient. The first group includes refracted P- and S- waves, which exhibit very high frequency and strength. The second group is the transmitted Love waves. The green tip is the location of the Airy Phase. The 3D display of the wavelet transform clearly illustrates the relationships among refracted P- and S-waves and Love waves simultaneously by time, frequency, and wavelet coefficient. The 3D image of the signal in terms of these three factors is very helpful to recognize the pattern of the seismic signals.

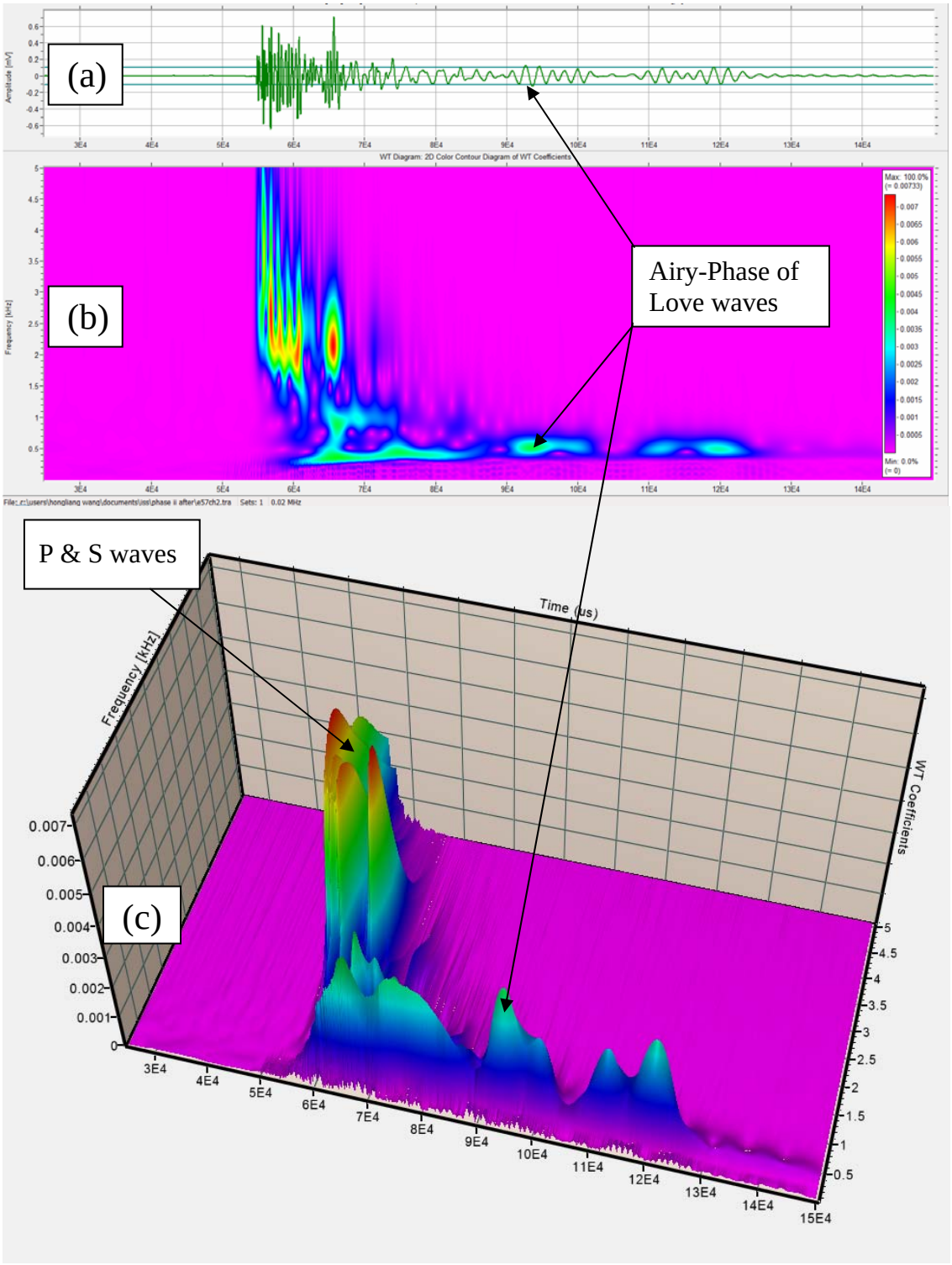

Figure 2.13 Analysis of transmission signals with wavelet transform.

Velocity calculations for Site I

The velocities of the P- and S-waves transmitted through the roof and the floor and the in-seam Love waves (the Airy Phase) were calculated based on the data from the transmission survey. The resulting calculated velocities are listed in Table 2.5. The raw data for the calculations are tabulated in Tables 2.6 – 2.9.

Table 2.5 Velocities associated with Site I, Nolo Mine**.**

Strata	Velocity Type	Velocity (ft/s)	Number of measurements	Standard deviation (ft/s)
Coal (bituminous)	Airy Phase	1590	30	58
Roof (sandy shale)	P-wave	15242	83	706
	S-wave	7320	35	832

Table 2.6 Source – receiver distances (ft) for transmission surveys at Site I.

	Channel #	2	3	4	5	7	8	9	10	11	12	13	14	15	16
Event #		S1	S2	S3	S4	S5	S6	S7	S8	S9	S10	S11	S12	S13	S14
71	T1	118.1	118.7	122.6	123.2	127.8	128.6	133.7	134.7	140.2	141.4	147.2	148.6	154.9	156.3
67	T2	120.2	120.9	125.2	125.8	130.8	131.7	137.1	138.1	143.9	145.1	151.2	152.6	159.2	160.6
63	T3	122.0	122.8	127.4	128.0	133.3	134.2	139.9	140.9	146.8	148.2	154.4	155.8	162.6	164.0
57	T7	130.1	131.1	136.6	137.4	143.5	144.6	151.0	152.1	158.7	160.2	166.9	168.5	175.7	177.3
52	T9	135.9	137.0	143.1	143.9	150.4	151.6	158.3	159.5	166.4	168.0	175.0	176.6	184.0	185.6
44	T10	138.0	139.2	145.3	146.2	152.9	154.1	160.9	162.1	169.1	170.7	177.8	179.4	186.9	188.5
28	T11	141.2	142.4	148.7	149.7	156.5	157.7	164.7	165.9	173.0	174.6	181.8	183.5	191.1	192.7

Table 2.7 The P-wave velocities in roof/floor determined from transmission surveys at site I

P-waves		Ch2	3	4	5	7	8	9	10	11	12	13	14	15	16
Event#	Source	S1	S2	S3	S4	S5	S6	S7	S8	S9	S10	S11	S12	S13	S14
71	T1	15141	15031	14956	15025	15216	14957	15198	14962	13877	14881	14432	14149	14897	14607
67	T2	15408	15305	15085	15345	15573	15313	15582	15343	14986	15277	15273	14531	15306	14870
63*	T3	10889	10960	10978	11036	11294	11183	11558	11360	10877	11574	11608	10530		10446
57	T7	15484	15420	15350	15441	15601	15548	15566	15523	15872	15551	14905	14043	14402	13957
52	T9	15446	15225	15058	15150	15672	15469	15678	15490	15131	15269	14705	14018		13550
44	T10	16631	16767	16706	16617	16801	16565	16762	16544	16107	16569	16460	14952	15196	14502
28	T11	15182	15146	15177	15116	15341	15161	15248	15222	14790	15452	14545	14335	14154	13964

* There was a problem on P-wave arrivals. However, we could not determine the cause.

Table 2.8 The S-wave velocities in roof/floor determined from transmission surveys at site I

S-waves		Ch2	3	4	5	7	8	9	10	11	12	13	14	15	16
Event#	Source	S1	S2	S3	S4	S5	S6	S7	S8	S9	S10	S11	S12	S13	S14
71	T1	8317	8246	8176	7605	6909									
67	T2	8772	8699	7975	7274	6995									
63	T3			7236		7363		7209	7114	7128					
57	T7			6797		6900	6427	6344	6312	7487					
52	T9			8670		8597		8700		8536					
44	T10			6760	6528	6735						7936			
28	T11	6537	6328	6495	6236	6493			6382						

Table 2.9 The in-seam Love wave (the Airy Phase) velocities determined from transmission surveys at site I

Ch.-waves		Ch2	3	4	5	7	8	9	10	11	12	13	14	15	16
Event#	Source	S1	S2	S3	S4	S5	S6	S7	S8	S9	S10	S11	S12	S13	S14
71	T1	1552		1568	1575	1570							1673		
67	T2	1557		1550	1550	1543			1744				1682		
63	T3	1566			1537								1660		
57	T7	1644							1551				1699		
52	T9	1672			1551				1575						
44	T10	1592	1533		1530	1532				1536					
28	T11	1649	1611		1557	1579	1586								

2.4 Reflection surveys at Site I

A total of 10 reflection surveys (blasting events) were accomplished at Site I in the Nolo Mine. The layout of the testing setup for the reflection surveys is illustrated in Figure 2.14. The seismic source for these surveys ranged from 120 to 240-gram dynamite and the event information is summarized in Table 2.10.

These surveys resulted in a successful demonstration of the observation and use of reflected Love waves for the detection of voids. In the following discussion, Event 110 is selected to demonstrate this conclusion.

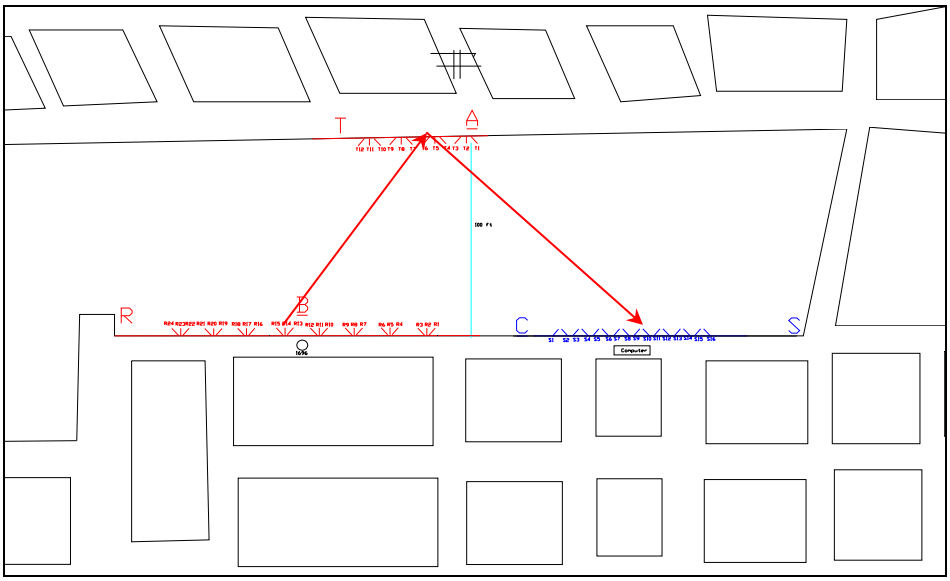

Figure 2.14 Testing setup for reflection surveys at Site I, Nolo Mine.

Table 2.10 A summary of the reflection surveys at Site I

Hole #	Explosive (gram)	Event #
R1	120	110
R3	120	106
R4	120	104
R6	120	102
R7	120	100
R9	120	98
R16	240	96
R18	240	94
R19	240	92
R20	240	90

Event 110 refers to the reflection survey with the seismic source at R1. The layout for this survey, including the locations of R1, the sensors, and the associated ray paths, is illustrated in Figure 2.15. The recorded event is presented in Figures 2.16 and 2.17, where Figure 2.16 is the complete record of the original waveform for the event and Figure 2.17 is a close-up of the reflected Love waves. A strong trend of the reflected Love waves is clearly shown in Figure 2.17. The arrival time readings for the reflected Love waves are listed in Table 2.11.

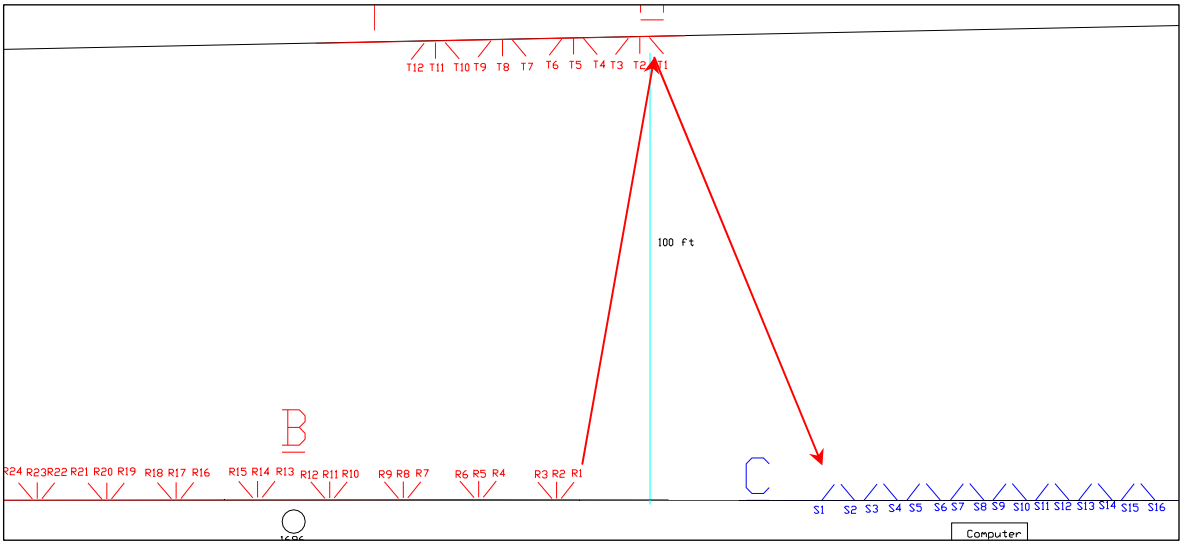

Figure 2.15 Testing setup for event 110.

Table 2.11 Arrival time readings for the reflected Love waves for event 110.

Triggering time (ms)	Sensor #	S1	S2	S3	S4
101.1	Arrival time	231	235	246	250

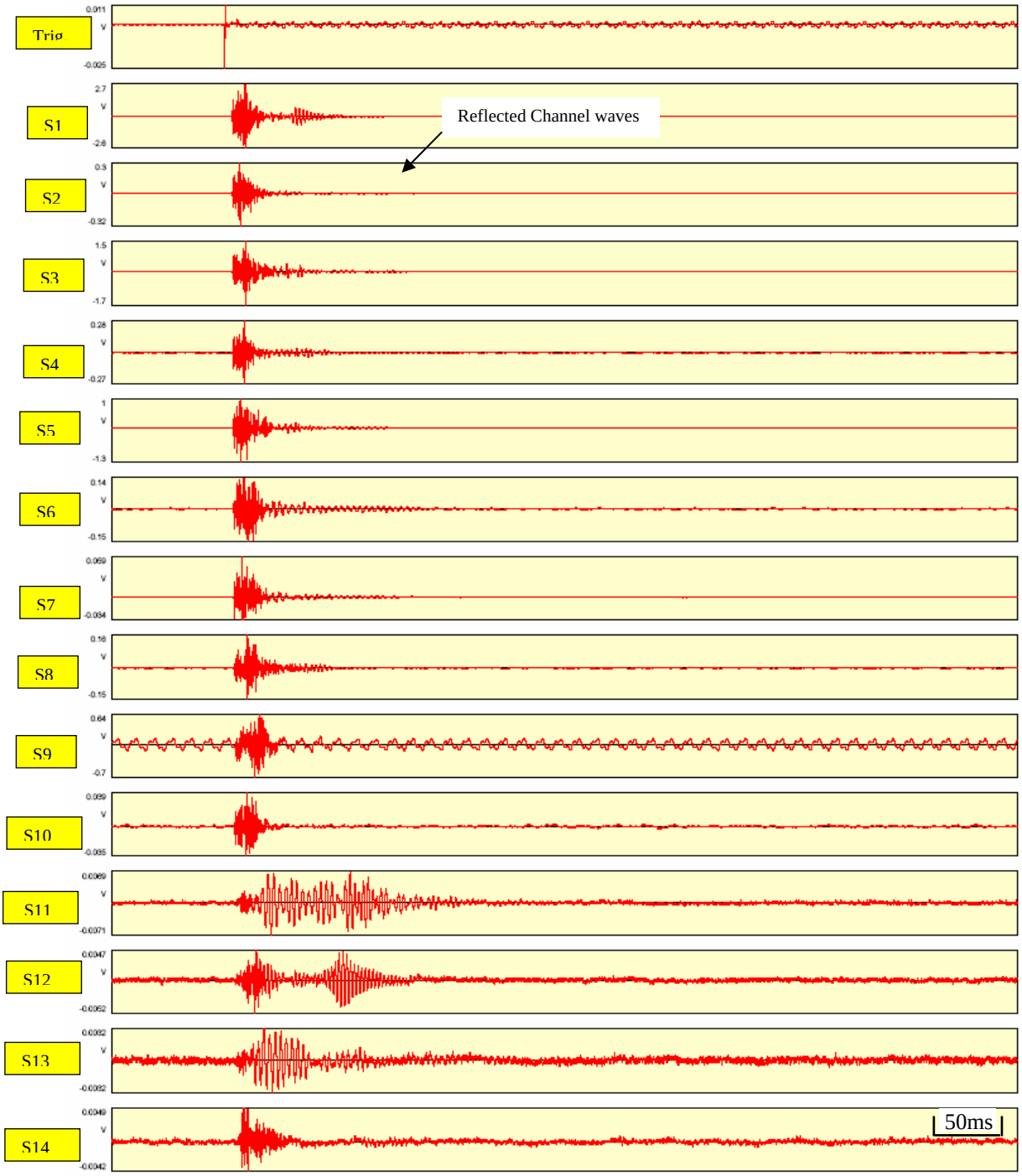

Figure 2.16 Waveform record for event 110 (display window: 0-800ms).

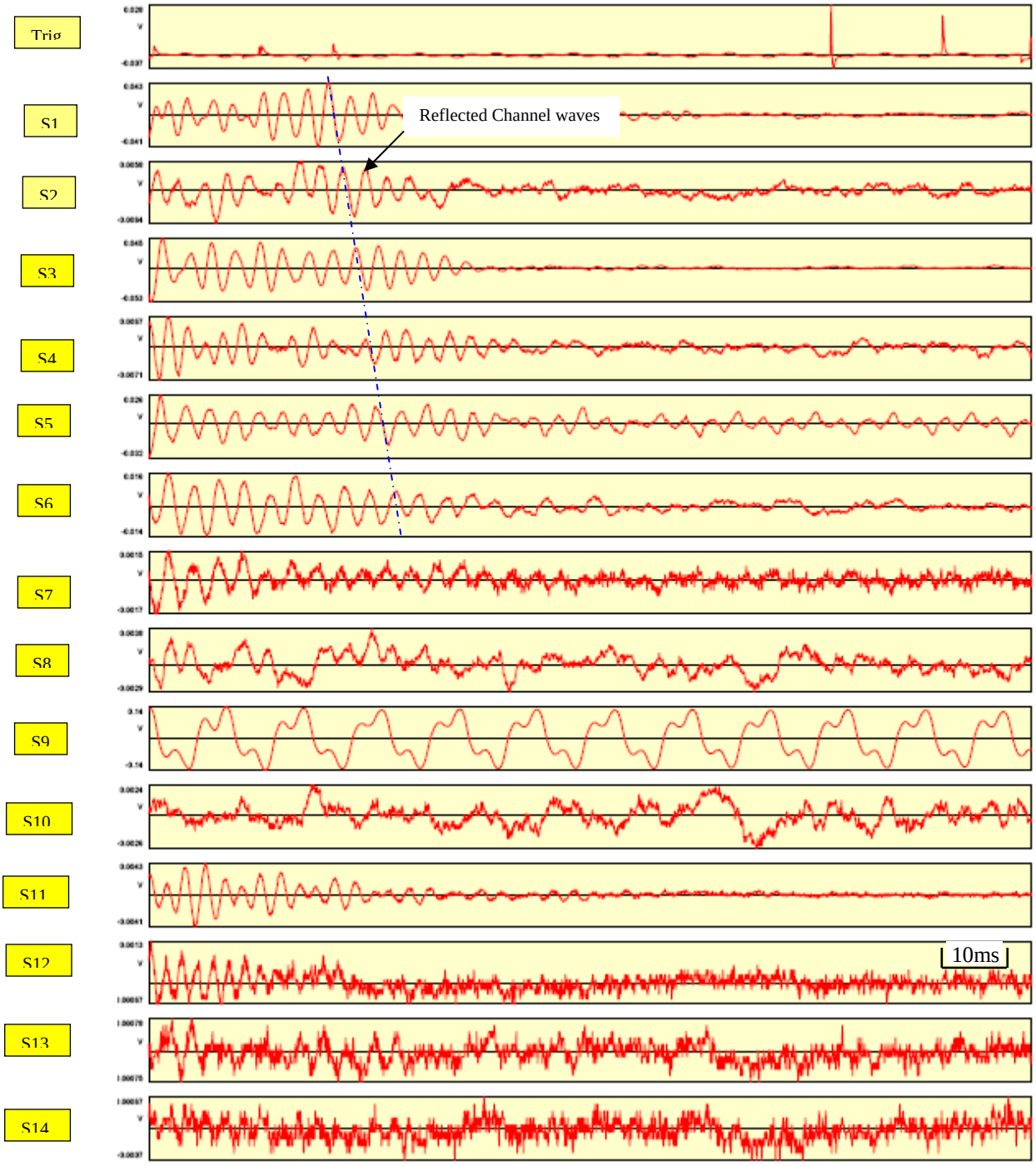

Figure 2.17 A close-up view of Love waves associated with event 110 (display window: 196-342ms).

2.5 Void mapping

The elliptical method was used to map the void location and the results are presented in Figures 2.18 and 2.19. The plot in Figure 2.18 was based on four arrival time information from event 110 and Figure 2.19 was based on the arrival time information of 16 reflected Love waves from four events. The pillar boundary is depicted with the red line in the figures. The travel velocity of Love waves used for void mapping is 1692 ft/s. This is the average of the wave velocity obtained from the transmission survey and the wave velocity calculated based on the information of the direct arrived Love waves recorded during the reflection survey. The mapping error as shown by the plot in Figure 2.19 is within ±20 feet.

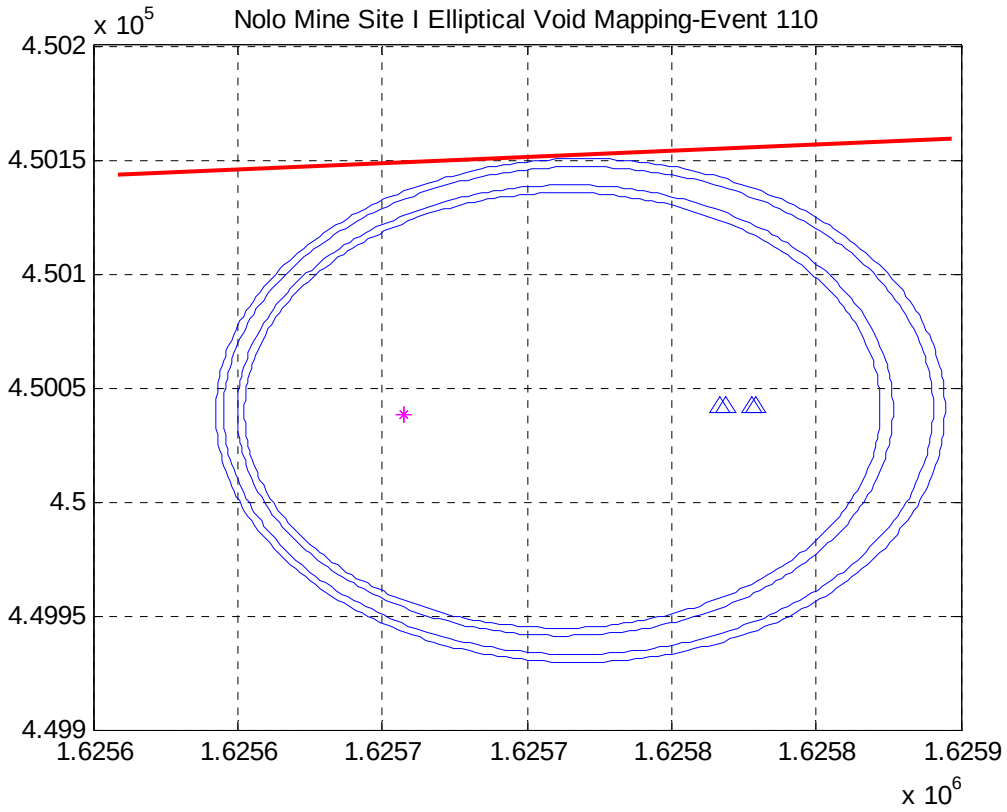

Figure 2.18 "Void" location determined by the elliptical location method using the information from event 110 at Site I, Nolo Mine. Red line denotes the location of the void.

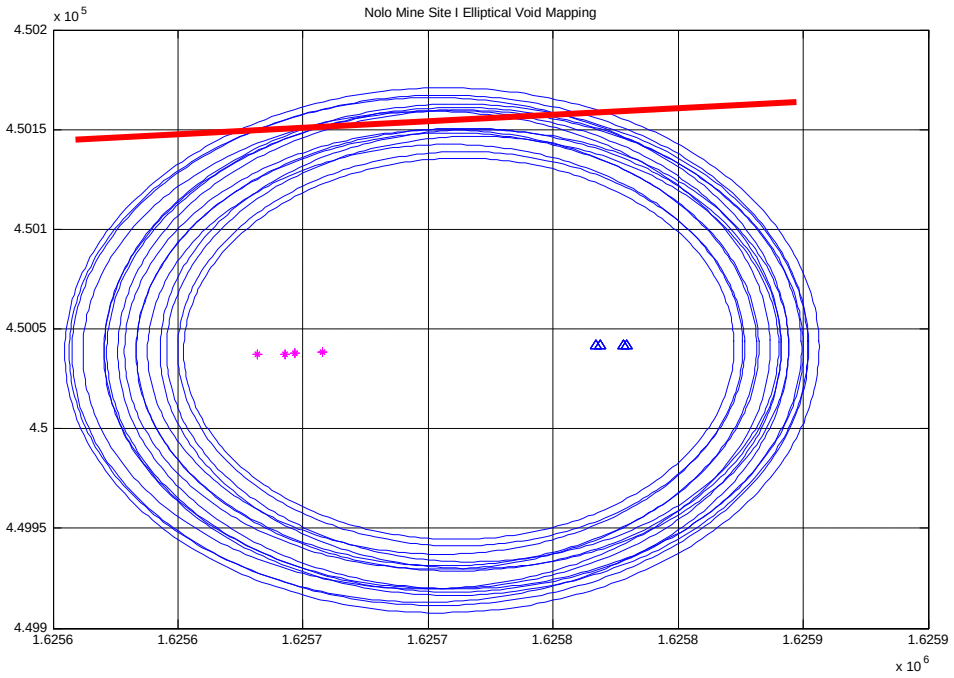

Figure 2.19 "Void" location determined by the elliptical location method at Site I, Nolo Mine. Red line denotes the location of the void.

2.6 Summary of the first test at the Nolo Mine

The test at the Nolo Mine Site I was the first opportunity for Penn State to test the ISS based void detection technique during Phase II of this project. The importance of this test might be viewed from two different perspectives.

First, from the ISS test point of view, the Nolo Mine almost certainly represents one of the most difficult conditions: a very low seam (4 ft at site I), an extremely weak and fragile coal seam, and weak roof and floor strata. The condition encountered at the Nolo Mine is typical for low seam mines in Pennsylvania, West Virginia and Kentucky. Because of the extreme nature of these conditions, the test at the Nolo Mine was considered very important.

Second, the test unequivocally demonstrated the existence of the channel waves in the fragile bituminous coal at this mine and the feasibility to use these waves for void detection. The Love waves at the site have a typical frequency range of 200 – 300 Hz and a traveling velocity of 1690 ft/s.

3. Second Field Test at Nolo Mine

3.1 Introduction

On August 29, 2007, the Penn State project team carried out the second field test on the ISS based void detection technique at the Nolo Mine. This second test involved surveys at Site II. The first test took place on June 23, 2007 at Site I of the mine. This initial test at the Nolo Mine was also the first field test for Phase II. The detection distance for the first test, that is, the pillar width for Site I, is 120 feet.

One of the advantages of using the Nolo Mine for the ISS based void detection test is that it has a number of long pillars and the width of these pillars ranges from 100 to 400 feet. If the ISS test can be carried out progressively with the increased pillar width, then the detection distance can be determined in an objective manner. The knowledge of the effective detection range is critical for reliable use of a void detection technique.

Furthermore, as has been discussed in Chapter 2, the test condition at the Nolo Mine represents one of the most difficult situations. If a detection distance is confirmed at this mine, it may be considered as a benchmark of the detection distance for the technique.

Because of these considerations, it was decided to have the second test at Site II after the first test was successfully completed. The pillar width at Site II is approximately 180 feet, a width that is 50% greater than Site I.

3.2. Testing site and experimental design

Both Site I and Site II are located down the length of a long pillar (Figure 3.1). Site I, which is about 120-feet wide, is on the east section of the pillar. Site II is located at the mid-point of the wide section of the pillar, where the width is approximately 180 feet.

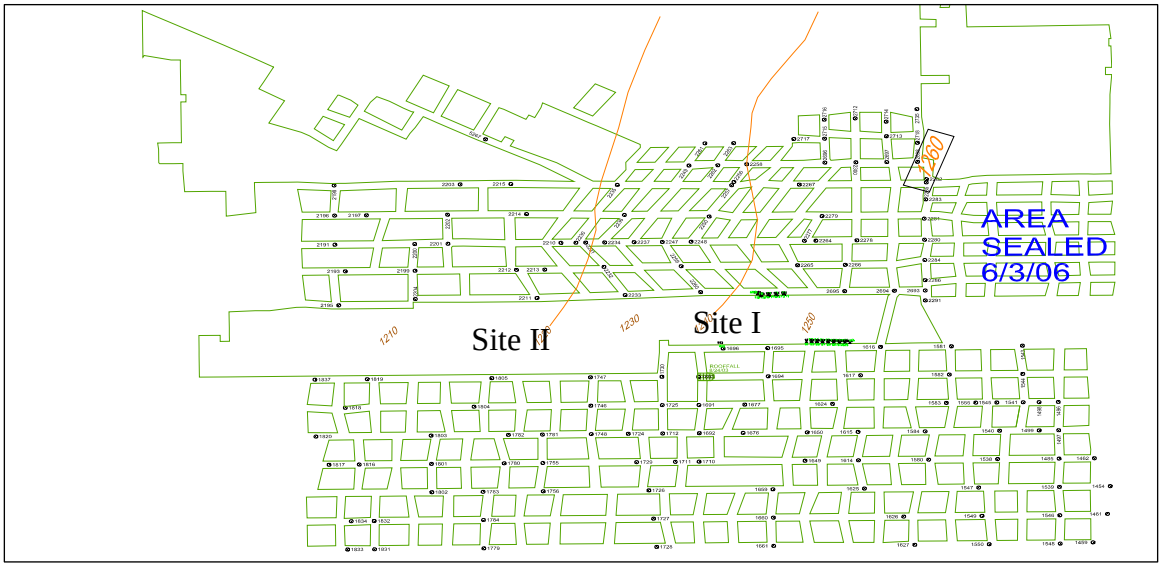

Figure 3.1 Locations of the test sites, Site I and Site II, at the Nolo Mine.

The testing setup for Site II included a sensor section and a blasting section. The general locations of these two sections are shown in Figure 3.2, where the blue and red segments on the lower side of the pillar denote the sensor and blasting sections, respectively. Mark M is a point to illustrate the location of in the middle of the two sections.

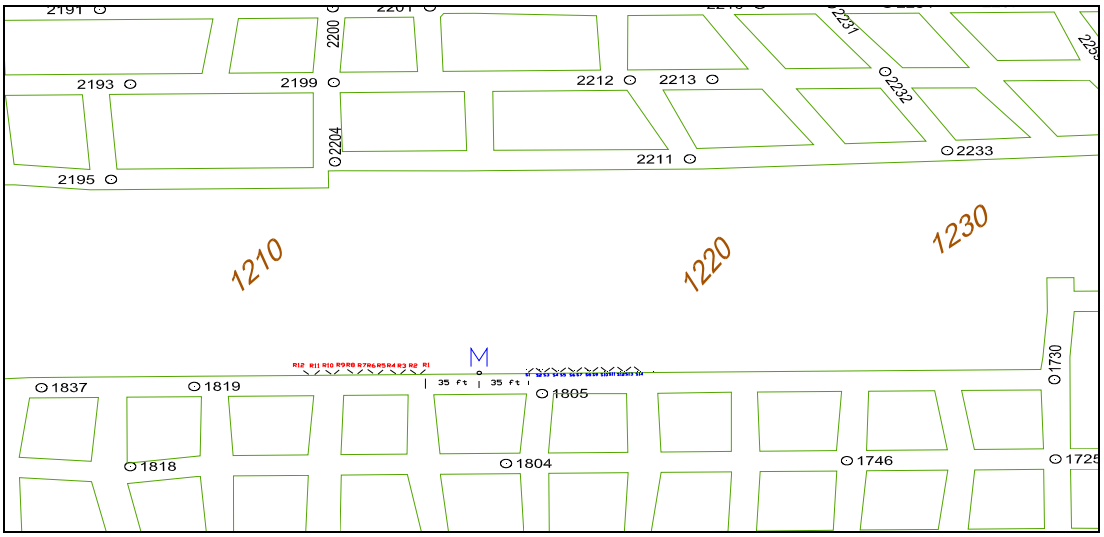

Figure 3.2 An overview of the test setup at Site II. The blue and red segments on the lower side of the pillar denote the sensor and blasting sections, respectively. M is a mark which is located in the middle between the two sections.

3.2.1 Sensor section

The sensor section consists of 14 sensor holes, numbered from S1 to S14. The locations and orientation of these sensor holes are shown in Figure 3.3. These sensor holes are 5-feet deep, drilled in pairs and oriented with a 45° angle in the middle of the coal seam. The diameter of the sensor holes is 1.75 inches. The related information for these sensor holes is summarized in Table 3.1.

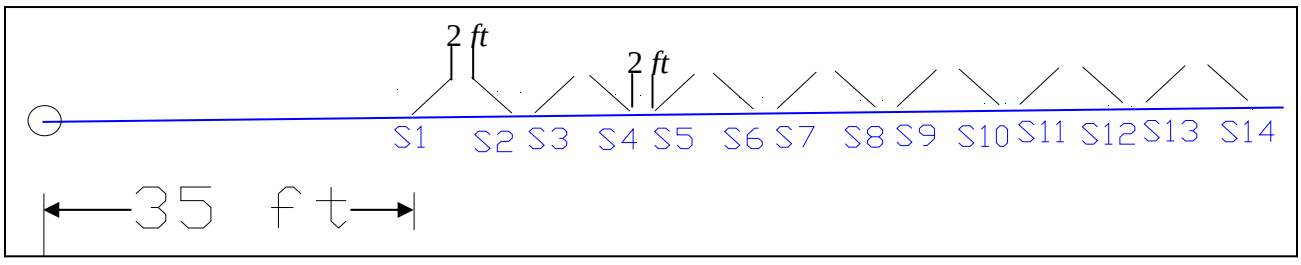

Figure 3.3 Layout of sensor section at Site II, Nolo Mine.

Table 3.1 Sensor hole information for Site I, Nolo Mine.

Hole #	Channel #	Length (ft)	Sensor coordinate (ft)	
			East (X)	North (Y)
S1	2	5	1625138.5	449961.4
S2	3	5	1625140.1	449961.7
S3	4	5	1625149.4	449961.8
S4	5	5	1625151.1	449961.9
S5	7	5	1625160.3	449961.9
S6	8	5	1625162.2	449962.0
S7	9	5	1625171.5	449962.1
S8	10	5	1625173.2	449962.1
S9	11	5	1625182.7	449962.2
S10	12	5	1625184.0	449962.2
S11	13	5	1625193.5	449962.3
S12	14	5	1625195.1	449962.3
S13	15	5	1625204.4	449962.4
S14	16	5	1625206.2	449962.4

Two types of sensors, the accelerometer and the geophone, were installed into the sensor holes. Accelerometers were placed in the first ten holes, S1 - S10, and geophones were placed in the remaining four holes, S11-S14.

3.2.2 Blasting section for reflection survey

A total of 12 blasting holes, numbered from R1 to R12, were prepared for reflection surveys, as shown in Figure 3.4. The dimensions of these holes were 5-ft deep and 1.75 inches in diameter. The coordinates of the drill holes are listed in Table 3.2.

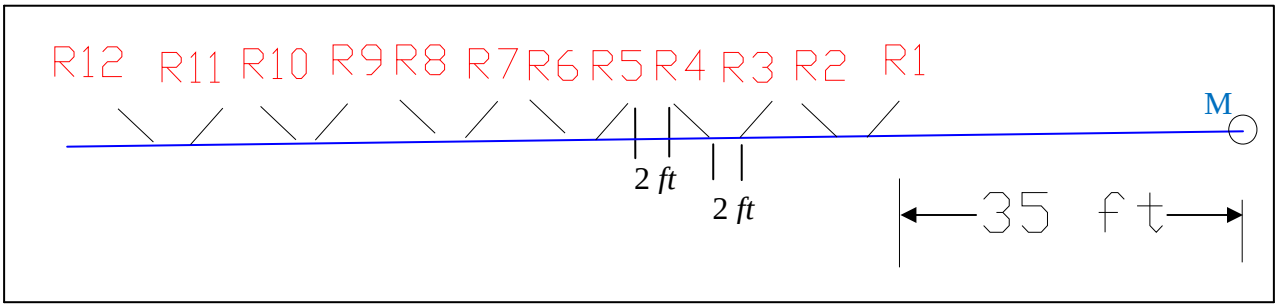

Figure 3.4 Blasting section for reflection survey at Site II, Nolo Mine.

Table 3.2 Coordinates of blasting holes for reflection survey at Site II, Nolo Mine

Hole #	Source coordinate (ft)	
	East (X)	North (Y)
R1	1625000.8	449961.1
R2	1625010.0	449961.4
R3	1625011.9	449961.4
R4	1625021.2	449961.7
R5	1625023.0	449961.7
R6	1625032.1	449962.0
R7	1625034.1	449962.1
R8	1625043.3	449962.3
R9	1625045.1	449962.4
R10	1625054.4	449962.7
R11	1625056.2	449962.7
R12	1625065.0	449963.0

3.3 Reflection surveys at Site II, Nolo Mine

A total of 12 reflection surveys (blasting events) were carried out at Site II in the Nolo Mine. The layout of the testing setup for reflection surveys is illustrated in Figure 3.5. The seismic source for these surveys ranges from 60 to 80-gram dynamite and the event information is summarized in Table 3.3. The surveys resulted in a successful demonstration of the observation and use of reflected Love waves for the detection of voids. In the following discussion, Event 63 is selected to demonstrate this conclusion.

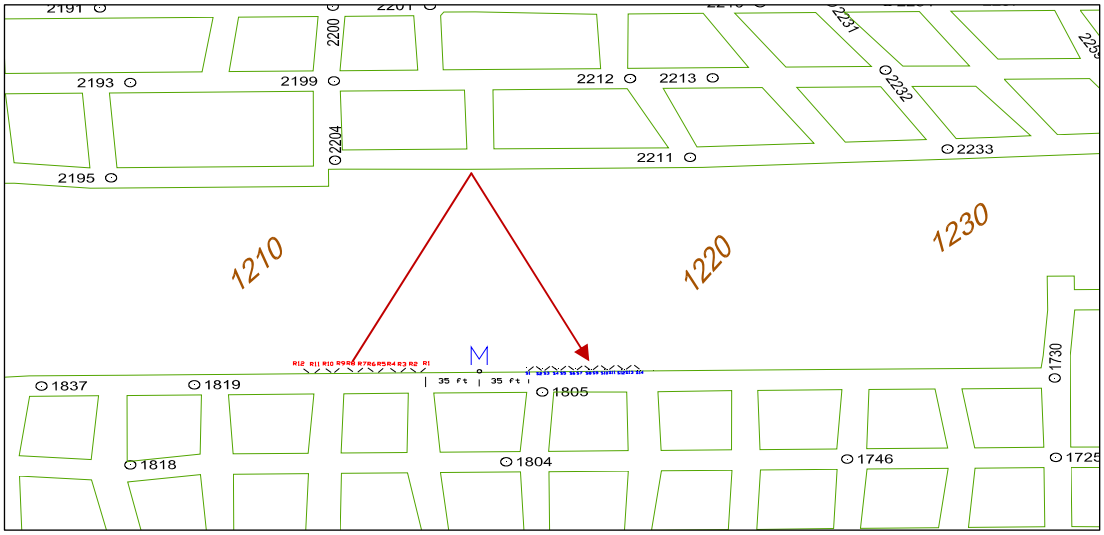

Figure 3.5 Testing setup for reflection surveys at Site II in the Nolo Mine.

Table 3.3 A summary of the reflection surveys at Site II in the Nolo Mine.

Hole #	Explosive (gram)	Event
R1	70	63
R2	70	61
R3	80	59
R4	80	54
R5	80	51
R6	80	48
R7	80	46
R8	80	41
R9	70	38
R10	60	35
R11	80	31
R12	80	29

Event 63 refers to the reflection survey with the seismic source at R1. The layout for this survey, including the locations of R1, the sensors, and the associated ray paths, is illustrated in Figure 3.6. The recorded event is presented in Figures 3.7 and 3.8. A magnified view of the reflected Love waves is provided in Figure 3.8. The arrival readings for the reflected Love waves are listed in Table 3.4.

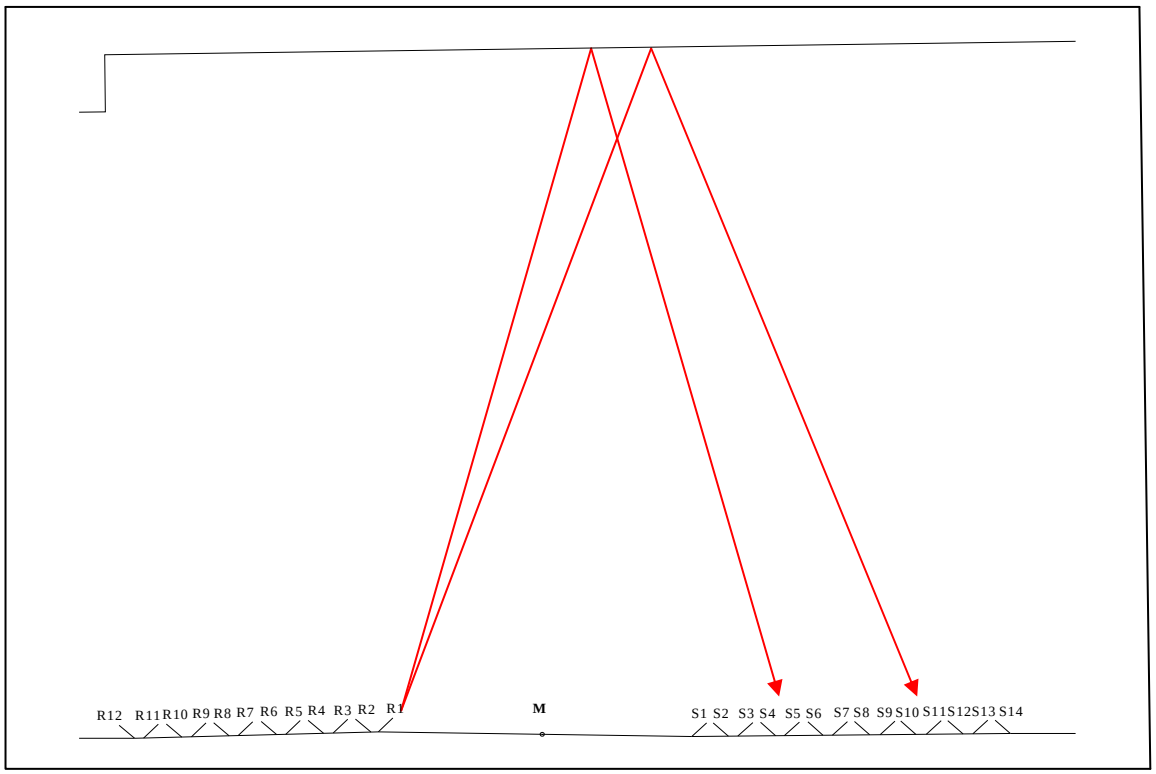

Figure 3.6 Testing setup for event 63.

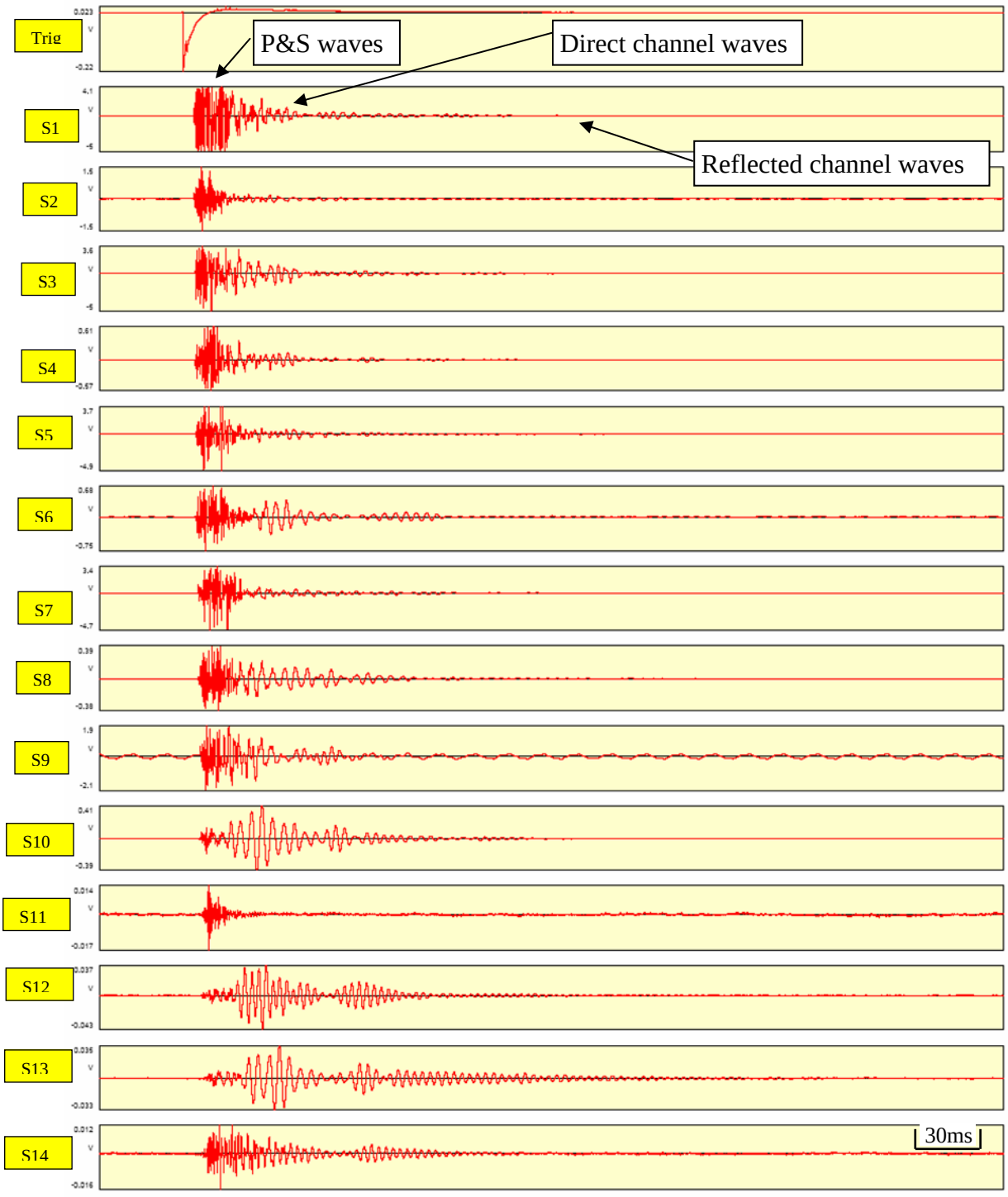

Figure 3.7 Signal waveform for event 63 (displaying window: 60-500 ms).

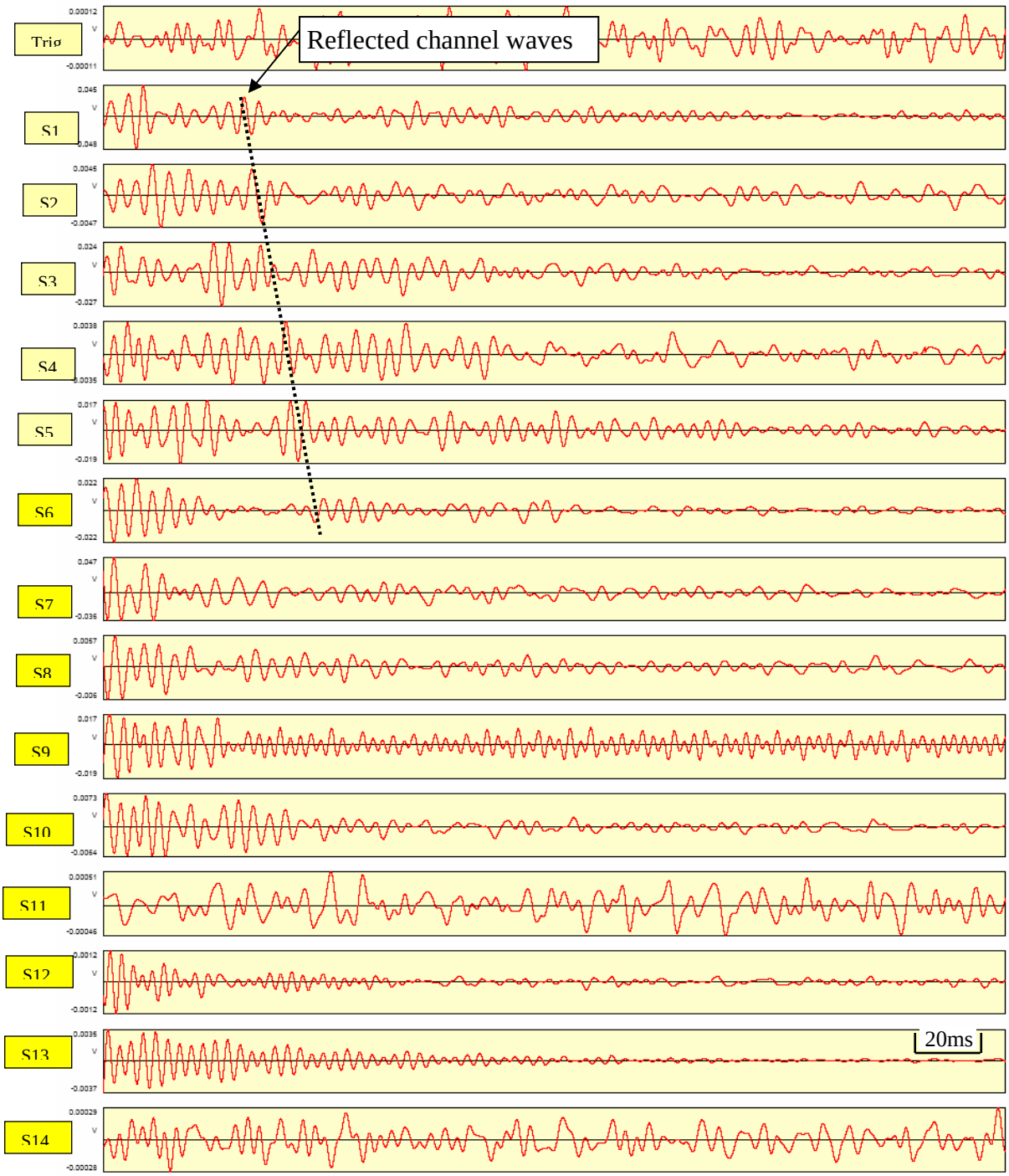

Figure 3.8 Signal waveform for event 63 (display window: 270-560 ms).

Table 3.4 Arrival time readings for the reflected Love waves for event 63.

Triggering time (ms)	S1	S2	S3	S4	S5	S6
101.2	316.8	319.6	322.3	330.4	331.5	337

3.4 Void mapping

The elliptical method was used to map the void location. Figure 3.9 shows the void location by using the information from event 63 only. The plot in Figure 10 was made based on the arrival time information from 16 reflected Love waves. The pillar boundary in these figures is depicted with the red line. The travel velocity of Love waves used for void mapping is 1642 ft/s. This is the average of the wave velocity obtained from the transmission survey and the wave velocity calculated based on the information of the direct arrived Love waves recorded during the reflection survey. The mapping error as shown by the plot in Figure 3.10 is within ±20 feet.

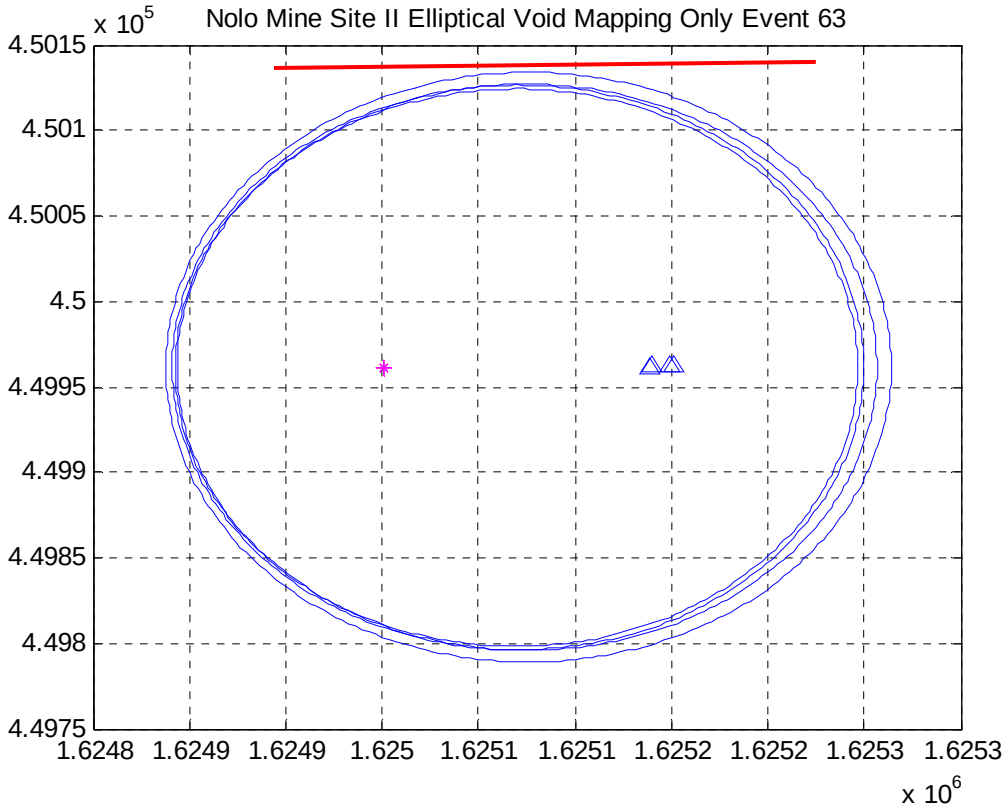

Figure 3.9 "Void" location determined by using the information of event 63 only at Site II, Nolo Mine. Red line denotes the location of the void.

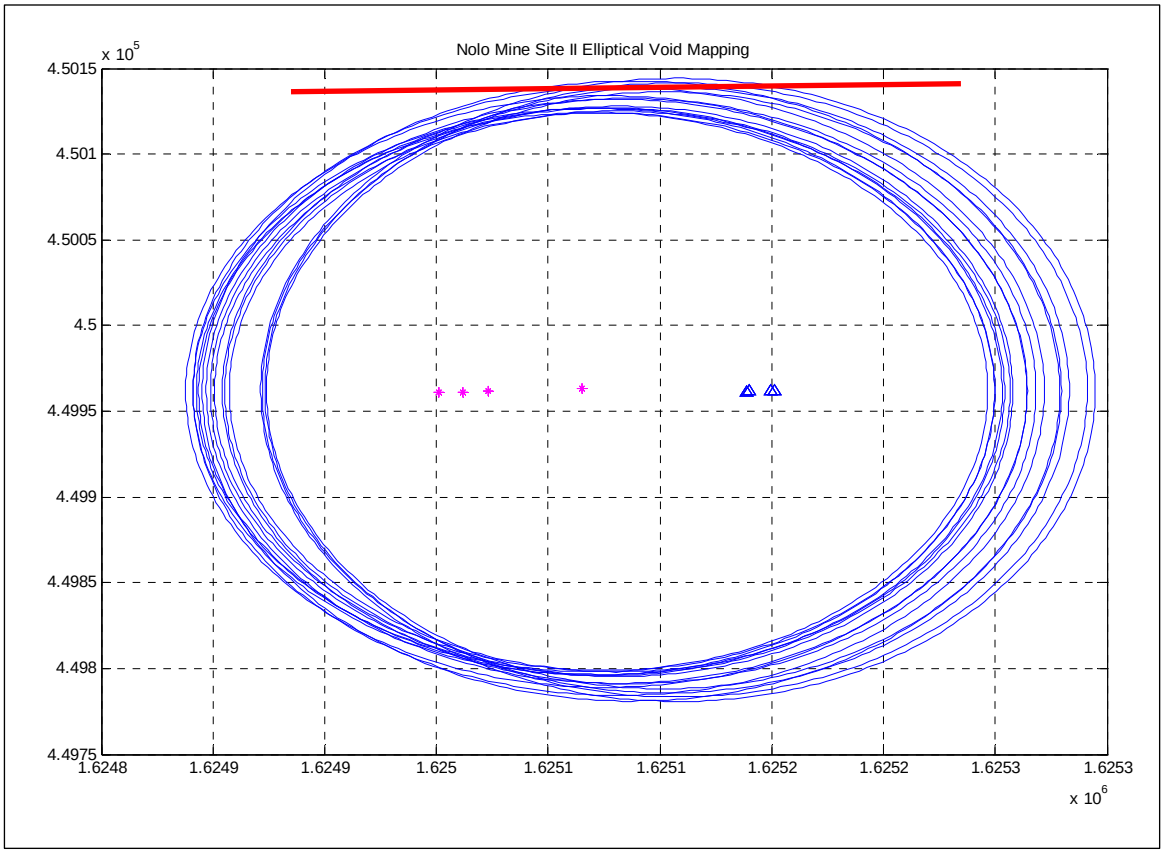

Figure 3.10 “Void” location determined by the elliptical location method at Site I, Nolo Mine. Red line denotes the location of the void.

3.5 Summary of the second test at the Nolo Mine

The reflected Love waves were consistently observed from the reflection surveys carried out at Site II of the Nolo Mine and were used for void mapping. The mapping error is estimated within ±20 feet based on the visual inspection of the plot.

4. Field Test at the Black King Mine

4.1 Introduction

On May 10, 2008, the Penn State project team carried out a field test of the ISS based void detection technique at the Black King Mine. The main objectives of this test were to investigate the characteristics of Love waves associated with an extremely thin bituminous seam (36 inches) and to determine the effectiveness of the ISS based void detection technique under these conditions.

Black King Mine

The Black King Mine is a small bituminous mine located in Sylvester, West Virginia (Figure 4.1). It is owned by a subsidiary of Massey Energy, the Elk Run Coal Co. The thin coal seam recovered by the Black King Mine is known as the Lower Cedar Grove, which measures 36 inches in thickness. Both the roof and the floor at the test site are sandstone. The overburden at the test site is approximately 700 feet.

Figure 4.1 Geographic location of Black King Mine

4.2 Testing site and experimental design

The testing site at the Black King Mine is a long pillar, approximately 100 ft wide (Figure 4.2). The site was utilized for both transmission and reflection surveys.

The general layout of the test setup is illustrated in Figure 4.2. The layout consists of four sections: a sensor section for reflection surveys, a blasting section for reflection surveys, a sensor section for transmission surveys, and a blasting section for transmission surveys.

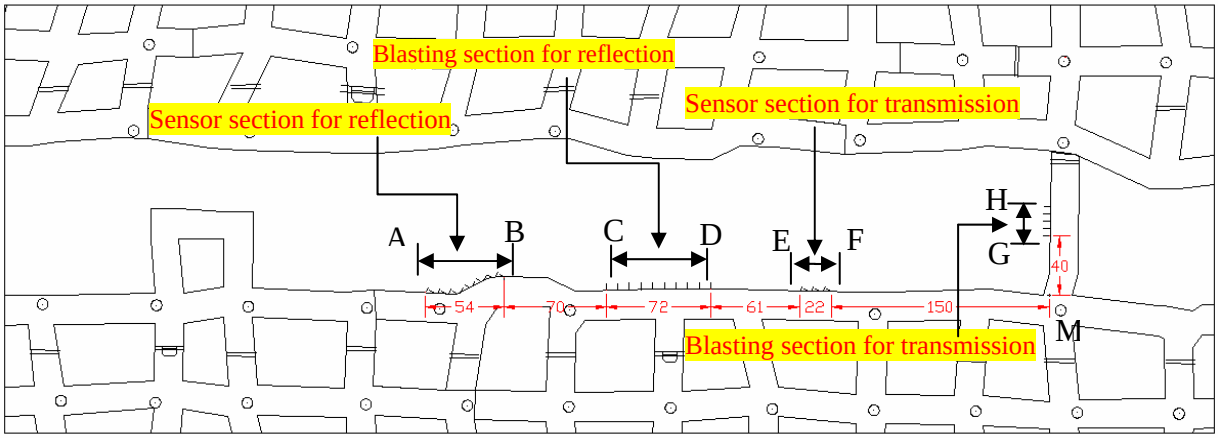

Figure 4.2 An overview of the test site at the Black King Mine.

4.2.1 Testing site condition

The coal seam recovered at the Black King Mine is known as the Lower Cedar Grove, which is only 36-inch thick at the site. From a perspective of underground mining, a coal seam of 36 inches is considered extremely thin. A thin coal seam presents a challenging condition for the ISS technique because the Love wave frequencies expected for this situation are high. The use of the Black King Mine as a test site is to examine the effectiveness of the ISS technique under this extreme condition.

Another difficult condition for the ISS technique is an irregular rib surface, such as the one shown in Figure 4.3, which is caused by the mining practice at the Black King Mine. In order to minimize the impact of this condition, the author carefully inspected the reflection side of the pillar during his site selection trip and located a section which was not as rugged as the one shown in Figure 4.3. The locations of the sensor section and the blasting section for the reflection survey were positioned to use this less rugged section as the reflector.

The advantages of this test site include a good strength for coal and an excellent roof/floor condition. The Lower Cedar Grove seam is considerably stronger than the Lower Kittanning seam mined by the Nolo Mine. Furthermore, both the roof and floor at the test site are sandstone. The roof condition is excellent at the site. These factors contribute positively towards the development and propagation of in-seam Love waves.

Figure 4.3 Rugged rib condition created by the local mining practice.

4.2.2 Testing setup for transmission surveys

The testing setup for transmission surveys at the Black King Mine was somewhat different from the one used at the Nolo Mine. Because the entry on the opposite side of the pillar was the return air passage and blasting was not allowed, the blasting section for transmission surveys had to be placed in the crosscut and a sensor section marked by EF had to be added for this purpose.

Blasting Section for Transmission Surveys

The blasting section for transmission surveys was located a distance of 40 feet from the corner of the crosscut (Figure 4.4). A total of 6 blasting holes were drilled at the coordinates listed in Table 4.1. The dimensions of the holes were 4-ft deep and 1.75 inches in diameter.

Sensor Section for transmission surveys

The sensor section for transmission surveys consisted of 6 sensor holes, which was located a distance of 150 ft away from the corner of the crosscut (Figure 4.5). The sensor holes were arranged in pairs and were drilled at the coordinates listed in Table 4.2. The dimensions of the holes were 4-ft deep and 1.75 inches in diameter.

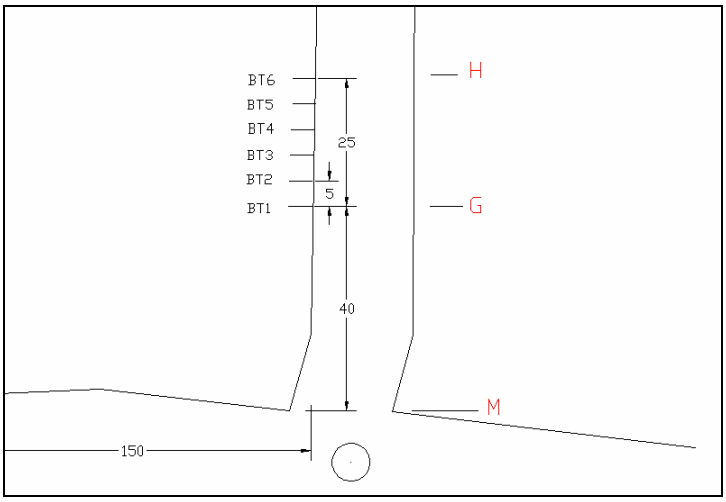

Figure 4.4 The layout of the blasting holes used for transmission surveys.

Table 4.1 Coordinates of blasting holes for transmission surveys

Hole #	Coordinates (feet)	
	x	y
BT6	1157.7	288.2
BT5	1157.7	283.2
BT4	1157.6	278.2

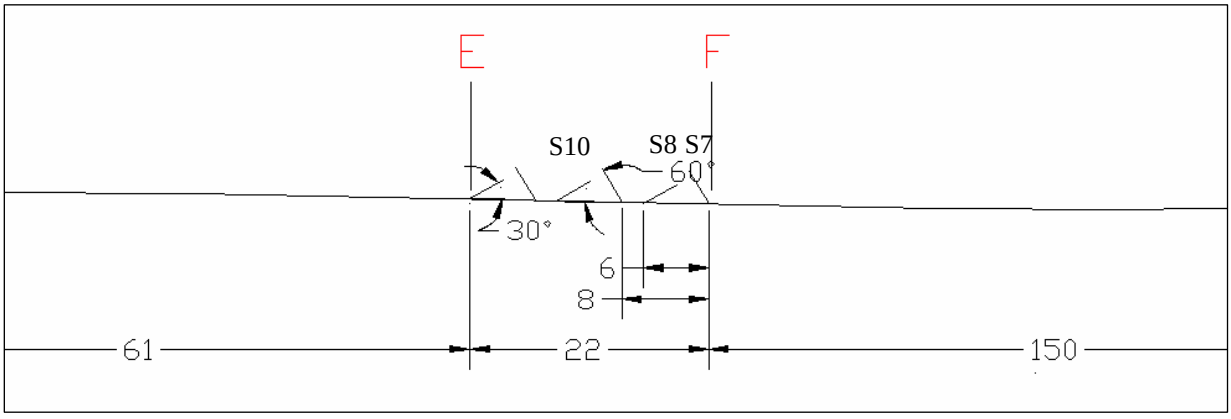

Figure 4.5 Layout of the sensor holes for transmission surveys.

Table 4.2 Coordinates of sensor holes for transmission surveys

Hole #	Coordinates (feet)	
	x	y
S7	1007.3	227.8
S8	1006.2	229.2
S10	998.2	229.2

4.2.3 Testing setup for the reflection surveys

The testing setup for the reflection surveys included a sensor section and a blasting section, located a distance of 70 feet apart from each other. The general placement of these two sections has been presented in Figure 4.2.

Sensor Section for reflection surveys

The sensor section consisted of 14 sensor holes arranged in pairs as shown in Figure 4.6. The dimensions of these holes were 4-ft deep and 1.75 inches in diameter. Both accelerometers and geophones were utilized for these surveys. Accelerometers were installed in the first ten sensor holes and geophones were installed in the last four sensor holes. The coordinates of these sensor holes are given in Table 4.3.

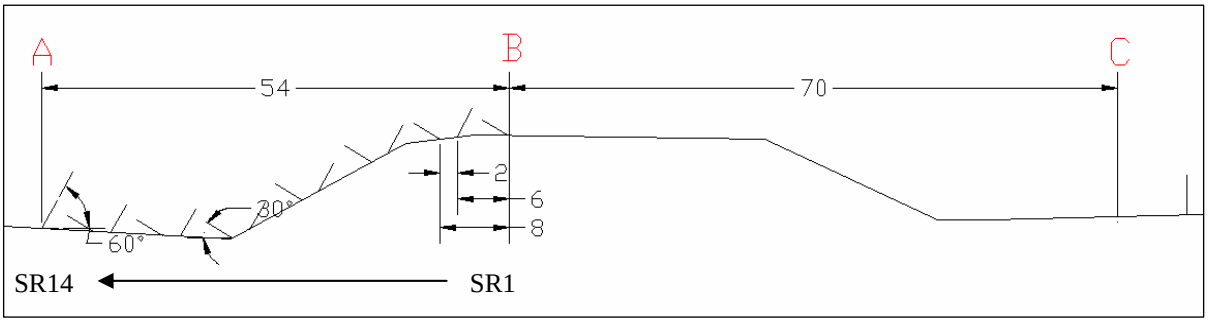

Figure 4.6 Layout of the sensor holes for reflection surveys.

Table 4.3 Coordinates of sensor holes for reflection surveys

Sensor hole #	Coordinates (feet)	
	x	y
SR1	782.0	237.3
SR2	780.8	238.6
SR3	774.0	237.0
SR4	772.8	236.8
SR5	766.0	234.4
SR6	764.8	232.4
SR7	758.0	230.2
SR8	756.8	228.0
SR9	750.0	225.8
SR10	748.8	227.3
SR11	742.0	226.1
SR12	740.8	227.8
SR13	734.0	226.5
SR14	733.0	228.2

Blasting Section for Reflection Surveys

The blasting section for reflection surveys consisted of 10 blasting holes (Figure 4.7), which were drilled at the coordinates listed in Table 4.4. The dimensions of these holes were 4-ft deep and 1.75 inches in diameter.

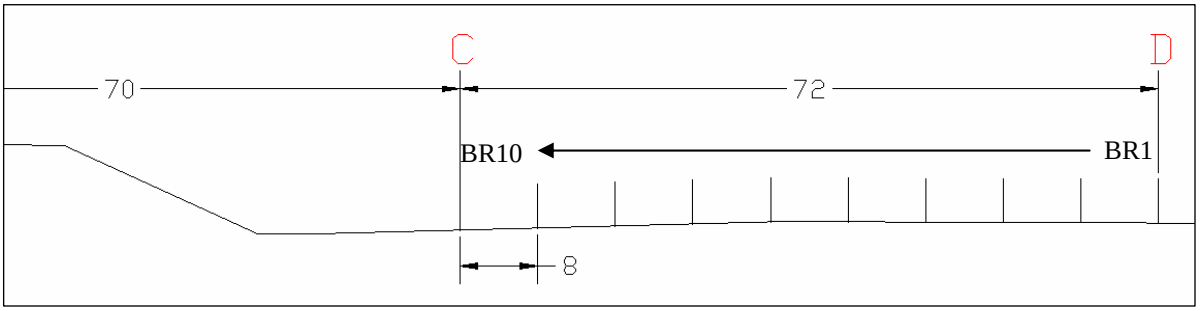

Figure 4.7 The layout of the blasting holes used for reflection surveys.

Table 4.4 Coordinates of blasting holes for reflection surveys

Blasting hole #	Coordinates (feet)	
	x	y
BR1	927.3	231.7
BR2	919.3	231.7
BR3	911.3	231.7
BR4	903.3	231.8
BR5	895.3	231.8
BR6	887.3	231.8
BR7	879.3	231.6
BR8	871.3	231.4
BR9	863.3	231.2
BR10	855.3	230.9

4.3 Transmission surveys

Three transmission surveys were performed at the Black King Mine. The seismic sources for the surveys were 38 and 50 grams of dynamite detonated at the boreholes of BT6, BT5 and BT4. Table 4.5 lists the related information for these survey events. The ray paths associated with these surveys are illustrated in Figure 4.8. The travel distances for these ray paths range from 159 to 170 feet with an average path distance of 164 feet (Table 4.6).

Table 4.5 A summary of the transmission survey sources

Hole #	Explosive (gram.)	Event #
BT6	50	1275
BT5	38	1276
BT4	38	1277

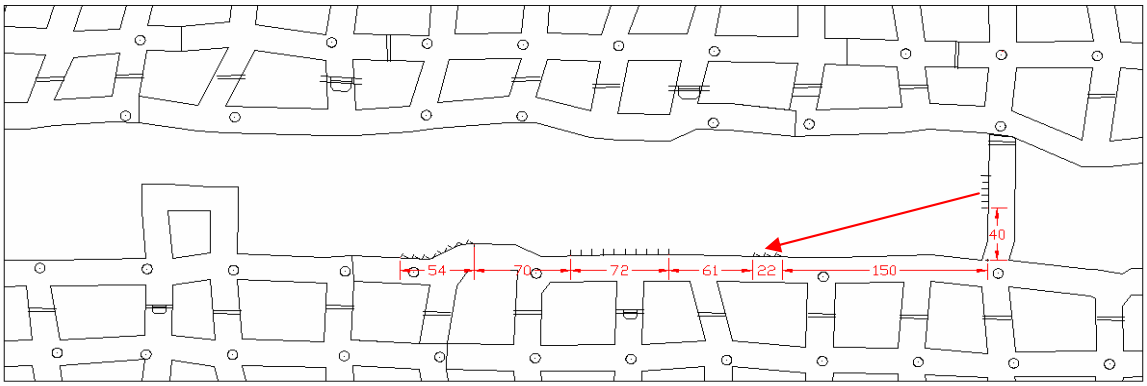

Figure 4.8 Ray paths associated with the transmission survey at Black King.

Table 4.6 Ray path distances for transmission surveys (feet)

Blasting hole #	Sensor #		
	S7	S8	S10
BT6	162.1	162.5	170.0
BT5	160.2	160.8	168.2
BT4	158.5	159.1	166.6
Average	160.3	160.8	168.3

The seismic signals recorded during the transmission surveys are of very good quality as demonstrated in Figures 4.9 - 4.11. Figure 4.9 shows the originally recorded data for event 1277. In addition to the well defined signal profile, it is noted that the arrivals of in-seam Love waves are clear. Event 1277 was originated at borehole BT4 with a seismic source of 38-gram dynamite. The layout for this transmission survey is shown in Figure 4.12.

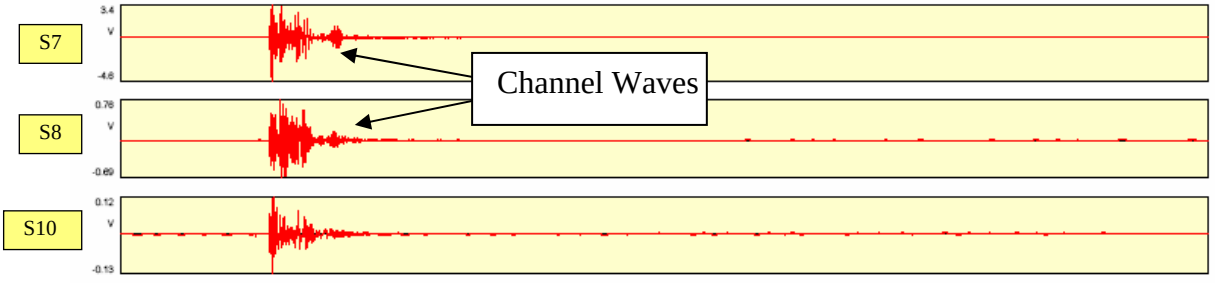

Figure 4.9 Signals originally recorded for a transmission survey (Event 1277) at the Black King Mine (displaying window: 0-800 ms)

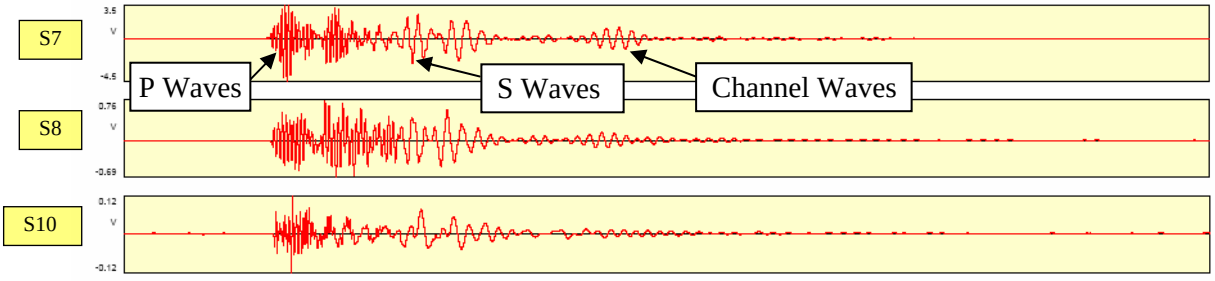

Figure 4.10 Details of P- and S-waves transmitted through the country rock and in-seam Love waves for Event 1277 (displaying window: 90-250 ms).

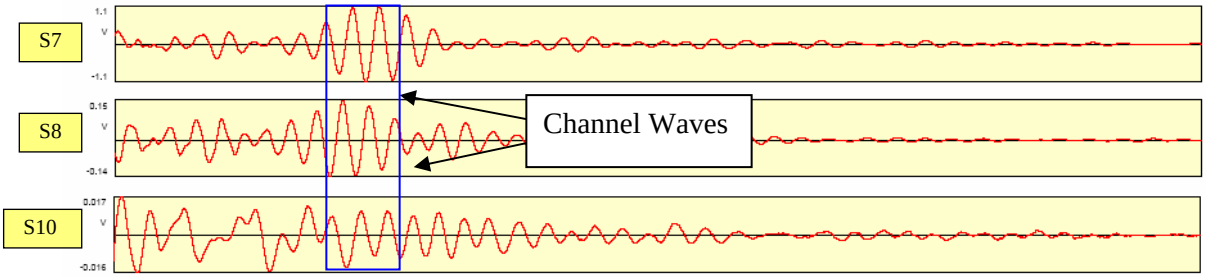

Figure 4.11 In-seam Love waves for Event 1277 (displaying window: 145-220 ms).

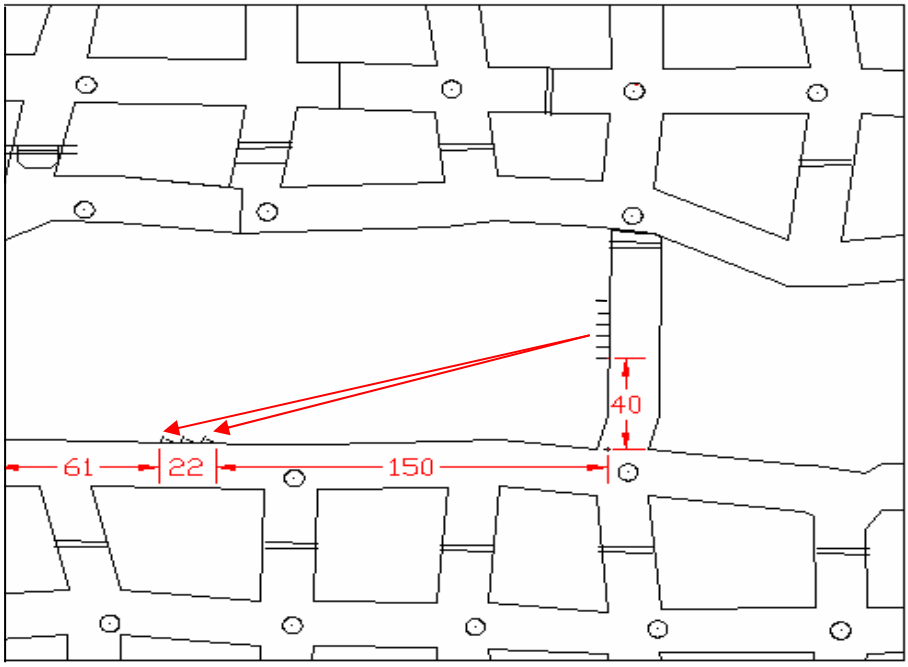

Figure 4.12 Testing setup for Event 1277.

The details of the transmission signal section are shown in figure 4.10. One can observe that all major wave groups, including P- and S-waves transmitted through the country rock and the in-seam Love waves, are well defined. Each group exhibits its own distinctive characteristics.

The dominant frequencies for the P-, S- and Love waves are 2000, 500 and 550 Hz, respectively. As noted earlier, the high frequency for the Love waves was expected due to the thin seam. Figure 4.13 shows the frequency spectra for the signals plotted in Figure 4.9.

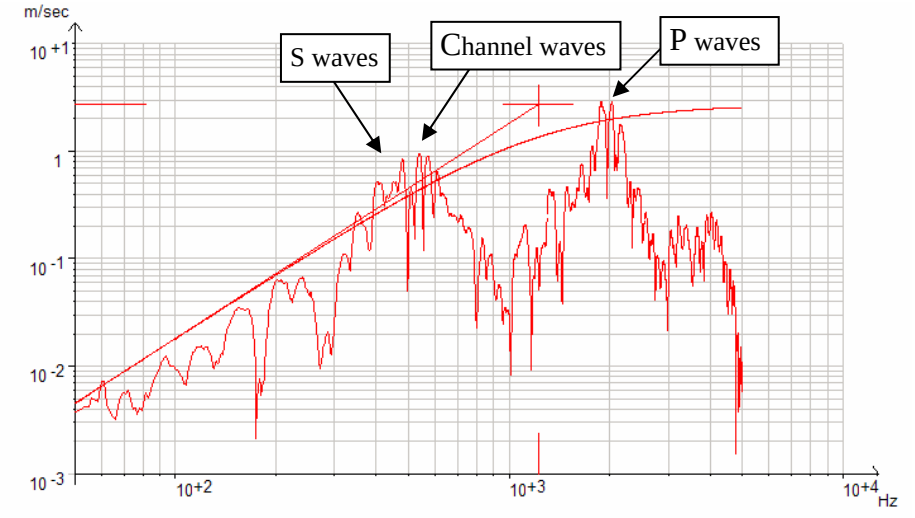

Figure 4.13 Frequency spectrum for signals recorded by sensor S7 shown in Figure 4.9.

The average velocities for these three wave groups are 15684 ft/s, 7862ft/s and 2705 ft/s, respectively. The related data for velocity calculations are presented in Tables 4.7 – 4.10.

Table 4.7 Velocities associated with Black King Mine**.**

Strata	Wave Type	Velocity (ft/s)	Number of measurements	Standard deviation (ft/s)
Coal (bituminous)	Airy Phase	2705	9	82
Roof (sandstone)	P-wave	15684	9	96
	S-wave	9101	9	95

Table 4.8 P-wave velocities determined from transmission surveys (ft/s)

Blasting hole # \ Sensor	S7	S8	S10
BT6	15738	15625	15741
BT5	15553	15612	15574
BT4	15693	15752	15867

Table 4.9 S-wave velocities determined from transmission surveys (ft/s)

Blasting hole # \ Sensor	S7	S8	S10
BT6	9006	8900	9057
BT5	9078	9136	9144
BT4	9189	9191	9204

Table 4.10 Love-wave velocities determined from transmission surveys (ft/s)

Blasting hole # \ Sensor	S7	S8	S10
BT6	2675	2764	2742
BT5	2539	2758	2785
BT4	2594	2715	2777

4.4 Reflection surveys

A total of 10 reflection surveys (blasting events) were executed at the Black King Mine. The layout of the testing setup for reflection surveys is illustrated in Figure 4.14. The seismic source for these surveys ranges from 25 to 50-gram dynamite and the event information is summarized in Table 4.11.

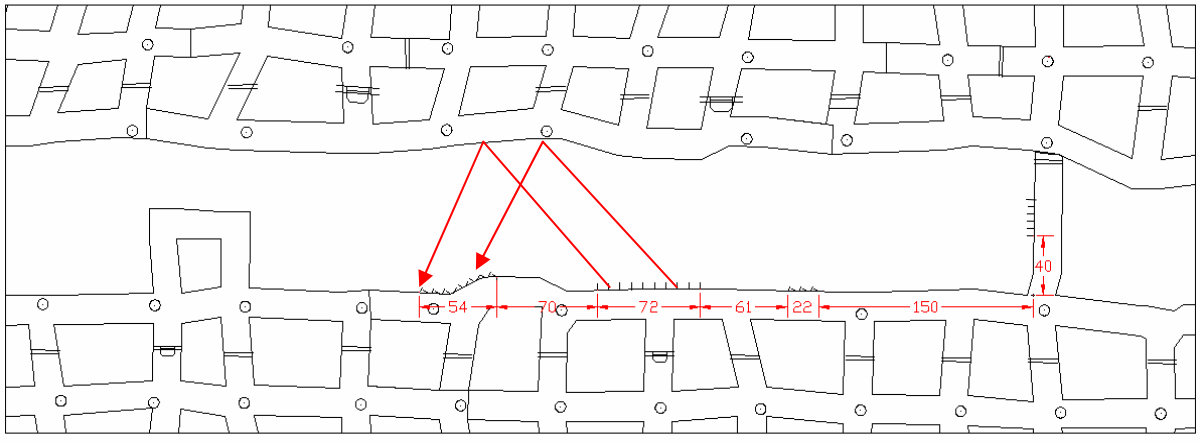

Figure 4.14 Testing setup for reflection surveys at the Black King Mine.

Table 4.11 A summary of the reflection surveys at Black King mine

Hole #	Explosive (gram)	Event
BR1	50	1595
BR2	25	1599
BR3	38	1600
BR4	25	1601
BR5	25	1602
BR6	25	1603
BR7	25	1604
BR8	25	1606
BR9	25	1607
BR10	25	1608

The surveys resulted in a successful demonstration of the observation and use of reflected Love waves for the detection of voids. In the following discussion, event 1600 is selected to demonstrate this conclusion.

Event 1600 was the reflection survey with the seismic source at BR3. The testing layout for this survey, including the locations of BR3 and the sensors, is shown in Figure 4.15. The recorded waveforms for this event are presented in Figure 4.16. An examination of the figure reveals that even the reflected Love waves can be observed directly from some channels.

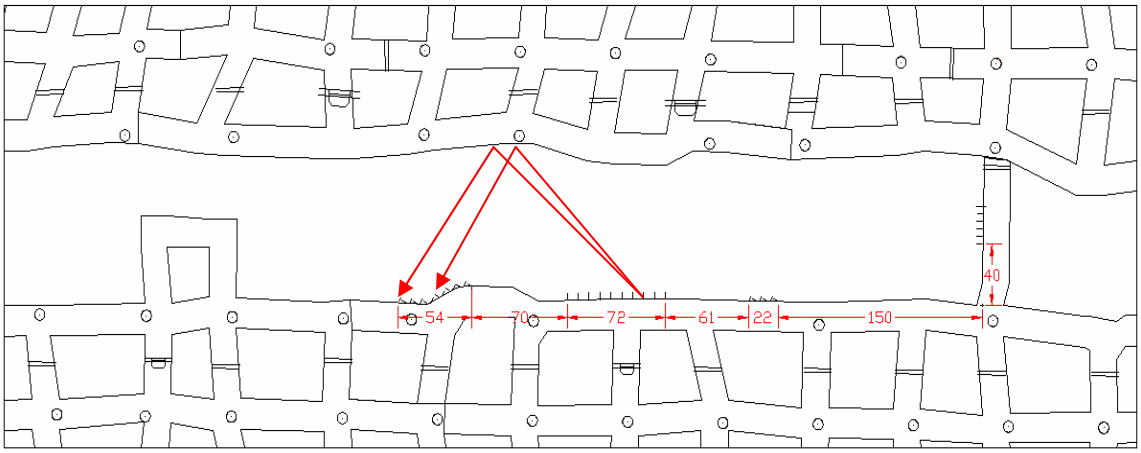

Figure 4.15 Testing setup for event 1600.

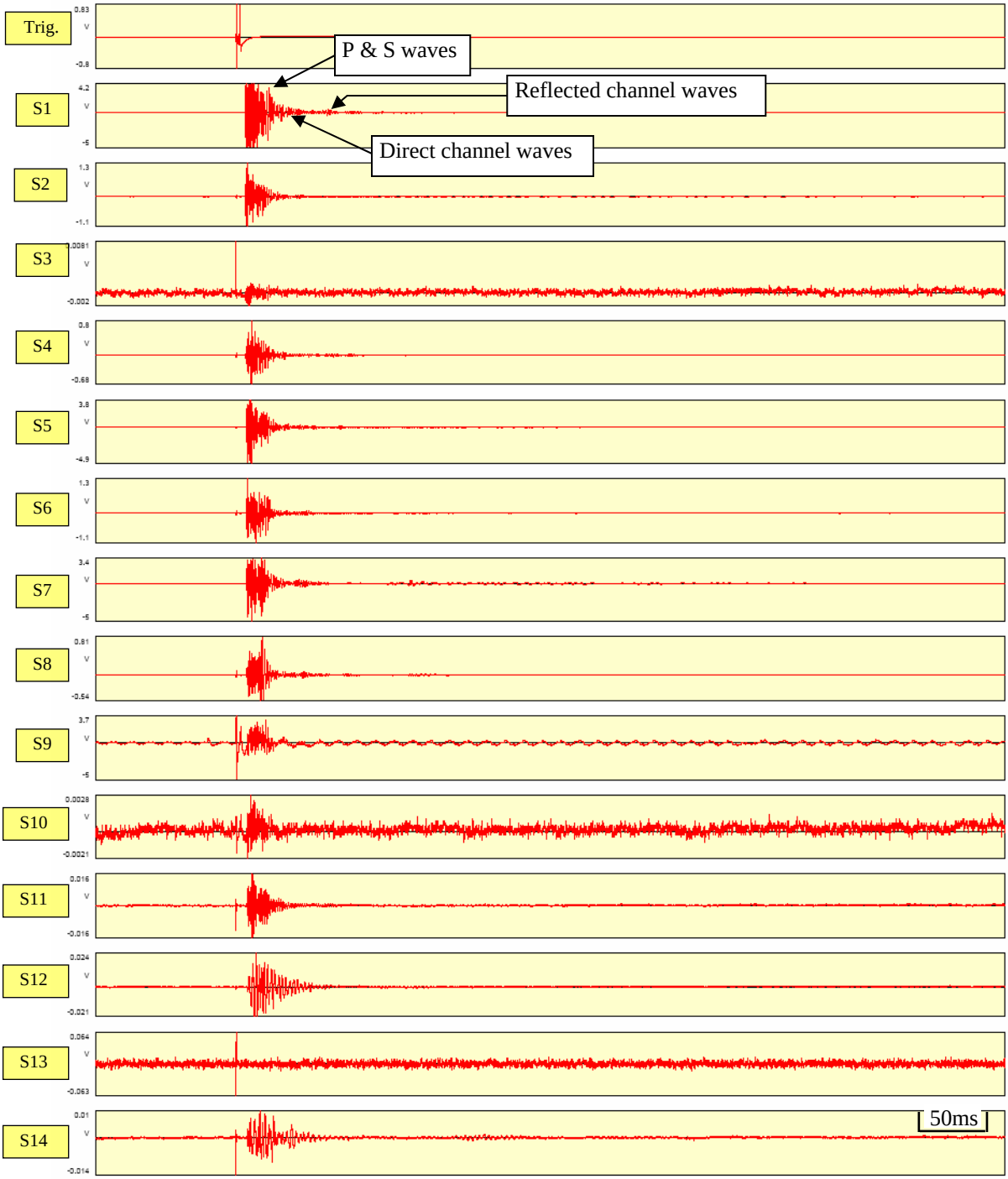

Figure 4.16 Original waveform record for event 1600 (displaying window: 0 – 800 ms)

An enlarged view of the direct arrived Love waves is presented in Figure 4.17 and the corresponding arrival time readings are listed in Table 4.12. Similar data for the reflected Love waves are presented in Figure 4.18 and Table 4.13, respectively.

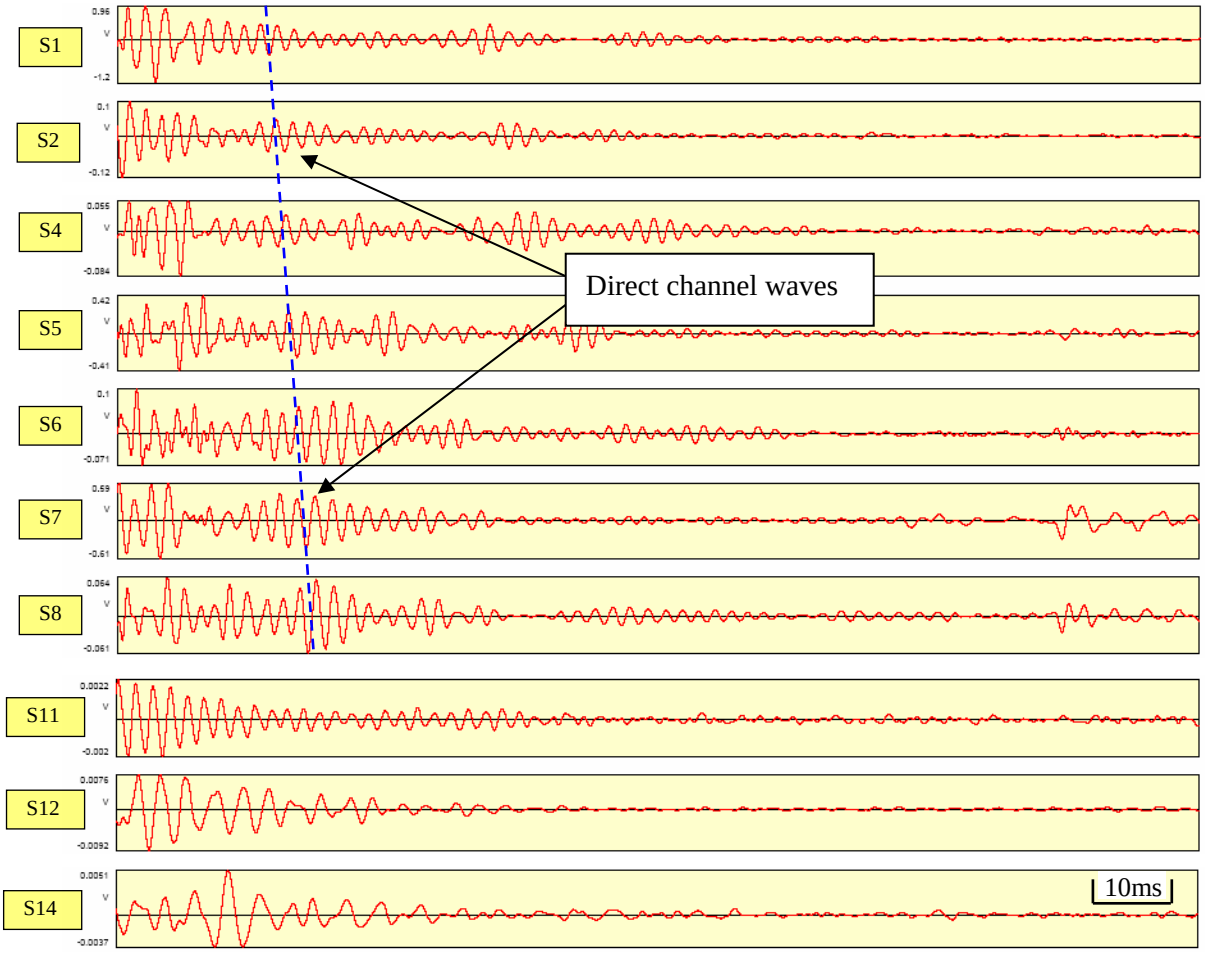

Figure 4.17 A close-up view of the direct arrived Love waves for event 1600 (display window: 162-300 ms).

Table 4.12 Arrival time readings for the direct arrived Love waves for event 1600.

Triggering Time (ms)	Arrival time (Airy Phase) (ms)						
	S1	S2	S4	S5	S6	S7	S8
126.2	173.1	182.9	183	184.5	190.1	183.4	186.9

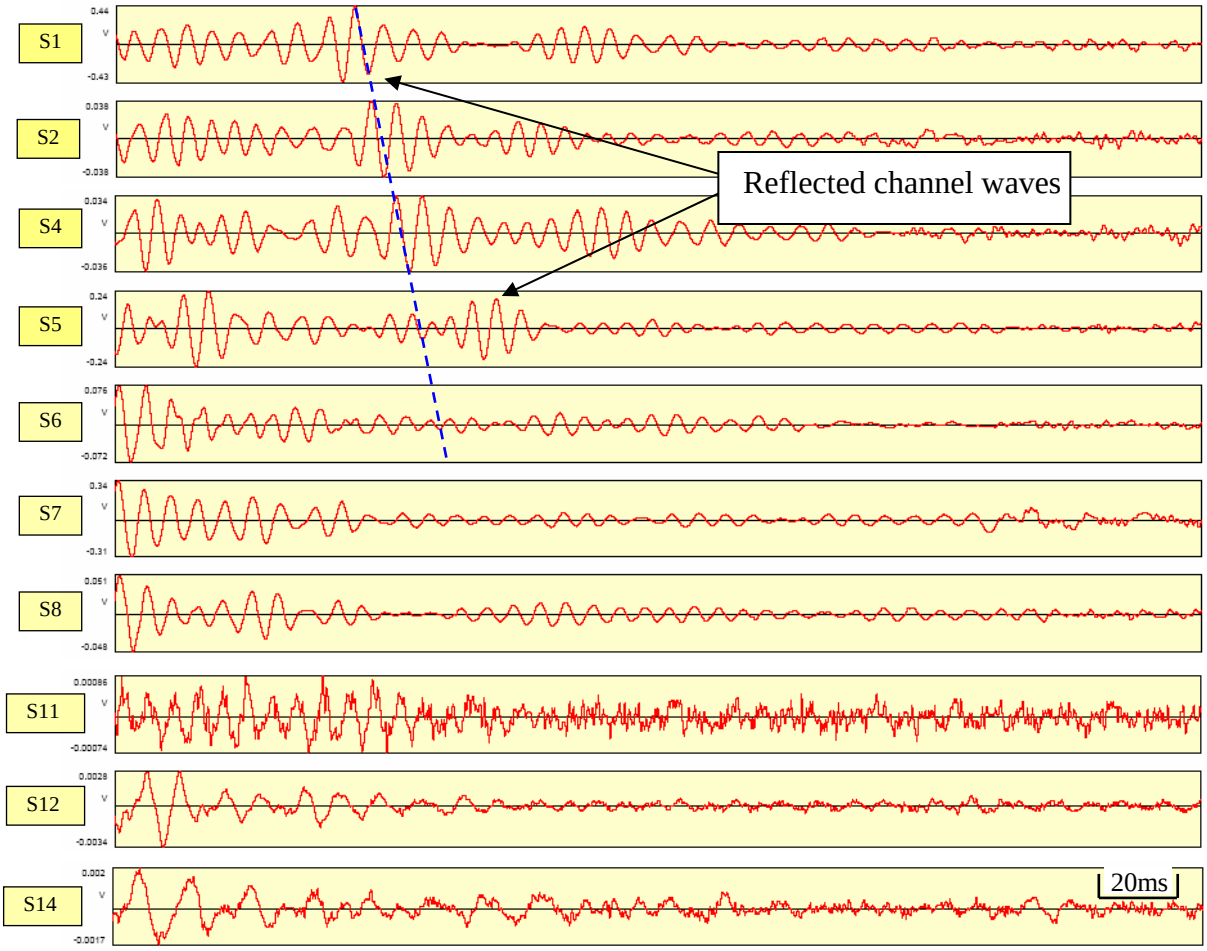

Figure 4.18 A close-up view of the reflected Love waves for event 1600 (display window: 270-560 ms).

Table 4.13 Arrival time readings for the reflected Love waves for event 1600.

Triggering Time (ms)	Arrival time (Airy Phase) (ms)				
	S1	S2	S4	S5	S6
126.2	208.8	211.3	214.5	220.8	226.1

4.5 Void mapping

The elliptical method was used to map the void location. Figure 4.19 shows the void location by using the information from event 1600 only. The plot in Figure 4.20 was made based on the arrival time information from 20 reflected Love waves. The pillar boundary is depicted with the red line. The travel velocity of Love waves used for void mapping is 2639 ft/s. This is the average of the wave velocity obtained from the transmission survey and the wave velocity calculated based on the information of the direct arrived Love waves recorded during the reflection survey. According to the plot, the maximum error is about 30 feet and the average error is about 15 feet.

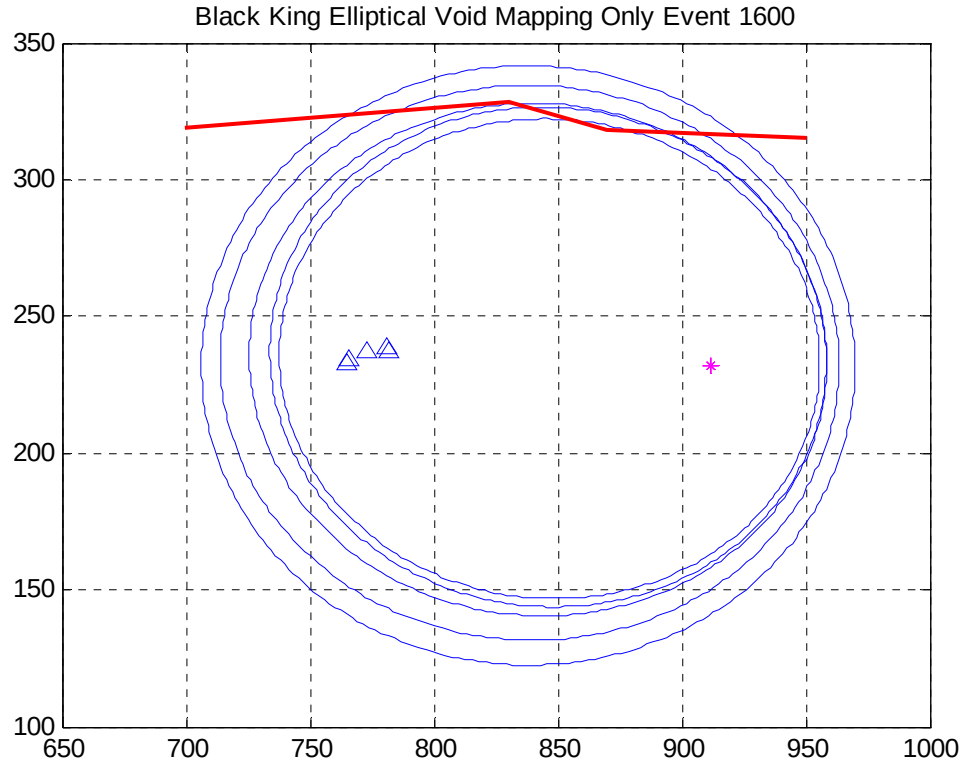

Figure 4.19 “Void” location determined by the elliptical location method using the information of event 1600 only at Black King Mine. Red line denotes the location of the void.

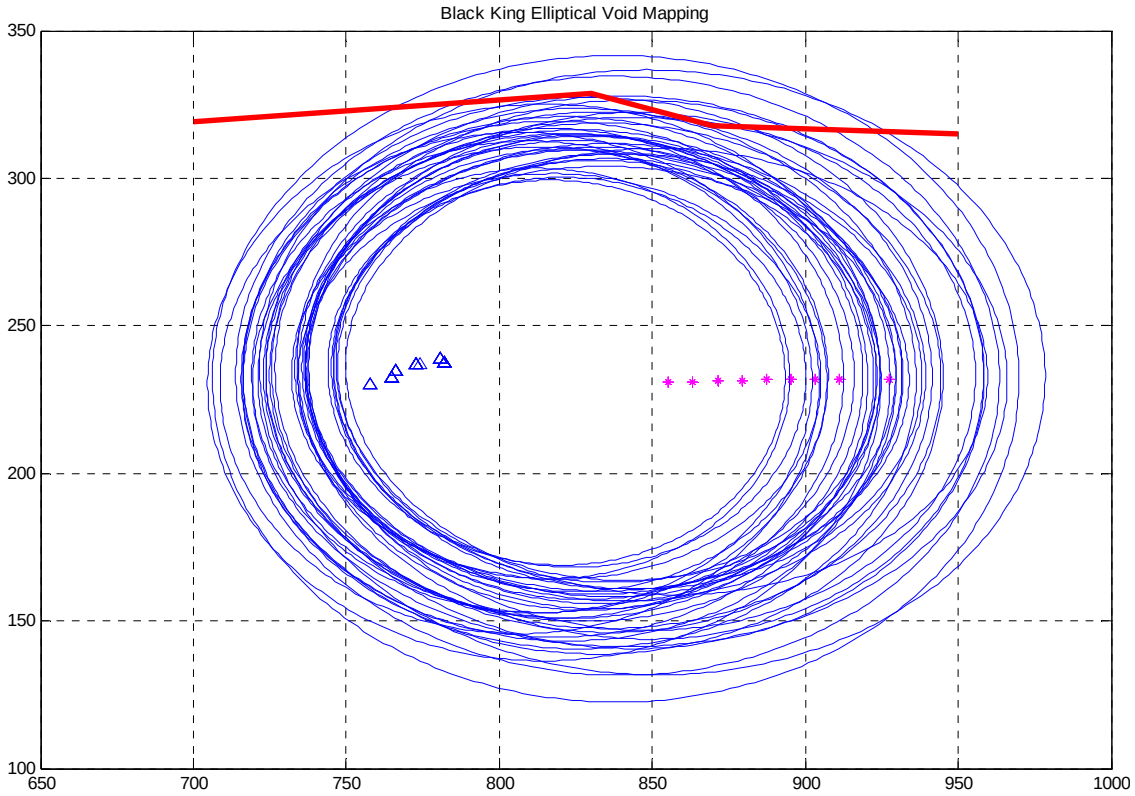

Figure 4.20 “Void” location determined by the elliptical location method at Black King mine. Red line denotes the location of the void.

4.6 Summary of the test result at the Black King Mine

The objectives of the test carried out at the Black King Mine were to investigate the characteristics of Love waves associated with an extremely thin bituminous seam (36 inches) and to determine the effectiveness of the ISS based void detection technique under these conditions.

In addition to the very thin seam, the other difficult condition for the ISS test is the irregular rib surface which is characteristic of the Black King Mine. The favorable conditions for the site are that the coal is relatively strong and the roof and the floor are sandstone, which are positive for the development and propagation of in-seam Love waves. The overburden is approximately 700 ft at the test site. The pillar under testing is 100-ft wide.

Both transmission and reflection tests were performed at the site.

Well developed and defined in-seam Love waves were consistently observed in both transmission and reflection surveys. The dominant frequency (Airy Phase) is 550 Hz with an average velocity of 2099 ft/sec. The in-seam Love waves at the site have a typical frequency of 550 Hz, with a traveling velocity of 2600-2700 ft/s.

The trend of the reflected Love waves is evident. The average mapping error is about 15 feet, with 30 feet being the maximum.

Based on the strength of the reflected signals, we believe that a detection range of 150 feet should be achievable for the ISS based void detection technique under similar physical conditions.

The dominant frequencies for P- and S-waves transmitted in roof/floor are 2000 and 500 Hz, respectively. The average P- and S-wave velocities are 15684 ft/s and 7862 ft/s, respectively.

5. Field Test at the Cumberland Mine

5.1 Introduction

On May 12, 2008, the Penn State project team completed a field test on the ISS based void detection technique at the Cumberland Mine. The purpose of this test was to investigate the effectiveness of the ISS based void detection technique for bituminous mines with a relatively thick seam. The coal recovered by the Cumberland Mine is the Pittsburgh seam, which is 84 inches. The Pittsburgh seam is the best known coal seam in the United States.

Cumberland Mine

The Cumberland Mine, a subdivision of Foundation Coal, is located approximately 12 miles south of Waynesburg, Pennsylvania (Figure 5.1). The mine uses the longwall mining method and produces about 7 million tons annually.

The test site is the barrier pillar for longwall panel 54 (LW 54), which is about 200-ft wide. The seam thickness at the site measures approximately 84 inches (7 feet). Both the roof and floor of the seam are shale with varying strengths. The overburden at the test site is approximately 800 feet and varies throughout the mine from 700 to 800 feet.

Figure 5.1 Geographic location of the Cumberland Mine

5.2 Testing site and experimental design

The test site is the barrier pillar for longwall panel 54, which is about 200-ft wide (Figure 5.2). The site was utilized for both transmission and reflection surveys.

The general layout of the testing setup is illustrated in Figure 5.2. The layout consists of three general sections: a sensor section, a blasting section for transmission surveys, and a blasting section for reflection surveys. The sensor section and the blasting section for reflection surveys were located on the upper side of the pillar. The locations of these two sections were measured from M as marked. The blasting section for transmission surveys was located on the left end of the pillar, marked by E and F.

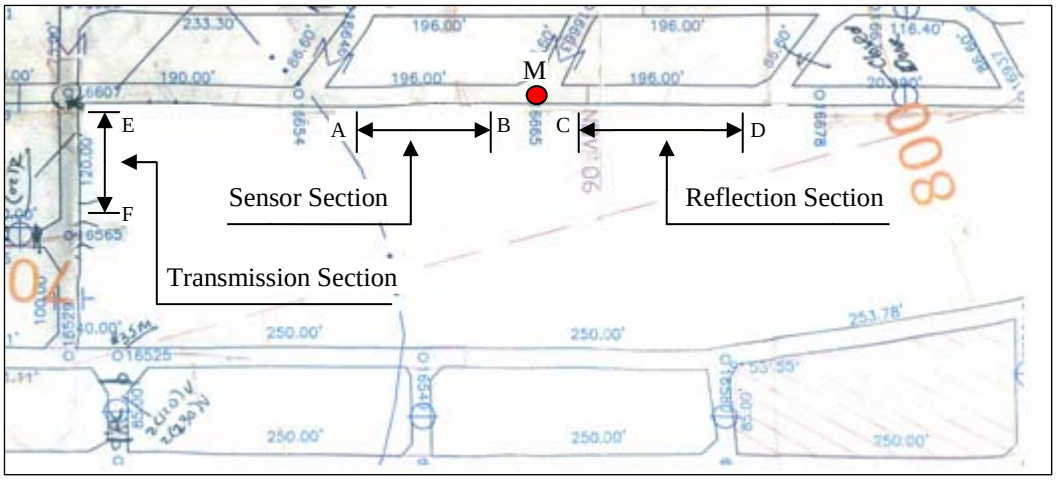

Figure 5.2 Test site used for the ISS test at the Cumberland Mine.

5.2.1 Sensor section

The sensor section was located on the left side of point M. The first sensor hole was placed a distance of 35-ft from this point. The section consisted of 14 sensor holes arranged in pairs as shown in Figure 5.3. The hole dimensions were roughly 3 feet deep and 1.75 inches in diameter. The coordinates of these sensor holes are given in Table 5.1.

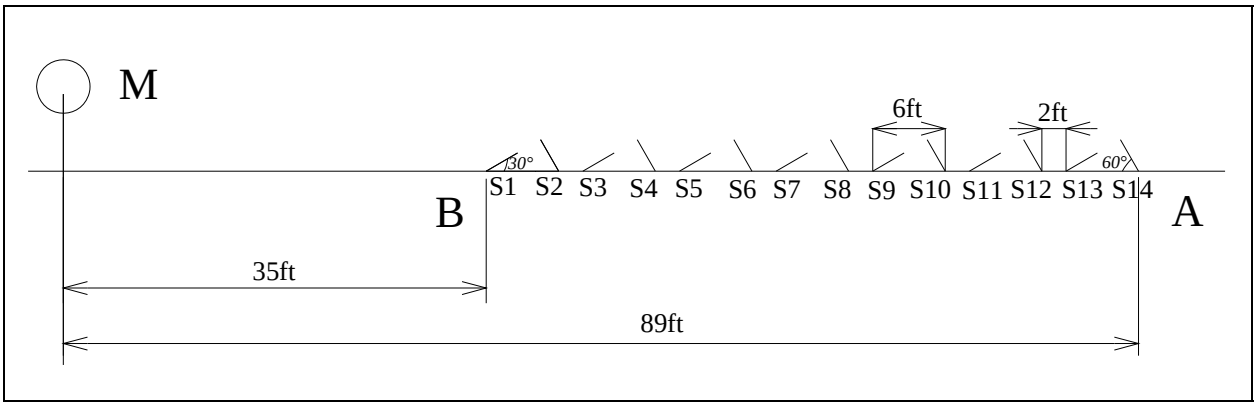

.

Figure 5.3 Sensor section used for the ISS based void detection test at the Cumberland Mine.

Table 5.1 Sensor hole coordinates

Sensor hole #	Coordinates (feet)	
	X	Y
S1	405.2	278.3
S2	404.0	277.0
S3	397.2	278.3
S4	396.0	277.0
S5	389.2	278.3
S6	388.0	277.0
S7	381.2	278.3
S8	378.0	277.0
S9	373.2	278.3
S10	372.0	277.0
S11	365.2	278.3
S12	364.0	277.0
S13	357.2	278.3
S14	356.0	277.0

5.2.2 Blasting section for the transmission surveys

The blasting section used for the transmission surveys was located on the left end of the pillar, indicated by points E and F. E was positioned at the corner of the pillar. A total of 10 blasting holes with the dimensions of approximately 3-ft long and 1.75 inches in diameter were drilled (Figure 5.4). The coordinates of these blasting holes are given in Table 5.2.

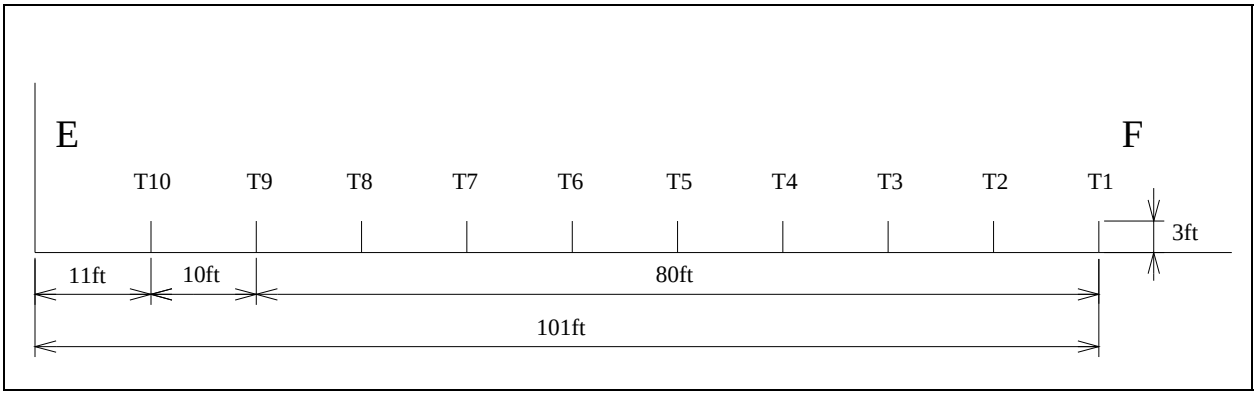

Figure 5.4 The layout of the blasting holes used for transmission surveys.

Table 5.2 Coordinates of blasting holes for transmission surveys

Blasting hole #	Coordinates (feet)	
	X	Y
T1	105.7	179.0
T2	105.7	189.0
T3	105.7	199.0
T4	105.7	209.0
T5	105.7	219.0
T6	105.7	229.0
T7	105.7	239.0
T8	105.7	249.0
T9	105.7	259.0
T10	105.7	269.0

5.2.3 Blasting section for the reflection surveys

The blasting section for the reflection surveys was approximately 100-feet long, with the first hole located a distance of 35 feet from mark M (Figure 5.5). The section consisted of 12 blasting holes, each approximately 3-feet deep with a diameter of 1.75 inches. The coordinates of these blasting holes are given in Table 5.3.

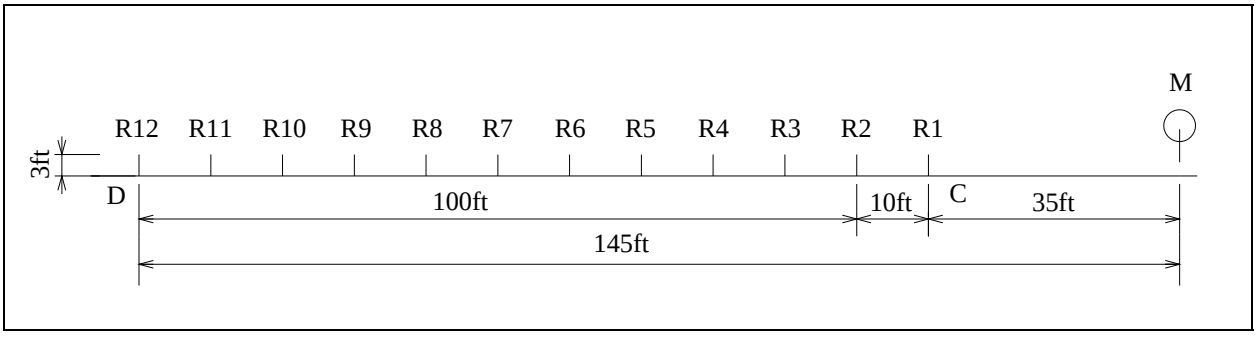

Figure 5.5 The layout of the blasting holes used for reflection surveys.

Table 5.3 Coordinates of blasting holes for reflection surveys

Blasting hole #	Coordinates (feet)	
	X	Y
R1	478.2	276.5
R2	488.2	276.5
R3	498.2	276.5
R4	508.2	276.5
R5	518.2	276.5
R6	528.2	276.5
R7	538.2	276.5
R8	548.2	276.5
R9	558.2	276.5
R10	568.2	276.5
R11	578.2	276.5
R12	588.2	276.5

5.3 Transmission surveys

A total of five transmission surveys were performed at the Cumberland Mine. The seismic sources for the surveys were 50 and 38 grams of dynamite. Table 5.4 lists the related information for these surveying events. The ray paths associated with these surveys are illustrated in Figure 5.6. The travel distance for these ray paths ranges from 255 to 316 feet with an average path distance of 285 feet (Table 5.5).

Table 5.4 A summary of the transmission survey

Hole #	Explosive (gram.)	Event #
T1	50	176
T2	38	185
T4	38	201
T5	38	208
T6	38	214

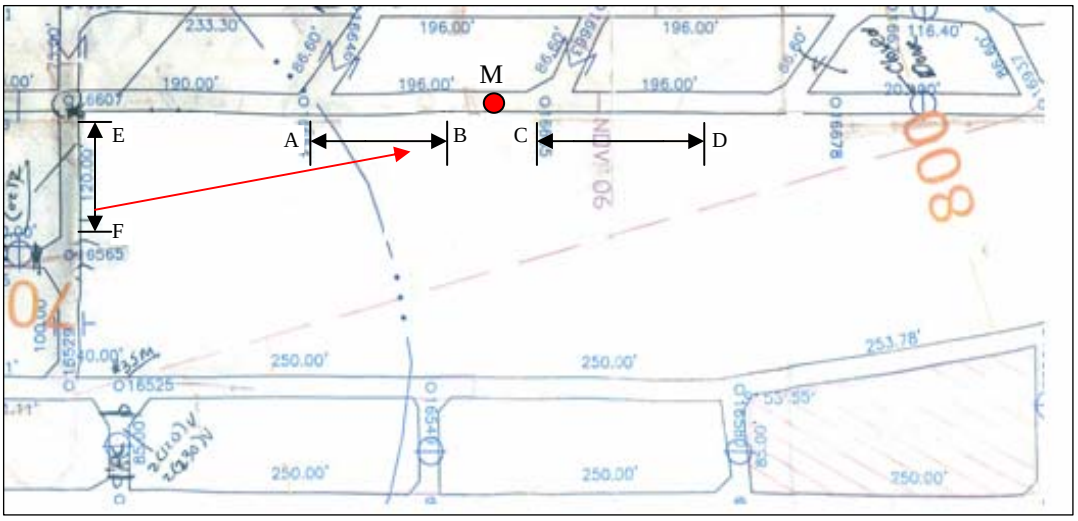

Figure 5.6 Illustration of ray paths associated with transmission surveys

Table 5.5 Ray path distances for transmission surveys (feet)

Blasting hole #	Sensor														Average distance
	S1	S2	S3	S4	S5	S6	S7	S8	S9	S10	S11	S12	S13	S14	
T1	316	314	308	306	300	299	293	291	285	284	278	276	270	269	292
T2	313	311	305	303	297	296	290	288	282	280	274	273	267	265	289
T3	310	308	302	301	294	293	287	285	279	277	271	270	264	262	286
T4	307	306	300	298	292	290	284	283	276	275	269	267	261	259	283
T5	305	304	297	296	290	288	282	280	274	273	266	265	258	257	281
T6	304	302	296	294	288	286	280	278	272	271	264	263	256	255	279
Average distance	309	308	301	300	294	292	286	284	278	277	270	269	263	261	285

The five transmission surveys were successful and the results from these surveys were very similar. Event 208 is selected for demonstration of the general features of the transmitted signals. The original waveform recorded for the event is presented in Figure 5.7 and a close-up view of the signal segment is shown in Figure 5.8. The experimental layout and the associated ray paths for the event are illustrated in Figure 5.9. The seismic source for this event was 38-gram dynamite at the location of blasting hole T5.

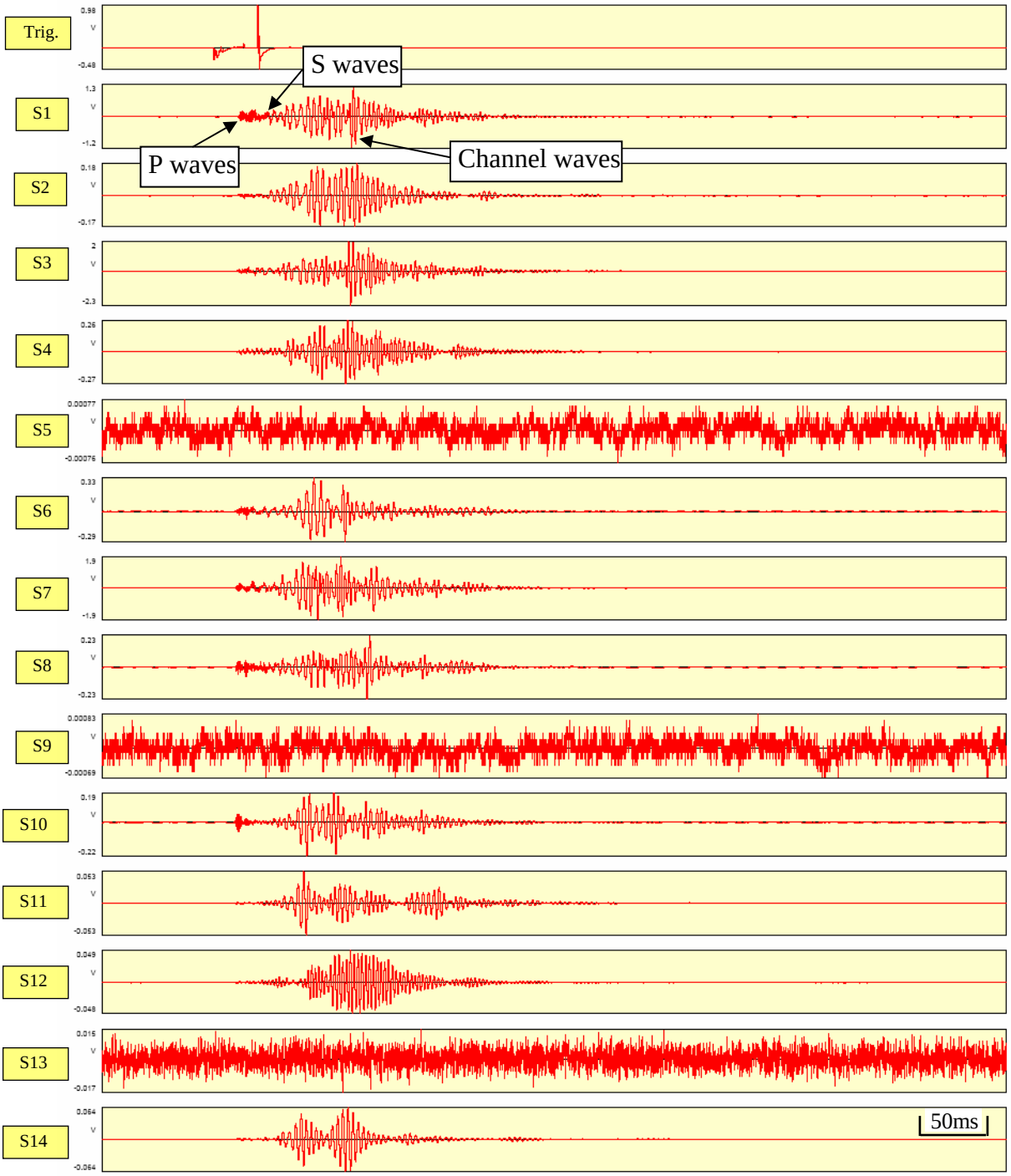

Figure 5.7 Original waveform record for a transmission survey (Event 208) at the Cumberland Mine (displaying window: 0-800 ms)

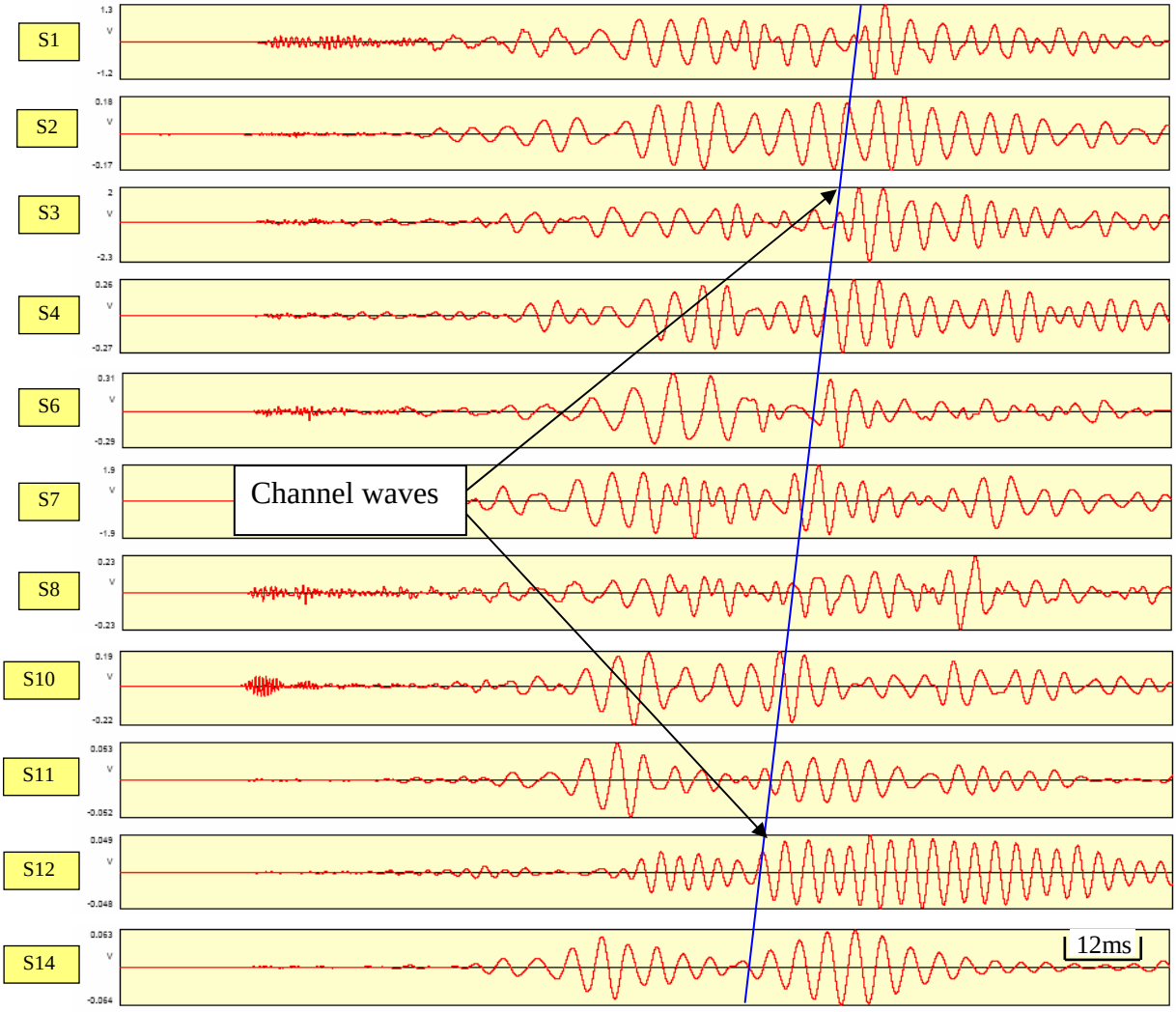

Figure 5.8 Details of P- and S-waves transmitted through the country rock and in-seam Love waves for Event 208 (displaying window: 100-275 ms).

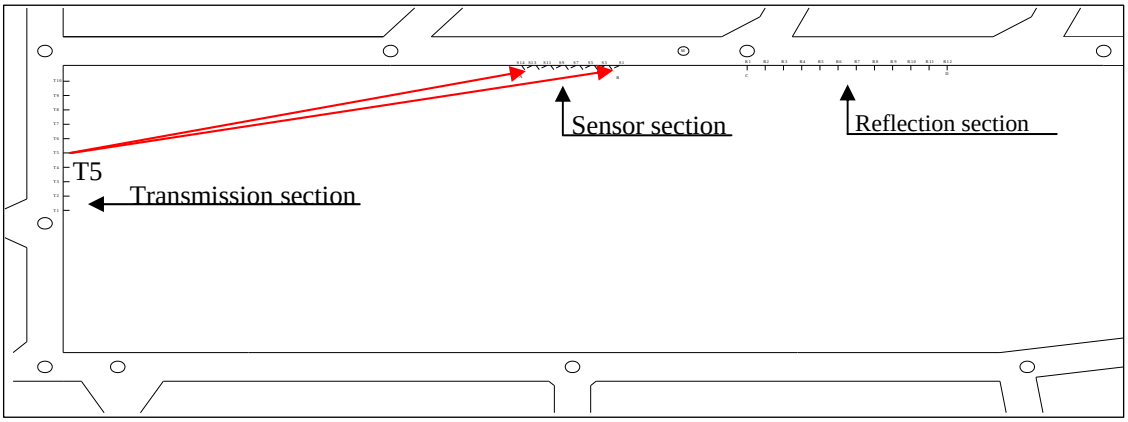

Figure 5.9 Testing setup for event 208.

It is seen from these figures that all major wave groups, including P- and S-waves transmitted through the country rock and the in-seam Love waves, are well defined. Each group exhibits its own distinctive characteristics. The trend of the Love wave arrivals, as shown in Figure 5.8, is clear and strong.

The dominant frequencies for the P-, S- and Love waves are 1000, 200 and 250 Hz, respectively. A typical frequency spectrum for the transmitted signals is given in Figure 5.10.

The average velocities for these three wave groups are 14220 ft/s, 7635ft/s and 2429 ft/s, respectively. The related data for velocity calculations are presented in Tables 5.6 – 5.9.

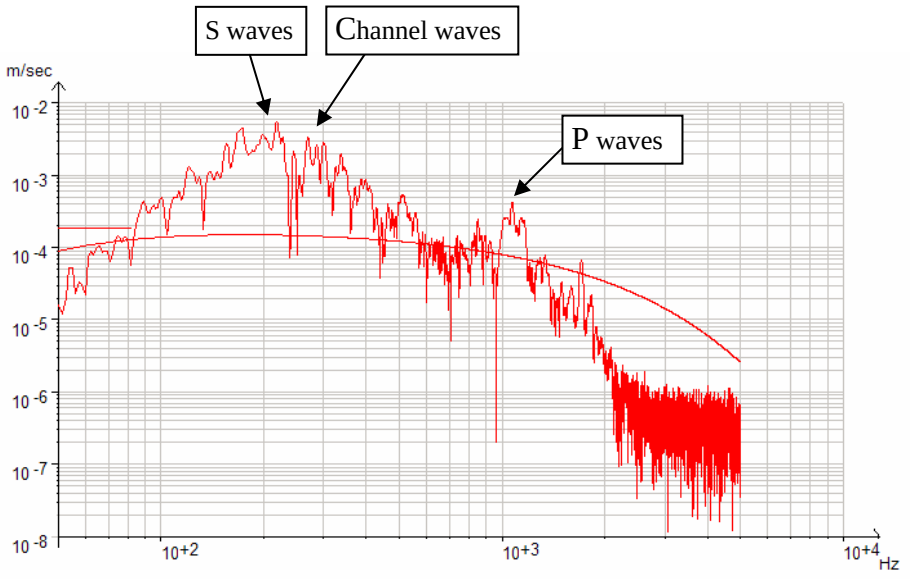

Figure 5.10 Frequency Spectrum for transmitted signals recorded by sensor S1

Table 5.6 Velocities associated with Cumberland Mine**.**

Strata	Wave Type	Velocity (ft/s)	Number of measurements	Standard deviation (ft/s)
Coal (bituminous)	Airy Phase	2429	18	103
Roof (sandy stone)	P-wave	14220	32	197
	S-wave	7635	17	281

Table 5.7 P-wave velocities determined from transmission surveys (ft/sec)

Blasting hole # \ Sensor	S1	S2	S3	S4	S6	S7	S8	S10
T1	13899	14333	14124	14313	14435	14214	14275	14256
T2	13889	14332	14111	14307	14420	14337	14328	14306
T5	13814	14196	14028	14231	14266	14551	14451	14753
T6	13858	14183	14009	14213	14173	14131	14132	14162

Table 5.8 S-wave velocities determined from transmission surveys (ft/sec)

Blasting hole # \ Sensor	S1	S2	S3	S4	S6	S7	S8	S10
T1	7337	7656	7736	7658	7681			
T2	7336		7776		7522			
T5	7269	7428	7931	8065	8135			
T6	7141	7888	7946		7495			

Table 5.9 Love-wave (Airy Phase) velocities determined from transmission surveys (ft/sec)

Blasting hole # \ Sensor	S1	S2	S3	S4	S6	S7	S8	S10	S11	S12	S14
T1	2438	2409					2609				
T2	2339		2299	2338				2587			
T5	2437	2366	2420	2463	2463	2490	2648	2562	2492	2511	2480
T6	2424	2360	2293								

5.4 Reflection survey at Cumberland Mine

A total of 11 reflection surveys (blasting events) were executed at the Cumberland Mine. The layout of the testing setup for reflection surveys is illustrated in Figure 5.11. The seismic source for these surveys ranges from 38 to 70-gram dynamite and the event information is summarized in Table 5.10.

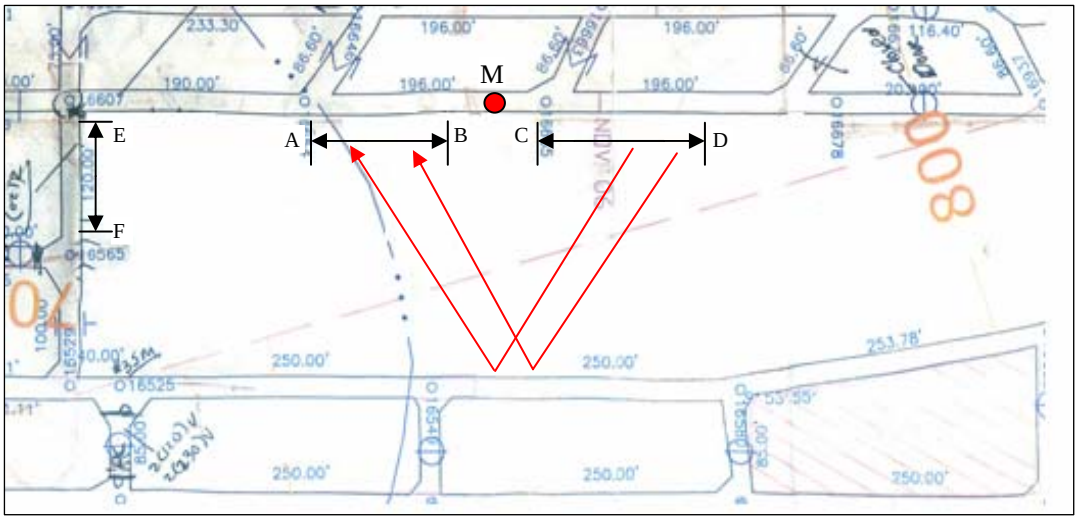

Figure 5.11 Testing setup for reflection surveys at the Cumberland Mine.

Table 5.10 A summary of the reflection surveys at the Cumberland Mine.

Hole #	Explosive (gram)	Event
R12	38	233
R11	50	242
R10	63	250
R9	63	256
R8	50	266
R7	50	278
R6	38	295
R5	70	302
R4	50	310
R3	50	316
R2	50	323

The reflection survey resulted in a successful demonstration of the observation and use of reflected Love waves for the detection of voids. In the following discussion, event 250 is selected to illustrate this observation. .

The seismic source for Event 250 was located at R10. The testing layout for this survey, including the locations of R10, the sensors, and the reflected ray paths, is shown in Figure 5.12.

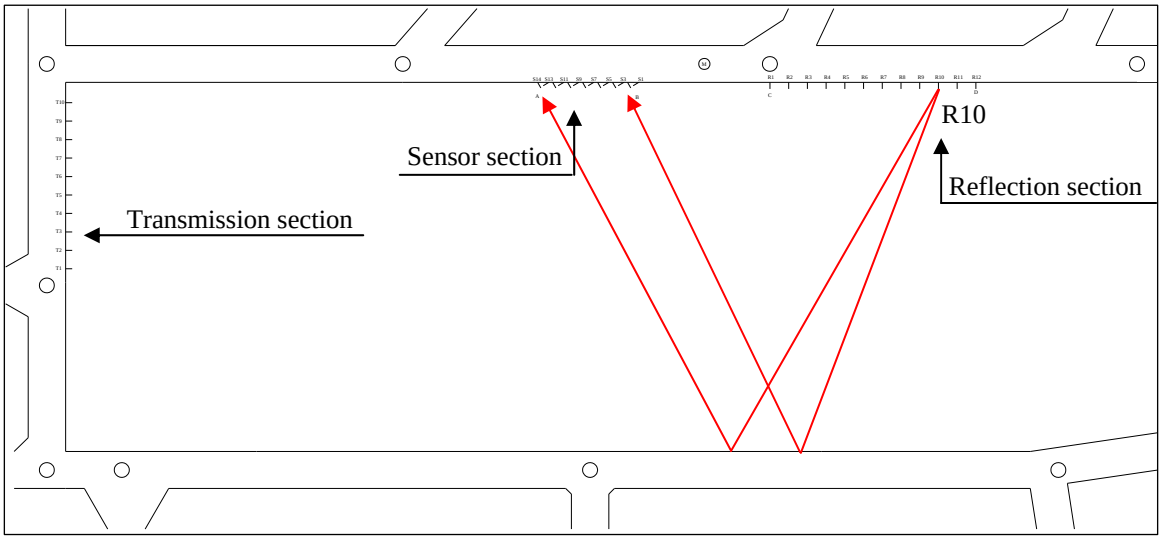

Figure 5.12 Testing setup for event 250.

The recorded waveforms for this event are presented in Figures 5.13 - 5.15. Figure 5.13 shows the original waveform record for the event. In this figure, the trend of the reflected Love waves is clearly seen. The direct arrived waves are shown in more detail in Figure 5.14. A close-up view of the reflected Love waves is provided in Figure 5.15. The arrival time readings of the reflected Loves waves (Airy Phase) for event 250 are listed in Table 5.11.

Table 5.11 Arrival time readings of reflected Love waves for event 250.

Triggering Time (ms)	Arrival time (Airy Phase) (ms)								
	S1	S2	S4	S5	S7	S8	S11	S12	S14
101.2	309.4	313.6	303.5	318.5	318.1	319.1	331.1	333.8	336.4

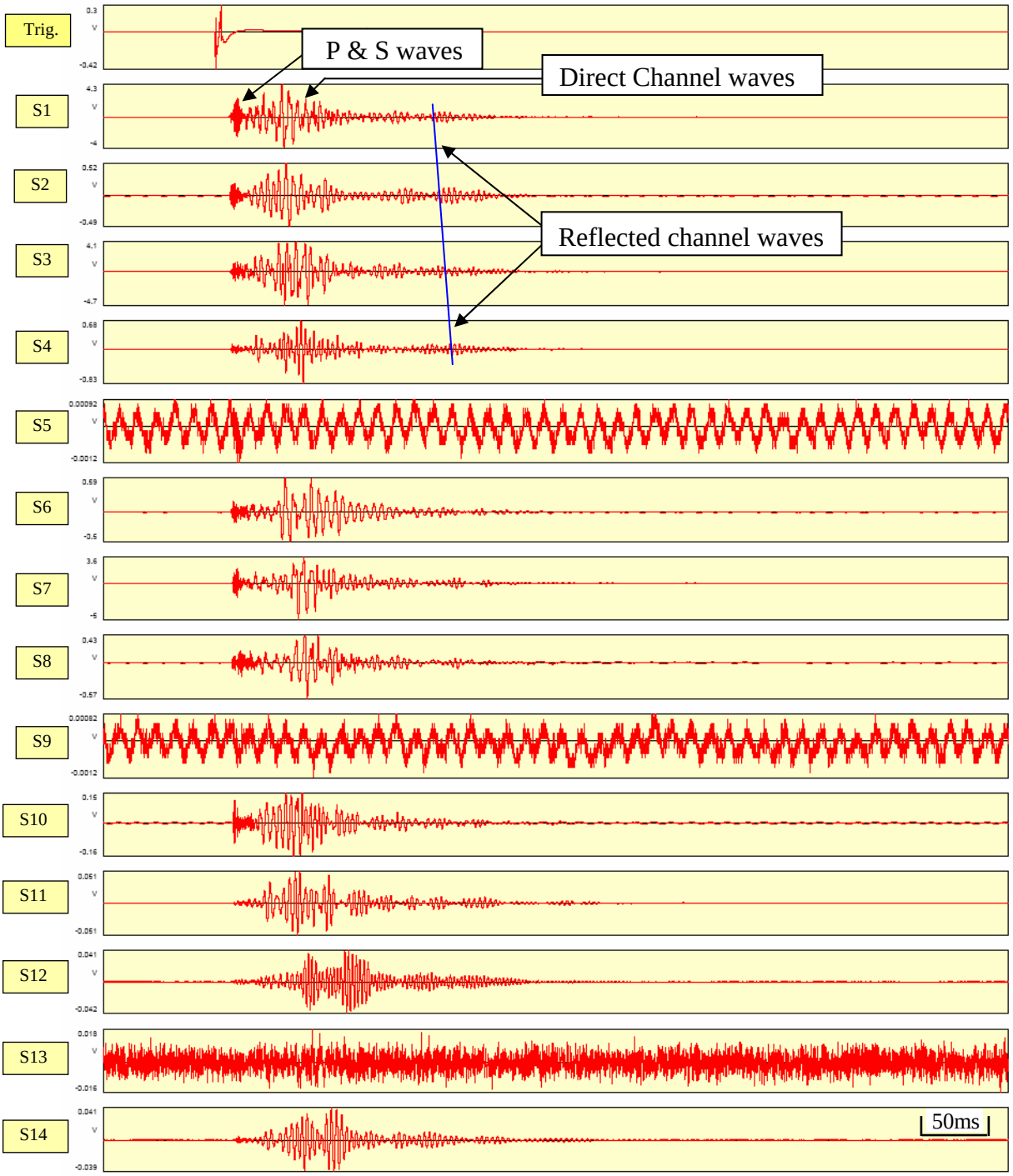

Figure 5.13 Original waveform record for event 250 (displaying window: 0 – 800 ms).

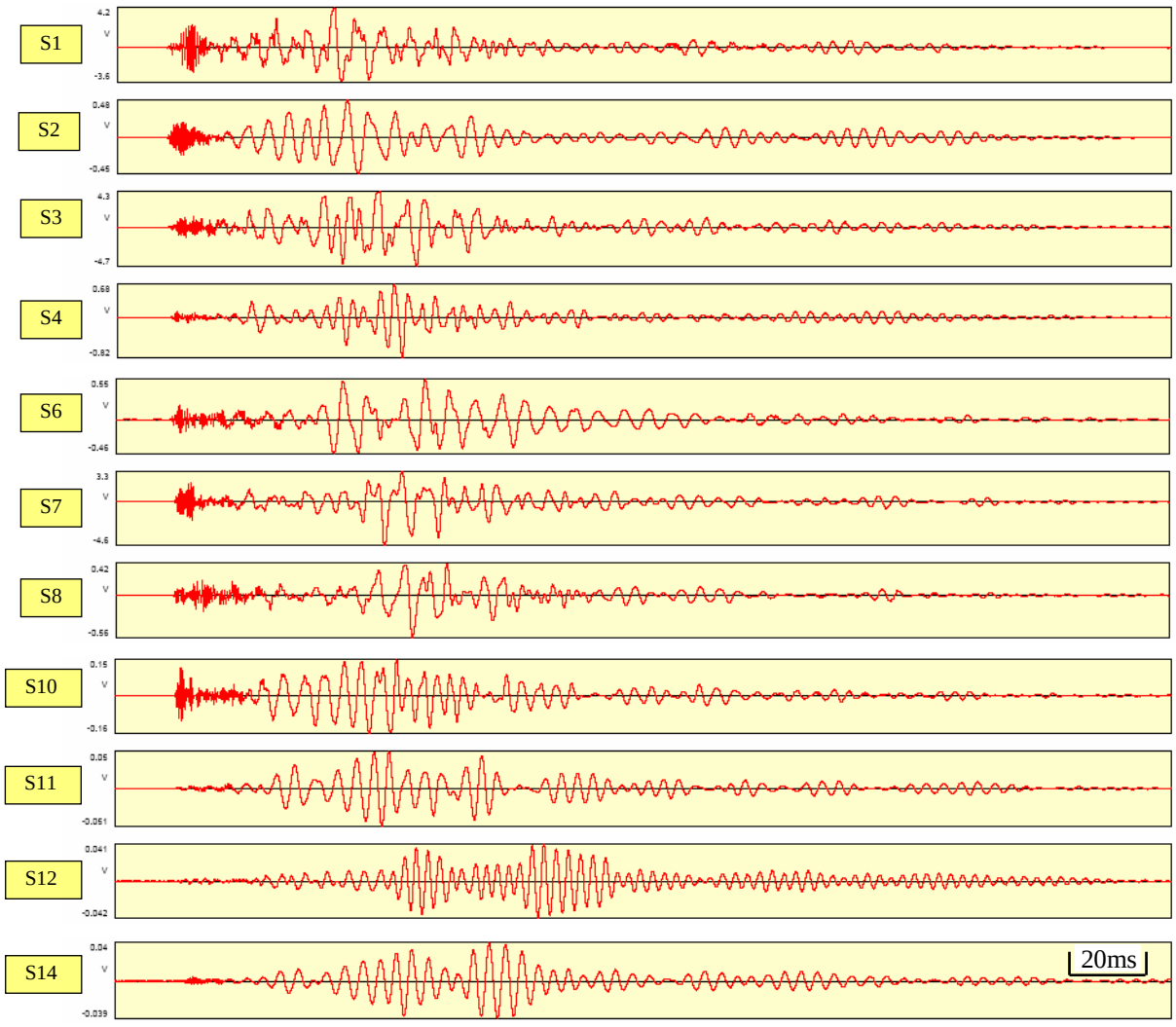

Figure 5.14 Details of the direct arrived signals for event 250 (displaying window: 100-400 ms).

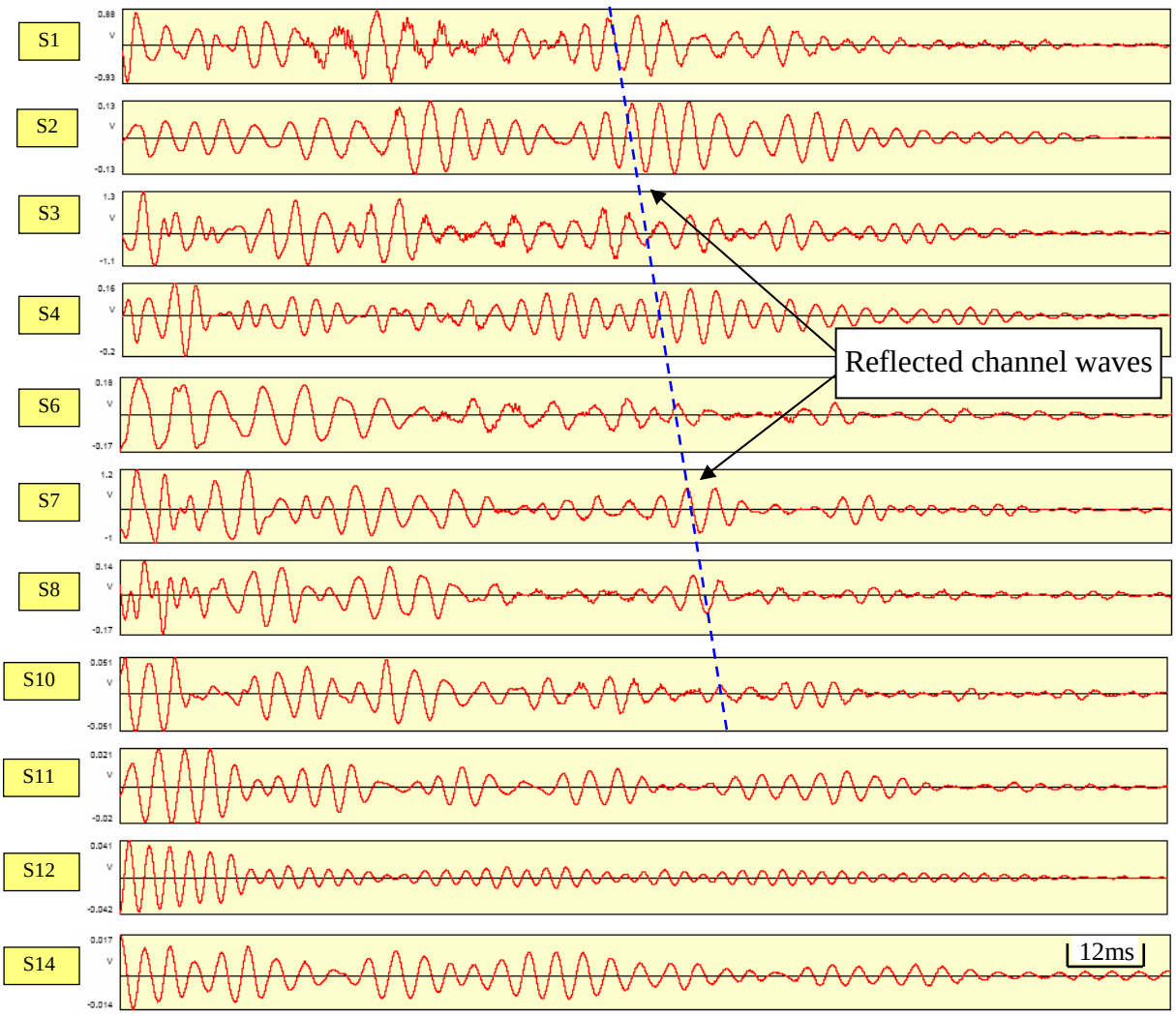

Figure 5.15 A close-up view of the reflected Love waves for event 250 (display window: 220-400 ms).

5.5 Void mapping

The elliptical method was used to map the void location. Figure 5.16 shows the void location by using the information of event 250. The void location is also presented in Figure 5.17, in which the plot was made based on the arrival time information from 20 reflected Love waves. The pillar boundary is depicted with the red line in the figures. The travel velocity of Love waves used for void mapping is 2099 ft/s. This is the average of the wave velocity obtained from the transmission survey and the wave velocity calculated based on the information of the direct arrived Love waves recorded during the reflection survey. The mapping error as shown by the plot is within ±15 feet.

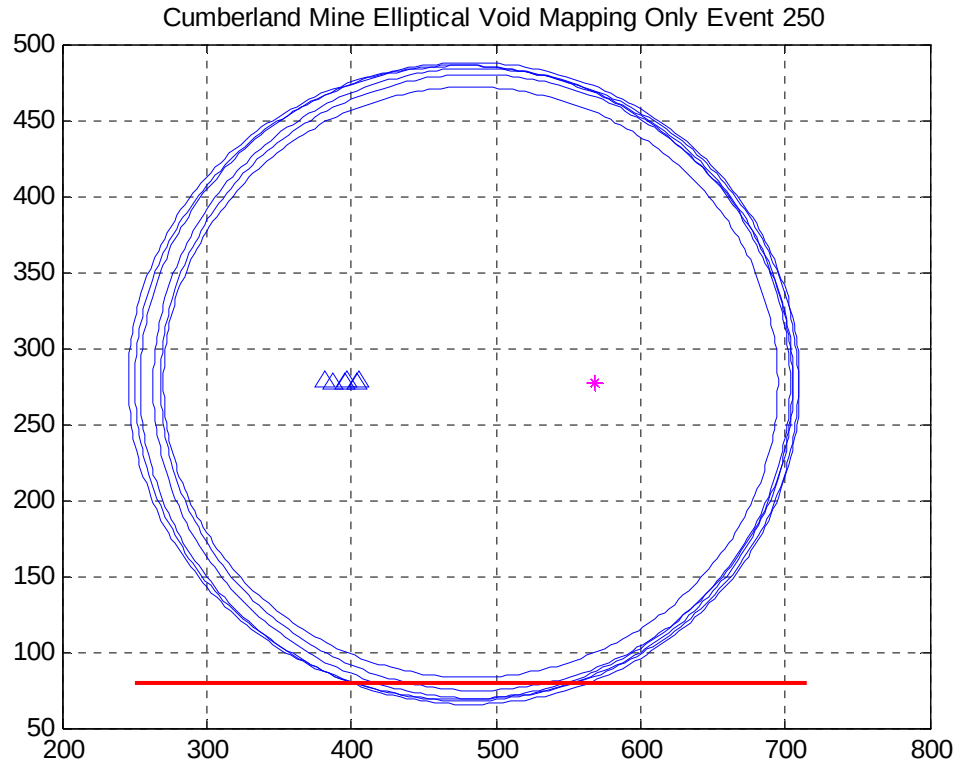

Figure 5.16 “Void” location determined by the elliptical location method using event 250 only at the Cumberland Mine. Red line denotes the location of the void.

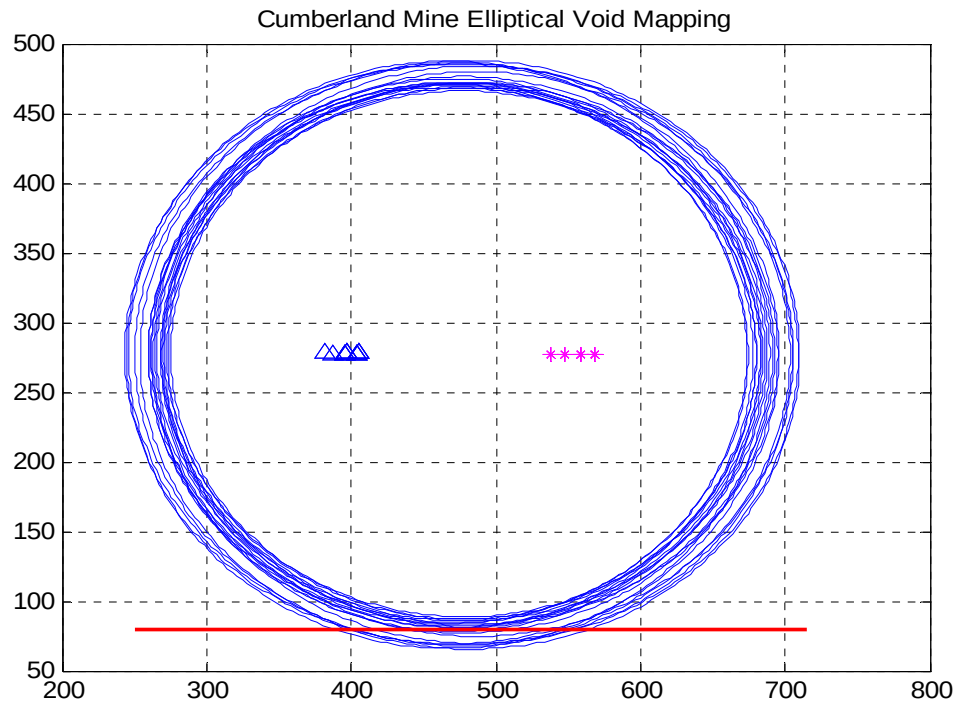

Figure 5.17 “Void” location determined by the elliptical location method at the Cumberland Mine. Red line denotes the location of the void.

5.6 Summary of the test result at the Cumberland Mine

The objective of the test carried out at the Cumberland Mine was to investigate the effectiveness of the ISS based void detection technique for bituminous mines with a relatively thick seam.

The seam thickness at the site is about 84 inches (7 feet). Both the roof and the floor of the seam are shale with varying strengths. The overburden is about 800 ft at the test site. The pillar under testing is 200-ft wide.

Both transmission and reflection tests were performed at the site.

Well developed and defined in-seam Love waves were consistently observed in both transmission and reflection surveys. The dominant frequency (Airy Phase) is in the range of 230 – 250 Hz with an average velocity of 2099 ft/sec.

The trend of the reflected Love waves is evident. The mapping error is estimated within ±15 feet based on plotting the result of 20 reflected signals.

Based on the strength of the reflected signals, we believe that a detection range of 250 feet should be achievable for the ISS based void detection technique under similar physical conditions.

The dominant frequencies for P- and S-waves transmitted in roof/floor are 1000 and 200 Hz, respectively. The average P- and S-wave velocities are 14220 ft/s and 7635ft/s, respectively.

6. Conclusions

The objective of Phase II was to investigate the effectiveness of the In-Seam Seismic (ISS) based void detection technique for bituminous mines.

6.1 Testing sites

Four sites from three mines were selected for the field test. These three mines are the Nolo Mine of the Amfire Mining Co., the Black King Mine of Massey Energy, and the Cumberland Mine of Foundation Coal. The Nolo Mine hosted two test sites.

The seam height for these test sites ranges from 36 to 84 inches. In addition to the fact that this range covers the coal seam thickness for most US bituminous mines, the seam height of 36 inches is almost the minimal limit height for underground mining. This height also represents a very difficult condition to apply the ISS technique as it implies much higher frequency for the associated Love waves.

Both the seam and country rock conditions associated with these mine sites are very different. The Nolo Mine may represent the most demanding condition for applying the ISS based void detection technique, where the seam is very low, only 48 inches, the coal is highly fractured, and the clay shale is a low strength rock material. The condition at the Cumberland Mine, on the other hand, may be considered ideal for the ISS based void detection technique, where the seam is relative thick, 84 inches, and both the coal and the shale, which forms both the roof and the floor, are fairly strong. The condition at the Black King Mine is mixed. It is extremely thin, only 36 inches, which is a negative for using the ISS technique. However, both the roof and the floor are sandstone, which is a preferred condition for using the ISS technique.

The detection distances for these four sites vary from 100 to 200 feet. Two sites were selected at the Nolo Mine. One site was 120-feet wide and the other site was 180-feet wide. As such, the detection distance was determined in an objective manner. Since the test condition at the Nolo Mine represents one of the most difficult situations, the detection distance determined from this mine may be considered as a benchmark of the detection distance for the bituminous mines.

In summary, the four sites used in Phase II represent diversified conditions for the bituminous mines in the United States, including those very unfavorable conditions for the ISS based void detection technique.

6.2 Signal characteristics

Well developed and well defined in-seam Love waves were consistently observed from the surveys performed at all four testing tests. The dominant frequencies (Airy Phase) vary from 200 – 300 Hz at the Nolo Mine to 550 Hz at the Black King Mine. The associated velocities range from 1692 ft/s at the Nolo Mine to 2639 ft/s at the Black King Mine.

The broadband data acquisition system and the advanced sensor installation technique also enabled us to record high frequency body waves transmitted through the country rock. For instance, the P-wave frequency at the Black King Mine is 2,000 Hz.

The dominant frequencies for in-seam Love waves and P- and S-waves transmitted in the roof and floor for the three mines are listed in Table 6.1. The associated velocities for these three wave groups are presented in Table 6.2.

Table 6.1 Signal frequencies at three mine sites

Mine site	Seam height (inch)	Frequency (Hz)		
		Love wave	P-wave	S-wave
Nolo	48	220	1,500	1,000
Black King	36	550	2,000	500
Cumberland	84	250	1,000	200

Table 6.2 Average signal velocities at three mine sites

Mine site	Velocity (ft/s)		
	Love wave (Airy phase)	P-wave	S-wave
Nolo	1,692	15,242	7,320
Black King	2,693	15,684	9,101
Cumberland	2,099	14,220	7,635

6.3 Mapping error and detection distance

The reflected Love waves were evident from the reflection surveys carried out at four testing sites. The Airy Phase can be identified from many channels and is used for void mapping. The detection distance and the associated mapping errors for the four sites are listed in Table 6.3.

Table 6.3 Void detection distance and the associated mapping error

Mine site	Detection distance (ft)	Average mapping error (±ft)
Site I, Nolo	120	20
Site II, Nolo	180	20
Black King	100	20
Cumberland	200	15

Based on the strength of the reflected signals, we believe that the detection range for all three mine conditions can be much greater. A conservative estimation of the expected detection range for these mine conditions is given in Table 6.4.

Table 6.4 Expected detection range for three mine site conditions.

Mine site	Actual detection distance (ft)	Expected detection range (ft)
Site II, Nolo	180	200 - 250
Black King	100	150 - 200
Cumberland	200	250 - 300

6.4 Effect of signal detection techniques

The test result from all four sites unequivocally demonstrated existence of well-developed and well-defined in-seam Love waves in bituminous mines, even under very difficult conditions, and the feasibility to use these waves for void detection.

An important reason for the success of these tests is the signal detection technique used, including the incorporation of accelerometers as primary sensors, using the advanced sensor installation technique developed in Phase I, and air-tight sealing of the sensor holes.

Using accelerometers as primary sensors

One of the major differences between our approach and previous ISS studies is that we demonstrated the use of accelerometers as the primary sensing units, instead of geophones. This practice allowed us to detect higher Love wave frequencies associated with thin seams. For instance, the geophones did not detect any in-seam Love waves at the Black King Mine because of the high frequency content of the Love waves at the mine site (550 Hz). This fact is plainly shown in Figure 4.17 where S1 – S7 are accelerometers and the Love waves are evident and where S12 and S14 are geophones and high frequency signals were not recorded.

Using the advanced sensor installation technique

In Phase I, an advanced retrievable sensor installation technique was developed (Ge, 2006b). This technique improves the capability of signal detection with two mechanisms. First, sensors are installed at the bottom of drill holes, which is beyond the fracture zone. Secondly, sensors are tightly screwed to their anchors which are grouted at the bottom of the borehole; this greatly improves the coupling effect.

If sensors are simply spiked into the rib surface, as conventionally done in ISS studies, most energy, especially the high frequency energy, will be attenuated. Unfortunately, pillar ribs for many bituminous mines are highly fractured, illustrated in Figure 2.3, a picture taken from the Nolo Mine. The picture in the text page was taken from the test site at the Cumberland Mine which displayed that a slab of coal, which was about 10-inch thick, was off from the rib. In fact, the fracture between the slab and the fresh wall extended several hundred feet along the rib, which passed the sensor section (we intersected the fracture while we were drilling the sensor holes). It is known from this case that, even the rib appears in excellent condition on the surface

as shown in the picture, major fractures could develop inside the rib, which are not visible. If the sensors had been installed at the rib surface, we might not have been able to detect any signals.

Table 6.1 The fracture between the felled coal slab and the fresh wall extended several hundred feet along the rib, which passed the sensor section for the ISS test.

Air-tight sealing of sensor holes
In Phase II, Play-Doh was used to seal all sensor holes during the test. This simple technique provided a convenient and effective air-tight seal for the sensor holes and completely eliminated the problems caused by (air) shock waves.

6.5 Recommendations for future work
Consideration of the future work for the ISS based void detection technique tested in Phase I and Phase II requires a philosophical discussion regarding how a geophysical method, such as the one discussed in this report, may be practically utilized by the mining industry.

An abandoned mine can pose a huge risk and cause enormous damage to an active mine nearby, such as the case of the Quecreek Mine incidence in 2002. Therefore, if an abandoned mine is suspected to exist within a certain range of an active mine, the potential risk must be explored. The existence or absence of the abandoned mine must be confirmed by a truth finding method. In general, one has to use the horizontal drilling method for this purpose.

The problem faced by the U.S. mining industry is that most active mines are near or surrounded by abandoned mines. However, it is neither economically nor technically feasible to use the horizontal drilling method as a general means to locate these abandoned mines. The geophysical methods, such as the ISS based void detection technique, are expected to fill the decision gap by answering the question whether there exist old mine workings within certain a certain distance. The expensive truth finding method, horizontal drilling, will be used if the geophysical method determines the presence of the old mine workings within a certain distance of the active mine. From this point of view, the most important criterion to measure the reliability of a geophysical based void detection method is that the method will *definitely* report the existence of the voids that are located within a certain range.

If we define the accuracy as the actual location error, then a high accuracy, such as an error of 15 feet, in my opinion, is not the most important claim. A given method will serve a great purpose to the mining industry if the method can claim that it will not miss-report a void within a certain range. This service will hold even the method has a relatively large location error.

In all our four tests, which were carried out with the range from 100 to 200 feet under varying and difficult conditions, well-developed Love waves were consistently generated and recorded. Focusing on the reliability of a geophysical method for void detection, as discussed above, we believe that the high quality data obtained from Phase II is the best evidence to demonstrate that there is a significant potential to develop the ISS method into an effective void location technique. In order to achieve this goal, there are a number of important issues to be further addressed.

Data analysis
Although we believe that we are able to acquire high quality data with the acquisition approach we used (data acquisition setting, sensor selection, sensor hole preparation, sensor installation technique, sensor hole sealing method, blasting procedure, and testing design), the method of data analysis remains a very challenging problem. We used the Airy Phase for timing Love waves. Although this method is relatively simple, easy to use and reliable, the problem is that the Airy Phase is not always clearly shown in the data. We need more robust methods for the data analysis.

More field tests
The tests executed to date have examined pillar width ranging from 100 to 200 feet. It is very important to test the pillar width up to four or five hundred feet.

Battery operated data acquisition system
The data acquisition system we employed needs 110v power. When the test site is located a long distance away from the power station, a stable power supply becomes a very serious issue. Our data acquisition was interrupted several times by this problem. In order to solve this problem, a smaller, battery operated system is necessary.

Blind tests
Blind tests are needed to examine the efficiency of the ISS based void detection technique.

References

Brentrup, F. K., 1970. Seismische vorfelderkundung zur ortung tektonischer storungen im steinkohlenbergbau. *Gluckauf* **106**, 933-938

Brentrup, F. K., 1971. Flozdurchschallung aus Tiefbohrlochern. *Gluckauf* **107**, 685-690.

Brentrup, F. K., 1979a. Die entwicklung einer schlagwettergeschutzten Digitalapparatur fur die Flozwellenmessung, *Gluckauf Forschungs Hefte* **40**, 11-15.

Brentrup, F. K., 1979b. Flozwellenseismische Vorfelderkundung. *Gluckauf* **115**, 820-823.

Darken, W. H., 1975. A finite-difference model of channel waves in coal seams. Golden, Colorado School of Mines, USA, Master's thesis No. 1729

Dresen and Ruter, 1994. Seismic Coal Exploration, Part B: In-seam Seismics. Pergamon, New York, NY.

Evinson, F. F., 1955. A coal seam as a guide for seismic energy. *Nature* **176**, 1224-1225.

Ge, M., 2006a. An in-seam seismic (ISS) method based mine void detection technique. Final report for Phase I of Geo-physical Void Detection Demonstrations (MSHA B2532532), submitted to U.S. Department of Labour, Mine Safety and Health Administration, October 29, 2006, pp227.

Ge, M., 2006b. User's manual for ISS based void detection technique. Special report for Phase I of Geo-physical Void Detection Demonstrations (MSHA B2532532), submitted to U.S. Department of Labour, Mine Safety and Health Administration, October 29, 2006, pp106.

Guu, J. Y., 1975. Study of seismic guided waves in the continuity of coal seams. Golden Colorado School of Mines, USA, Ph.D. thesis No. T 1770.

Krey, T., 1962. Boundary waves as a tool of applied geophysics in coal mining. Paper presented at the 32nd SEG Meeting, Calgary, Canada.

Krey, T., 1963. Channel waves as a tool of applied geophysics in coal mining. *Geophysics* **28**, 701-714.

Krey, T., 1976a. In-seam seismic exploration techniques, in coal exploration 1, Proc.1st International coal exploration symposium, London, U.K., (ed) W.L.G. Muir, Miller-Freeman Publishers, San Francisco, USA.

Krey, T., 1976b. Possibilities and limitation of in-seam seismic exploration. Coal seam discontinuity symposium, Pittsburgh, Pennsylvania, USA.

Leitinger, H., 1969. Investigations of displacements in a layered halfspace by the finite-difference method. Golden, Colorado School of Mines, USA, Ph.D. thesis No.T. 1770.

Rodriguez R., R. Brendlinger, H. Naumann, and L. Browning, 1994. Underground high resolution seismic method as a low cost alternative for mapping sandstone replacement channels in coal mines. Proc. 13th International Conference on Ground Control in Mining, pp. 233-238.

Rodriguez, R., E. and H. Naumann, 1995. Application of underground in-seam seismic methods (UISS) to map the coal seam structure across longwall panels. Proc. 14th International Conference on Ground Control in Mining, pp. 261-272.

Rodriguez, R., 1996. Theoretical aspects of in-seam 3-D channel waves. Geophysics Journal. This paper may not be published.

Su, F. C., 1976. Seismic effects of faulting in coal seams: numerical modeling. Golden, Colorado School of Mines, USA, Ph.D. thesis No. 1869.

Young, G. B. and L. W. Braile, 1976. A computer program for the application Zoeppritz's amplitude equations and Knott's energy equations. *Bull. Seism. Soc. Am.* **66**, 1881-1885.

Appendix I

Testing equipment, material and software used for the project

This appendix lists the major equipment, material and software used for field tests.

Table I – 1 Equipment and material used for field tests

Equipment/material	Description	Manufacturer
ESG Hypersion data acquisition system	16-channel, 16-bit resolution, MSHA certified	ESG
A1030 uniaxial accelerometer	Sensitivity: 30V/g, frequency response: 50 – 5000 Hz to within ±3 dB, 3 V/g, MSHA certified	ESG
Wire-breaking recording device	For system triggering	ESG
Sensor cable	20 AWG, 2 pair copper w/shielding	Belden Electronics
Sensor installation kit	For installing retrievable sensors	Penn State
Lokset Resin	For grouting sensor anchors	Minova USA
Stemming clay	For stemming blasting holes	Webb Manufacturing

Table I – 2 Software used for data analysis

Software	Description	Developer
ESG –IS-001L	This software was purchased along with the data acquisition system. It is a general software package used for seismic data processing and visualization.	ESG
AGU-Vallen Wavelet	Wavelet analysis package	Vallen
Matlab 7.0	Drawing ellipses	The MathWorks

Table I – 3 Parameters for data recording

Mode	Recording window (second)	Sampling Rate (samples/second)
Mode I	0.4	50k
Mode II	0.8	25k